The Identification and Validation of Novel Aptamers to Glioma

By

Karl Norris

A thesis submitted in partial fulfilment for the requirements of the degree of *Master of Science (by Research) in Pharmacy* at the University of Central Lancashire

Submitted: September/2014

Declaration

Concurrent registration for two or more academic awards

I declare that while registered as a candidate for the research degree, I have not been a registered candidate or enrolled student for another award of the University or other academic or professional institution.

_____

Material submitted for another award

I declare that no material contained in the thesis has been used in any other submission for an academic award and is solely my own work except where due reference is made.

_____

Collaboration

Where a candidate's research programme is part of a collaborative project, the thesis must indicate in addition clearly the candidate's individual contribution and the extent of the collaboration. Please state below:

Signature of Candidate

_____

Type of Award

_____

School

_____

Abstract

Glioma is a cancer derived from transformed glial cells; these tumours are often invasive and display a heterogeneous cell population, with various phenotypes. Current treatment modalities for glioma are ineffective, with minimal improvement to overall patient survival over the last decade. Targeted approaches that take advantage of the various biomarkers displayed within glioma are required to deliver therapeutics more specifically. Aptamers are short oligonucleotides that conform to unique three dimensional structures based on sequence and are able to target molecules selectively, in order to deliver therapeutic agents directly to the tumour.

Aptamers can be selected against whole cells via cell-SELEX, for production of a targeting ligand, which may also have the secondary advantage of revealing novel biomarkers if the target of the aptamer is elucidated. Previously, the glioblastoma cell line U87MG has been utilised in cell-SELEX for aptamer identification, however cell lines may not ubiquitously express all biomarkers indicative of glioblastoma. Consequently, cell-SELEX using short term cultures from human tissue may produce aptamers that target novel biomarkers. As primary cells are only available in small numbers, a cell-SELEX procedure was developed that was able to identify aptamers using 100 cells. Utilising this procedure, seven novel DNA aptamers were selected to short term cultures. Validation studies using oligohistochemistry showed the aptamers may interact with a protein on the cell surface.

DNA aptamers were also identified towards two known biomarkers important for gliomagenesis; EGFRvIII and PDE1C. Ten DNA aptamers were isolated towards a peptide within the mutated region for EGFRvIII and four aptamers were targeted towards the PDE1C protein. Whilst validation studies via Western blot showed no aptamer-protein interaction when using the EGFRvIII aptamers, denaturing and native Western blots showed positive results displaying 3 bands indicative of PDE1C isoforms. PDE1C aptamer targets were pulled out of native cell lysate via an aptoprecipitation assay, which showed similar banding patterns to the Western blots.

The results presented suggest the potential of aptamers to target short term cultures and also protein biomarkers that are over-expressed or truncated within glioma. Whilst further studies are required to elucidate binding characteristics, these aptamers have the potential to assist therapeutic agents become more specific.

Table of Contents

Declaration i

Abstract ii

Table of Contents iii

Table of Figures x

Table of Tables xiv

Acknowledgements xvi

List of Abbreviations xvii

Chapter 1: Introduction 1

1.0 Introduction 2

1.1 Glioma 2

1.1.1 Classification and grading of glioma 2

1.1.2 Epidemiology 7

1.1.3 Aetiology 8

1.1.3.1 Tyrosine Receptor Kinases (RTKs) 9

1.1.3.2 Oncogenes and Tumour Suppressor Genes (TSGs) 11

1.1.4 Prognostic factors 13

1.1.5 Diagnosis 15

1.1.6 Current treatment 15

1.1.6.1 Surgery 16

1.1.6.2 Radiotherapy....16

1.1.6.3 Chemotherapy....17

1.2 Aptamers....19

1.2.1 History of Aptamers....19

1.2.2 Structure and function....19

1.2.3 Aptamers *versus* antibodies....21

1.2.4 Identification of aptamers by SELEX....23

1.2.5 Review of aptamer applications....25

1.2.5.1 Aptamers as therapeutic agents....25

1.2.5.2 Aptamers for target identification....26

1.2.6 Use of aptamers in the targeting of glioma....27

1.3 Aims and objectives of study....28

Chapter 2: Methods and materials....30

2.1 Cell culture and maintenance.....31

2.1.1 Cell lines and primary cell cultures....31

2.1.2 Cell Culture and Subculture....31

2.2.3 Cell Viability....31

2.3 Optimisation and establishment of an aptamer library.....32

2.3.1 The DNA aptamer library....32

2.3.2 Amplification of the DNA aptamer library....32

2.3.3 Separation and visualisation of PCR products....34

2.3.4 Purification of DNA via ethanol precipitation....34

2.3.5 Preparation of ssDNA aptamers from concentrated PCR product....35

2.4 Systematic evolution of ligands by exponential enrichment using cell lines (cell-SELEX)....36

2.4.1 Negative Selections of amplified library against SVGp12 cell line....36

2.4.2 Positive selections against U87MG cell line....36

2.4.3 Minimum number of cells required to return specific aptamers....37

2.5 Primary cell SELEX....37

2.6 Identification of DNA aptamers towards purified biomarkers via Counter-SELEX...38

2.6.1 Counter-SELEX against Phosphodiesterase 1C (PDE1C)....38

2.6.1.1 Expression of glutathione S-transferase (GST)....38

2.6.1.2 Immobilisation and negative selection against GST....40

2.6.1.3 Positive selection against immobilised PDE1C....41

2.6.2 Counter-SELEX against EGFRvIII peptide....42

2.7 Establishing aptamer sequences....42

2.7.1 Transformation and cloning of identified DNA aptamers....42

2.7.2 Identifying novel aptamer sequences....44

2.8 Validation of aptamer-target specificity....44

2.8.1 Preparation of biotinylated ssDNA aptamers for validation studies....45

2.8.2 Denaturing and non-denaturing Western blot 45

2.8.3 Oligohistochemistry..... 46

2.8.4 Aptoprecipitation (AP) assay 47

Chapter 3: Results and analysis..... 48

3.0 Results 49

3.1 Optimisation of DNA aptamer amplification and purification..... 49

3.1.1 Optimisation of DNA aptamer amplification via polymerase chain reaction (PCR) 49

3.1.2 Optimisation of DNA aptamer purification via ethanol precipitation 52

3.2 Optimisation of cell-SELEX for use on primary cells 55

3.2.1 Minimum cell number to return bound DNA aptamers 55

3.2.2 Optimisation of amplification during each round of Cell-SELEX using minimal cell number. 56

3.2.3 Novel DNA aptamer sequences..... 58

3.2.4 Structural determination of aptamer sequences..... 59

3.3.4 Structural determination of aptamer sequences..... 67

3.3.5 Validating identified aptamers against primary cells..... 71

3.4 Identification of DNA aptamers towards EGFRvIII peptide through tailored counter-SELEX. 73

3.4.1 Optimisation of DNA amplification via TD-PCR during 6 rounds of Counter-SELEX 73

3.4.2 Identified novel DNA aptamer sequences, selected towards EGFRvIII.....75

3.4.4 Structural determination of aptamers identified towards EGFRvIII peptide...79

3.4.5 Validation of novel DNA aptamers, targeted towards an EGFRvIII peptide 84

3.5 Identification of DNA aptamers towards PDE1C through tailored counter-SELEX...85

3.5.1 Optimisation of DNA amplification via TD-PCR during 6 rounds of Counter-SELEX 85

3.5.2 Identified novel DNA aptamer sequences, selected towards PDE1C 89

3.5.3 Structural determination of aptamer sequences, selected towards PDE1C ...91

3.5.4 Validation of novel DNA aptamers, targeted towards PDE1C 92

Chapter 4: Discussion.....98

4.1 Discussion.....99

4.2 Producing sensitive and specific cell-SELEX and counter-SELEX procedures 99

4.2.1 Amplification of DNA aptamers by TD-PCR.....100

4.2.2 Purification of DNA aptamers via ethanol precipitation.....101

4.2.3 Utilisation of minimal biological material for aptamer identification 103

4.2.3.2 Minimal amount of protein for aptamer identification 104

4.3 The identification and validation of DNA aptamers towards short-term cultures 105

4.3.1 Aptamers identified towards primary cells.....106

4.3.2 CLL aptamers in comparison to DNA aptamers derived against the U87MG cell line 108

4.3.3 Validating target interaction using aptamers identified towards short term cultures 111

4.3.4 Utilising primary cells to identify novel aptamers 112

4.4 The identification and validation of DNA aptamers towards EGFRvIII peptide. 113

4.4.1 Aptamers identified towards EGFRvIII peptide 113

4.4.2 Validating target interaction using aptamer identified towards EGFRvIII 115

4.4.3 EGFRvIII specific aptamers in glioblastoma therapy 116

4.4 The identification and validation of DNA aptamers towards PDE1C.....116

4.4.1 Aptamers identified towards PDE1C 117

4.4.2 Validating target interaction using aptamer identified towards PDE1C.....118

4.4.3 PDE1C specific aptamers in glioblastoma therapy.....119

4.5 Study limitations 120

4.5.1 Aptamer amplification via PCR.....120

4.5.2 Aptamer-protein interaction via Western blots.....120

4.5.3 Aptamer-protein interaction via oligohistochemistry 121

4.6 Future studies 122

4.6.1 Establishing aptamer binding sites.....122

4.6.2 Establishing aptamer affinity towards protein epitope 123

4.6.3 Establishing aptamer target epitope.....123

4.6.4 Establishing aptamer localisation and enzymatic inhibition.....124

4.6.5 Enhancing the pharmacokinetic profile of aptamers.....125

4.7 Conclusion.....126

Appendix : Miscallaenous aptamer sequences.....- 127 -

Appendix 1: Non-specifc PDE1C aptamer sequences.....- 127 -

References.....- 129 -

Table of Figures

Figure 1.1- Tissue sections of glioma corresponding to cellular lineage and grade. 6

Figure 1.2- Brain, other CNS and intracranial tumour incidence during 2010 in the United Kingdom. 8

Figure 1.3 – The primary, secondary and tertiary structure of RNA and DNA aptamers. 20

Figure 1.4 – Systematic Evolution of Ligands by Exponential Enrichment (SELEX). 24

Figure 2.1 – Map of the pGEX-KG vector transformed in to chemically competent BL21 *E.coli* for the expression of GST. 40

Figure 2.2 – A map of the pCR 2.1 TOPO vector used to ligate aptamers in to, which were subsequently transformed in to chemically competent DH5α *E.coli* and cloned. 43

Figure 3.1 – Comparison of TD-PCR vs. Standard PCR programme and optimising the number of phase two cycles 50

Figure 3.2 – Ratio change of aptamer amplification, using TD-PCR across varied numbers of phase two cycles, in comparison to the standard PCR programme. 52

Figure 3.3 – Comparison of the standard ethanol precipitation protocol with the modified protocol and optimisation of the incubation conditions. 53

Figure 3.4 – Comparison of DNA purification by the standard procedure and the modified procedure, all with varied conditions. 54

Figure 3.5 – Determination of the lowest cell number to return bound aptamer through the use of cell lines. 56

Figure 3.6 – Optimisation of TD-PCR cycle number during 5 iterative rounds of Cell-SELEX using 100 cells. 57

Figure 3.7 – Colony screening for positive aptamer insert into pCR 2.1 plasmids. 58

Figure 3.8 – Predicted secondary structure of novel DNA aptamer sequences selected towards U87MG, determined by MFold software.....60

Figure 3.9 – DNA aptamers following recovery and amplification after each round of Cell-SELEX selection. 61

Figure 3.10 – Colony screening for positive aptamer insertion into pCR 2.1 plasmid. ..62

Figure 3.11 – A phylogram of identified aptamers selected towards BTNW390 and BTNW914 short-term cultures, by Clustal Omega software. 66

Figure 3.12 – Consensus sequences displaying similar bases within familial sequences identified towards short-term cultures, as determined by Clustal Omega software. ...66

Figure 3.13 – Predicted secondary structure of novel DNA aptamer sequences selected towards short-term cell cultures and determined by MFold software. 68

Figure 3.14 – Western blot analysis of native cell lysate from five glioblastoma tissue samples, using biotinylated CLL001(U) and CLL002(U) aptamers. 71

Figure 3.15 – Oligohistochemistry using the biotinylated CLL001(U) and CLL002(U) aptamers to detect aptamer-protein interactions within BTNW390 and BTNW914 tissue sections. 72

Figure 3.16 – Optimisation of the number of TD-PCR phase two cycles following EGFRvIII peptide selection. 74

Figure 3. 17 – Colony PCR screening of chemically competent DH5α *E.coli* transformants for positive aptamer inserts. 75

Figure 3.18 – Phylogram of identified novel aptamer sequences selected towards EGFRvIII peptide, determined by Clustal Omega. 78

Figure 3.19 – Consensus sequences displaying similar bases within familial sequences identified towards primary cultures, as determined by Clustal Omega software. 78

Figure 3.20 – Predicted secondary structure of novel DNA aptamer sense sequences, selected towards an EGFRvIII peptide and determined by MFold software. 80

Figure 3.21 – Western blot analyses of native cell lysate from five *EGFR* amplification positive glioblastoma tissue samples. 84

Figure 3.22 – SDS-PAGE of BL21 *E. coli* cells before and after GST induction. 86

Figure 3.23 – Optimisation of the number of TD-PCR phase two cycles following PDE1C selection. 87

Figure 3. 24 – Colony PCR screening of chemically competent DH5α *E.coli* transformants for positive aptamer inserts. 88

Figure 3.25 – Phylogram of identified novel aptamer sequences selected towards EGFRvIII peptide, determined by Clustal Omega. 90

Figure 3.26 – Consensus sequences displaying similar bases within familial sequences identified towards primary cultures, as determined by Clustal Omega software. 90

Figure 3. 27 – Predicted secondary structure of novel DNA aptamer sequences, selected towards PDE1C and determined by MFold software. 92

Figure 3.28 – Western blot analysis of cell lysate from SVGp12 and U87MG cell lines, using biotinylated XApt004 aptamer. 93

Figure 3.29 – A native Western blot, using cell lysate from SVGp12 (S) and U87MG (U) to show any aptamer-protein binding. 94

Figure 3.30 – Visualisation of aptoprecipitations, utilising biotinylated aptamers to pull out the aptamer target from SVGp12 (A) and U87MG (B) cell lysate. 96

Figure 4.1 – A phylogram grouping CLL aptamers and U87TDM aptamers based on sequence similarities, as determined by Clustal Omega software. 109

Figure 4.2 – Consensus sequences between familial CLL and U87TDM aptamers, determined by Clustal Omega software. 110

Figure 4.3 – Examples of nucleotide modifications to reduce degredation, increase half-life and facilitate functionality. 125

Table of Tables

Table 1.1 – The histological classification of glioma according to The World Health Organisation (WHO), adapted from (Ricard et al., 2012). 4

Table 1.2- Two year survival rates of glioma with respect to age of diagnosis and glioma-type, from 1973-2002. 13

Table 1.3 – SELEX modifications to select aptamers more effectively or of higher quality 25

Table 2.1 – Primer sequences and properties 33

Table 2.2 – Reagents used for amplification of DNA aptamer library 33

Table 2.3 – Touchdown and Standard PCR programmes used for the amplification of the DNA aptamer library. 34

Table 2.4 – The different precipitation protocols and varied temperatures and glycogen concentrations used to optimise DNA precipitation 35

Table 2.5 – Colony PCR programme used to screen for positive aptamer insert..... 44

Table 3.1 – The TD-PCR and standard PCR programmes. 50

Table 3.2 – Aptamer primer sequences and their respective complementary sequence. 58

Table 3.3 – Aptamer and complementary aptamer sequences selected towards the primary cell cultures U87MG. 59

Table 3.4 – Aptamer sequences and complementary sequences selected towards the primary cell cultures BTNW390 and BTNW914. 64

Table 3.5 – Identified novel DNA aptamer sequences selected towards EGFRvIII peptide following 6 rounds of Counter-SELEX. 76

Table 3.6 – Novel DNA aptamer sequences selected towards PDE1C. 89

Table 4.1 – Families of aptamers derived against primary cells, based on sequence similarities as determined by Clustal omega. 106

Table 4.2 – Families of aptamers derived against EGFRvIII peptide, based on sequence similarities as determined by Clustal omega. 114

Table 4.3 – Families of aptamers derived against EGFRvIII peptide, based on sequence similarities as determined by Clustal omega. 117

Acknowledgements

Many thanks to my supervisors; Dr. Clare Lawrence, Dr. Lisa Shaw and Dr. Jane Alder. Their patience, encouragement, knowledge and insight were not only instrumental to the production of this study, but to my own development.

I would also like to acknowledge Kerry. A Rostron, her guidance and knowledge has been essential in producing experimental data and troubleshooting experiments.

A special thanks to Chrissie Woodcocks and Tony Dickson, for their technical help and advice during the course of this study.

We would also like to thank and acknowledge Kate Ashton, Royal Preston hospital (UK) and Brain Tumour North West for providing tissue samples and tissue sections.

List of Abbreviations

ABC	Avidin-biotin complex
Akt	Protein kinase B
AMD	Age-related macular degeneration
AP	Aptoprecipitation
ATCC	American Type Culture Collection
BBB	Blood brain barrier
BCL-2	B-cell lymphoma protein 2
BSA	Bovine serum albumin
cAMP	Cyclic adenosine monophosphate
Cbl	Casitas B-lineage lymphoma
CD133	Promanin-1
CE-SELEX	Capillary electrophoresis systematic evolution of ligands by exponential enrichment
cGMP	Cyclic guanosine monophosphate
CNS	Central nervous system
DAB	3,3'-Diaminobenzidine
ddH_20	Double distilled water
dH_20	Distilled water
DNA	Deoxyribonucleic acid
dNTPs	Deoxyribose nucleoside triphosphates
DPBS	Dulbeccos phosphate buffered saline
E.coli	*Escherichia coli*
ECACC	European Collection of Cell Cultures
EGF	Epidermal growth factor
EGFR	Epidermal growth factor receptor
EGFRvIII	Epidermal growth factor variant III
EGFRwt	Epidermal growth factor receptor wild type
ELISA	Enzyme linked immunosorbant assay

EMEM	Eagles minimal essential medium
Fc	Fragment crystallisable
FDA	Food and Drug Administration
FISH	Fluorescence *in situ* hybridisation
GBM	Glioblastoma
GMBO	Glioblastoma with oligodendroglioma componenet
Grb2	Growth factor receptor bound protein 2
GST	Glutathione S-transferase
H&E	Haematoxylin and eosin
HER2	Human epidermal growth factor 2
HIV	Human immunodeficiency virus
HRP	Horse radish peroxidase
IDH1/2	Isocitrate dehydrogenase 1/2
IDT	Integrated DNA Technologies
IHC	Immunohistochemistry
IPTG	Isopropyl beta-D-1-thiogalactopyranoside
K_d	Disassociation constant
LB	Lysogeny broth
LOH	Loss of heterozygosity
MDM2	Mouse double minute 2
MGMT	O^6-methylguanine-deoxyribonucleic acid methyltransferase
miRNA	Micro ribonucleic acid
MRI	Magnetic resonance imaging
mRNA	Messenger ribonucleic acid
MRPs	Multidrug-resistant proteins
NADPH	Nicatinamide adenine dinucleotide phosphate (NADPH)
NEAA	Non-essential amino acids
NHA	Normal human astrocytes
NHS	N-hydroxysuccinimide
NICE	National Institute for Health and Care Excellence

NOS	Not otherwise specified
PBS	Phosphate buffered saline
PCR	Polymerase chain reaction
PCV	Procarbazine, lomustine, vincristine
PD	Primer dimer
PDE1C	Phosphodiesterase 1C
PDGF	Platelet derived growth factor
PDGFR	Platelet derived growth factor receptor
PDGFRα	Platelet derived growth factor receptor alpha
PDGFRβ	Platelet derived growth factor receptor beta
PEG	Polyethylene glycol
PI3K	Phosphoinositide 3-kinase
PIP_3	Phosphatidylinositol (3,4,5)-triphosphate
ppt	Precipitation
PSMA	Prostate specific membrane antigen
PTEN	Phosphate and tensin homologue
PVDF	Polyvinylidene fluoride
qPCR	Quantitative polymerase chain reaction
Rb	Retinoblastoma protein
RNA	Ribonucleic acid
ROS	Reactive oxygen species
RTKs	Receptor tyrosine kinase
SDS	Sodium dodecyl sulphate
SDS-PAGE	Sodium dodecyl sulphate polyacrylamide gel electrophoresis
SELEX	Systematic evolution of ligands by exponential enrichment
siRNA	Small interfering ribonucleic acid
SPR	Surface plasmon resonance
ssDNA	Single stranded deoxyribonucleic acid
TAE	Tris-base, acetic acid, EDTA
TAR	Trans-activation response

Tat	Trans-activator
TBA	Thrombin binding aptamer
TBST	Tris buffered saline, tween-20
TCGA	The Cancer Genome Atlas
TD-PCR	Touch down polymerase chain reaction
TGF-α	Transforming growth factor alpha
T_m	Melting temperature
TMZ	Temozolomide
TP53	Tumour protein p53
TSGs	Tumour suppressor genes
UV	Ultra-violet
VEGF	Vascular endothelial growth factor
VEGF-A	Vascular endothelial growth factor A
WHO	World Health Organisation

Chapter 1: Introduction

1.0 Introduction

A major challenge in the diagnosis and treatment of cancer is the identification of molecules that recognise cellular and molecular differences between diseased and healthy tissue. With respect to these criteria, aptamers have received high interest ever since they were first described in 1990 (Ellington and Szostak, 1990). Aptamers, regarded as chemical antibodies, are selected through systematic evolution of ligands by exponential enrichment (SELEX); an *in vitro* process that can accommodate various targets such as peptides, proteins and whole cells (Tuerk and Gold, 1990). To date, many aptamers have been selected against cancer, such as breast, liver and prostate cancer (Lupold *et al.*, 2002, Shangguan *et al.*, 2008, Liu *et al.*, 2012). Selective aptamers rely on truncated, defective or overexpressed biomarkers observed within disease state for differential recognition from healthy tissue. For example, the aptamer HB5 targets human epidermal growth factor receptor 2 (HER2), a biomarker specific to breast cancer (Liu *et al.*, 2012).

Glioma is a cancer of the central nervous system (CNS) originating from neuroglia. The utilisation of aptamers to target glioma has been of interest in the last decade, with numerous groups selecting aptamers that offer various biomedical applications, such as diagnostics and biosensors (Song *et al.*, 2008), therapeutics (Bates *et al.*, 2009) including drug delivery (Huang *et al.*, 2009). Although glioma only represent a small percentage of cancer incidences, mortality rates are often high (Schwartzbaum *et al.*, 2006). Currently, diagnosis involves hospitalisation for an invasive biopsy and treatment is non-selective which is usually intolerable in the elderly (Brandes *et al.*, 2009, Weller, 2011).

1.1 Glioma

1.1.1 Classification and grading of glioma

Glial cells are the most common cell type within the central nervous system (CNS). The transformation of these cells leads to invasive tumours forming in the brain called gliomas. Glioma comprises a group of heterogenous tumours derived from

glial progenitor cells, stem cells or de-differentiated cells that are defined by cell lineage, such as ependymal, astrocytic or oligodendrocytic (Ricard *et al.*, 2012). Different types of glioma are matched to a grade (I – IV) via the World Health Organisation (WHO) classification system (Louis *et al.*, 2007). The grade allocated to each tumour type is dependent on histological criteria which corresponds to severity (benign grade I – malignant grade IV), facilitates diagnosis and predicts prognosis (Louis *et al.*, 2007, Ricard *et al.*, 2012).

During histological examination, the morphology of the tissue is examined and abnormalities representative of glioma are noted (Table 1.1) (Ricard *et al.*, 2012).

Table 1.1 – The histological classification of glioma according to The World Health Organisation (WHO), adapted from (Ricard et al., 2012).

	Grade	Histological subtype	Phenotype	Grading						Median Survival (Years)
				Differentiation	Cell density	Nuclear atypia	Mitotic activity	Microvascular proliferation	Necrosis	
Astrocytoma	Grade II	Diffuse astrocytoma	Fibrillary or gemistocytic neoplastic astrocytes	Well differentiated	Moderate	Occasional	Generally absent	Absent	Absent	6 - 8
	Grade III	Anaplastic astrocytoma	Same as grade II	Regional or diffuse anaplasia	Regionally	Present	Present	Absent	Absent	3
	Grade IV	Glioblastoma	Pleomorphic astrocytic tumour cells	Poor	High	Marked	Marked	Prominent	Present	1 - 2
Oligodendroglioma	Grade II	Oligodendroglioma	Monomorphic cells, uniform round nuclei, perinuclear halos	Well differentiated	Moderate	Possibly marked	Absent or occasional	Not prominent	Rare	12
	Grade III	Anaplastic oligodendroglioma	Same as grade II	Regional or diffuse anaplasia	Increased	Marked	Prominent	Often prominent	Possible	3 - ≥10
Oligoastrocytoma	Grade II	Oligoastrocytoma	Neoplastic glial cells with both phenotypes	Well differentiated	Moderate	Occasional	Rare	Absent	Absent	6
	Grade III	Anaplastic oligoastrocytoma	Same as grade II	Anaplasia	High	Marked	High	May be present	Absent	3

GMBO = Glioblastoma with Oligodendroglioma component

The qualitative assessment of mitosis, cellular density, tumour differentiation and the presence of blood vessels predict the aggressiveness of the cancer (Louis *et al.*, 2007, Ricard *et al.*, 2012). As the grade increases, morphological features observed in glioma become more exaggerated (Fig 1.1). Grade I, such as pilocytic glioma present with little proliferation, are well differentiated and are generally curable by resection (Louis *et al.*, 2007). Grade II, such as diffuse astrocytoma or oligodendroglioma, are infiltrative neoplasms with low proliferation which are well differentiated (Louis *et al.*, 2007). Associated with grade II tumours are high rates of recurrence, this is caused by the infiltrative nature of the tumour in to the surrounding tissue with unpredictable growth patterns (Duffau, 2013, Ellenbogen *et al.*, 2013). Anaplastic grade III gliomas are malignant neoplasms with abnormal proliferative behaviour that display hyperchromatism and pleomorphic cellularity (Engelhard *et al.*, 2002, Reifenberger and Collins, 2004, Louis *et al.*, 2007). Grade IV malignant glioma features prominent proliferation and evidence of necrosis (Louis *et al.*, 2007). Glioblastoma (GBM), an astrocytic grade IV tumour, can arise as a direct transformation from astroglia cells (primary or *de* novo) or indirectly (secondary), progressing from benign grade II through to malignant grade IV (Wen and Kesari, 2008). GBM incur high rates of recurrence and are often fatal. Glioma stem cells or de-differentiated cells present in GBM are liable to genotypic evolution after therapy, resulting in therapeutic resistance (Salmaggi *et al.*, 2006, Bao *et al.*, 2006, Schwartzbaum *et al.*, 2006). Many characteristics are shared between different histological sub-types, however some are specific to tumour type, such as the appearance of perinecrotic palisading in glioblastoma (Weller, 2011) (Figure 1.1D).

The validity of the WHO classification system has been questioned due to varied interobserver reliability (van den Bent, 2010). Morphological classification is subjective and is therefore liable to observational error, reducing reproducibility (Ricard *et al.*, 2012). Efforts in the last decade have been focused towards producing a classification system based on molecular aberrations. This would provide a standardised system which is more reproducible (further discussed in Section 1.1.3).

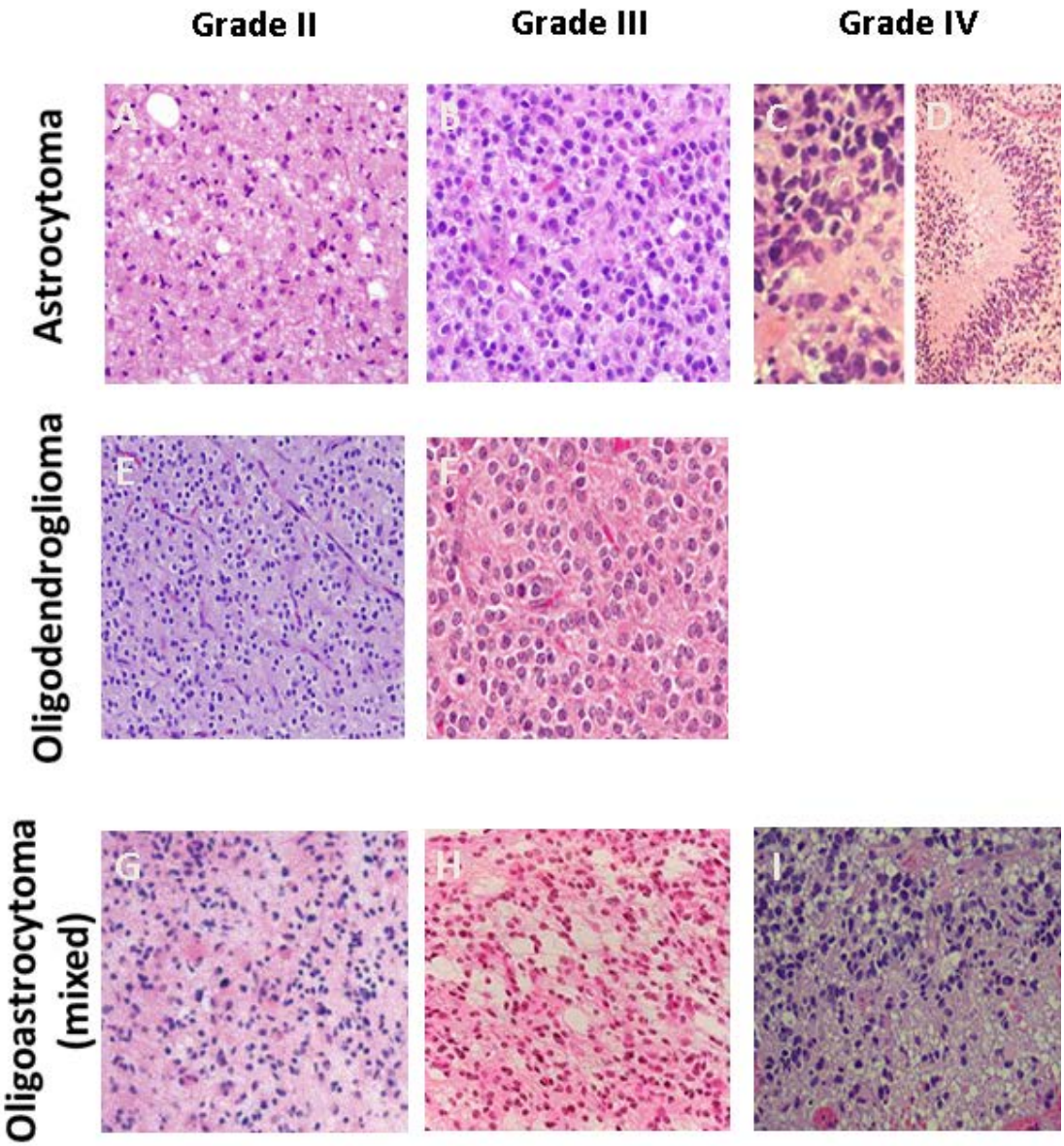

Figure 1.1- Tissue sections of glioma corresponding to cellular lineage and grade. The tissue sections show the morphology of astrocytoma (A-D), oligodendroglioma (E and F) and oligoastrocytoma (G-I), which are of differing grade. As the grade increases, the degree of abnormal cellularity and nuclear atypia increases. Some characteristics are specific to cell lineage due to their phenotype, such as the uniform round cells observed in oligodendrogliomas (E and F). Other features are specific to tumour type, such as perinecrotic palisading in glioblastoma (D) or the 'honeycomb' effect as seen in anaplastic oligodendroglioma (F). Figure adapted from (Cavaliere *et al.*, 2005, Salvati *et al.*, 2009, Martens *et al.*, 2013)

1.1.2 Epidemiology

Globally collated evidence shows there are several epidemiological factors predisposing individuals to glioma, such as sex, age, ethnicity, exposure to radiation and inherited mutations (Bondy *et al.*, 2008). Each year there is an estimated 6.3 cases of primary brain cancer per 100,000 population worldwide (Bondy *et al.*, 2008), with glioma accounting for approximately 80% of all brain tumour cases (Ohgaki, 2009). Incidences are higher in developed countries (9.9 cases compared per 100,000 population) compared to undeveloped countries (5.1 cases per 100,000 population) (Ohgaki, 2009). The large variation may be explained by inadequate detection in underdeveloped regions or by ethnicity, as Caucasians are twofold more likely to develop glioma than people of African or Asian descent (Fan and Pezeshkpour, 1992). Nevertheless, this requires further investigation in order to prevent under-observation of incidences.

Males are more likely to develop malignant brain tumours than females, who are more likely to develop benign tumours (Ostrom *et al.*, 2013). In the UK during 2010 (Fig 1.2), 34% of brain, CNS and intracranial tumours were astrocytomas, of which 80% were glioblastoma (GBM); a highly aggressive astrocytoma more prevalent in men. Worldwide data shows that the majority of GBMs are primary (90%) with a higher tendency to develop in men (1.33 male:female ratio) (Ohgaki and Kleihues, 2007, Ohgaki and Kleihues, 2005). In contrast to the aggressive malignant primary sub-type, secondary tumours are less aggressive with higher incidence in females (0.66 male:female ratio) (Ohgaki and Kleihues, 2005). Epidemiological information regarding glioma in the United Kingdom (UK) has been criticised due to under-recording of cases, with records currently lacking detailed information on the incidence of different tumour types (Chalmers, 2011). Consequently there is no definitive epidemiological data regarding primary or secondary GBM, possibly due to the differential tumour genotypes often displaying no phenotypical differences, therefore being histologically indistinguishable (Ohgaki and Kleihues, 2007). In addition, Ohgaki observed that the majority of GBMs diagnosed in the US are primary or *de novo* tumours. This is because the initial diagnosis is recorded and not the tumour grade where it has progressed from grades I to IV, which can happen with secondary GBMs.

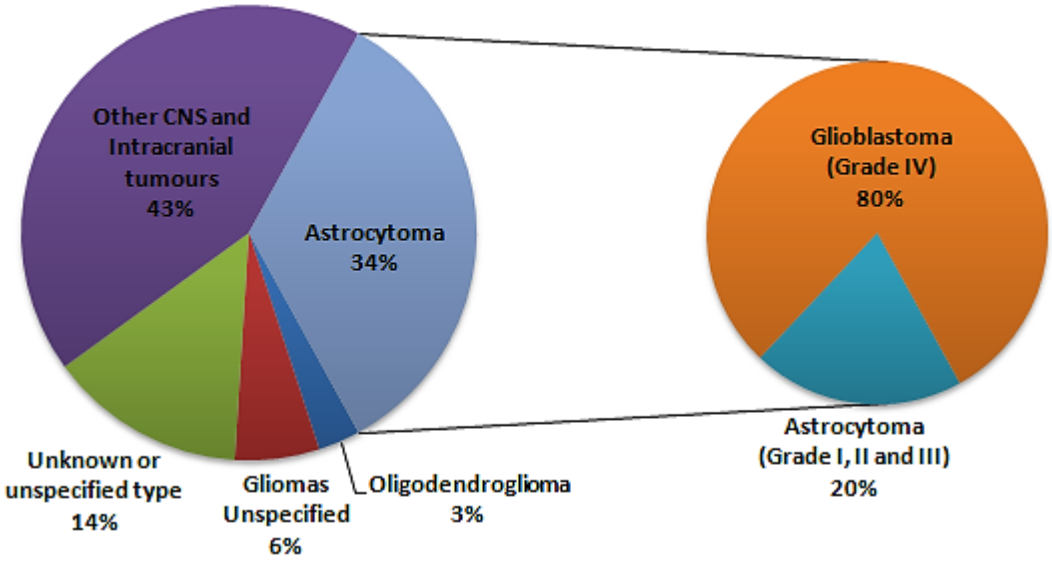

Figure 1.2- Brain, other CNS and intracranial tumour incidence during 2010 in the United Kingdom. Adapted using statistics provided by Cancer Research UK (CRUK, 2014)

Primary or *de novo* GBM appear within weeks often without presenting any clinical signs, in contrast secondary GBM tumours progress from benign grade I through to malignant grade IV GBM (Ohgaki and Kleihues, 2007). Primary GBM mortality rates are high in comparison to secondary tumours, with median survival rates of 4.7 months and 7.8 months respectively (Ohgaki *et al.*, 2004). The varied clinical features of both primary and secondary GBM can be explained by dysregulated signal transduction pathways which contribute to gliomagenesis. Mutated epidermal growth factor receptor (EGFR) and phosphate and tensin homologue (PTEN) are indicative of primary GBM, wereas isocitrate dehydrogenase 1 and 2 (IDH1/2) mutations are indicative of secondary GBM (Goodenberger and Jenkins, 2012). Both routes to gliomagenesis may also converge to vascular endothelial growth factor (VEGF) mutations for angiogenesis.

1.1.3 Aetiology

Indeed, no single mutation will ensure the transformation of a cell from healthy to cancerous. Instead a set of mutations must be present to guarantee cancer cell survival by preventing apoptosis and enhancing proliferation. In 1940, Hans-Joachim Scherer noticed a clear distinction between primary and secondary glioblastoma which was based upon clinical presentation (Peiffer and Kleihues, 1999). Unknown to him,

differences in clinical presentation was caused by expression of different sets of aberrant proteins, which have since been elucidated. Gliomagenesis may occur when proteins important to the regulation of cellular pathways become abnormally expressed or truncated. Gain and loss of function mutations within proto-oncogenes and tumour suppressor genes (TSGs) can be observed throughout each glioma grade; however each grade may confer a unique set of mutations in order to become biologically immortal.

1.1.3.1 Tyrosine Receptor Kinases (RTKs)

The receptor tyrosine kinase (RTK) pathway is activated in 88% of glioma tumours, with mutations occurring in the RTK receptor and downstream signalling components. RTKs are a superfamily of transmembrane proteins involved in signalling to the cell when to proliferate. Upon interacting with growth factors, a conformational change results in the activation of kinases within the intracellular domains of the receptor. Subsequently, other proteins, such as Ras and phosphoinositide 3-kinase (PI3K) are recruited and the cell initiates proliferation. Over-expressed or truncated RTKs, such as platelet derived growth factor receptor (PDGFR) and epidermal growth factor receptor (EGFR) may result in the dysregulation of cellular proliferation. In addition mutations must also be present in TSGs that regulate the activation of downstream mediators, such as PTEN, p53 and retinoblastoma protein (Rb).

EGFR is an RTK that may play an important role in gliomagenesis. Epidermal growth factor (EGF) can bind to a homodimer of EGFR resulting in allosteric transphosphorylation of the receptor between the intracellular kinase domains (Zhang *et al.*, 2006). Downstream mediators are then recruited to the tyrosine kinases and the subsequent phosphorylation of the recruited proteins induces proliferative pathways and represses anti-apoptotic mechanisms. The most common mutation seen in glioma is the amplification of the *EGFR* gene. Low levels of *EGFR* repeats are often seen within chromosome 7. Higher levels of gene amplification are usually observed when *EGFR* copies exist in extrachromosomal double minutes (dmins) (Vogt *et al.*, 2004). *EGFR* copies can be as high as 100 in extreme cases, which translate to the over-expression of EGFR (Lopez-Gines *et al.*, 2010). Glial cells are not capable of producing EGF,

however they may produce transforming growth factor alpha (TGF-α), another EGFR activator. This growth factor initiates similar effects to EGF and, as both receptor and ligand are produced by the cell, an autocrine loop is produced initiating proliferative behaviour further (von Bossanyi *et al.*, 1998). The amplification of *EGFR* is noted to occur in 36% of primary glioblastomas and 8% of secondary glioblastomas (Ohgaki *et al.*, 2004). A second mutation of *EGFR* is seen in 75% of cases exhibiting *EGFR* amplification, known as EGFR variant III (EGFRvIII) (Sugawa *et al.*, 1990).

EGFRvIII is a constitutively active receptor independent of ligand interaction that is co-expressed with the wild type receptor (EGFRwt) (Ge *et al.*, 2002). A rearrangement of the *EGFR* gene results in the deletion of exons 2-7. The amino acids 6-273, usually present in the extracellular domain, are therefore lost producing a truncated EGFR that is constantly active (Prigent *et al.*, 1996). Under the influence of growth factor binding, EGFRwt dimerises and the intracellular kinase domains become activated (Zhang *et al.*, 2006). Initially, it was thought that the truncated EGFRvIII did not dimerise and propagated intracellular signalling in monomeric form (Chu *et al.*, 1997, Gajadhar *et al.*, 2012). The absence of a ligand binding site on the oncogenic protein further supported this theory, as the binding site was instrumental for dimerisation. Later studies showed monomeric EGFRvIII to have no activity and therefore conferred no tumorigenicity, implying the protein must dimerise in order to signal to the cell (Kancha *et al.*, 2013). EGFRvIII possesses the ability to either homodimerise with another EGFRvIII protein or heterodimerise with the wild type version (Gajadhar *et al.*, 2012, Luwor *et al.*, 2004). Within the heterologous version, EGFRvIII activates EGFRwt independent of its ligand through transphosphorylation, furthering the tumorigenic potential of this oncogenic protein (Fan *et al.*, 2013). Post-signal transduction, RTKs are normally internalised quickly and ubiquitinated ready to be degraded to prevent prolonged signals. The ubiquitin ligase enzyme Cbl is usually recruited to the EGFR receptor following signal transduction; however if the Cbl-EGFRvIII interaction is perturbed, it can lead to prolonged proliferative signalling. Cbl can internalise the EGFRvIII directly, through the phosphorylation of the amino acid Y^{1045}, or indirectly, through the adapter protein Grb2 (Davies *et al.*, 2006, Waterman *et al.*, 2002). Hypophosphorylation of Y^{1045} on EGFRvIII leads to poor internalisation and, rather than

lysosomal degradation, the receptor is recycled in the cytoplasm and re-expressed on the cell surface (Grandal *et al.*, 2007). Poor internalisation of the constantly active receptor and improper degradation enhances the oncogenic potential of EGFRvIII, leading to prolonged signal transduction and an increased half-life within the cell. EGFRvIII is not expressed in non-cancerous cells therefore is a potential target for selective therapy to cancer cells. Antibodies have been produced against EGFRvIII, however many cross react with the EGFRwt (Gupta *et al.*, 2010).

Glial cells can produce platelet derived growth factor (PDGF), which is required for differentiation of glial cells and also promotes proliferation. PDGFR is produced by the dimerisation of PDGFRα and PDGFRβ, either homogenously or heterogeneously (Lokker *et al.*, 2002). PDGF and PDGFR (specifically PDGFRα) is overexpressed in low-grade astrocytomas and oligodendrogliomas, and the PDGFRα genes are amplified in 10% of secondary glioblastomas (Ohgaki *et al.*, 2004, Karcher *et al.*, 2006). The overexpression of both ligand and receptor produces an autocrine loop resulting in recurrent proliferation.

One feature almost exclusive to primary glioblastoma is the production and secretion of vascular endothelial growth factor A (VEGF-A) (Karcher *et al.*, 2006). When secreted, the growth factor binds VEGF receptors located on surrounding epithelial cells which induces angiogenesis. The integration of blood vessels in to the tumour provides the cancer with its own blood supply, allowing the uptake of nutrients and a way of metastasising to other areas of the body.

1.1.3.2 Oncogenes and Tumour Suppressor Genes (TSGs)

Whilst RTK signalling may signal to proliferate, downstream mediators may become active to deminish the proliferative signal or to stop it all together. Therefore mutations must occur in downstream mediators to allow the signal to fully instigate proliferation. During RTK signalling, phosphatidylinositol (3,4,5)-trisphosphate (PIP_3) is phosphorylated which propagates the proliferative activity of PI3K and Akt. PIP_3 is normally regulated by the phosphatase activity of PTEN, however loss of function mutations within this tumour suppressor gene will leave the proliferative activity

unchecked and the cell liable to become cancerous (Dahia, 2000). Not only are PTEN mutations commonly seen in primary GBMs, but complete removal of the PTEN gene is also common due to loss of heterogeneity in chromosome 10, at the P arm (LOH 10p).

TP53 point mutations are present in 70% of secondary glioblastomas and 30% of primary glioblastomas. Loss of heterozygosity (LOH) mutations prevents TP53 from carrying out functions which include DNA repair and apoptosis. Mutations can be found throughout this pathway and are not just confined to the TP53 protein. Amplification of *MDM2* and LOH mutations in $p14^{ARF}$ further dysregulate the TP53 DNA repair pathway. Mdm2 is involved in TP53 ubiquitination and subsequent degradation. Higher levels of the protein due to gene amplification will see intracellular levels of TP53 diminish. Mdm2 is subject to regulation by $p14^{ARF}$, however LOH mutations and point mutations make $p14^{ARF}$ redundant and consequently leave Mdm2 to bind and degrade TP53.

A novel aberration that has recently been implicated in glioblastoma is the over-expression of phosphodiesterase 1C (PDE1C). Although little work has been produced on glioma, PDE1C has been implicated in other cancers, such as malignant melanoma and osteosarcoma (Ahlstrom *et al.*, 2005, Shimizu *et al.*, 2009). PDE1C hydrolyses the second messengers cyclic adenosine monophosphate (cAMP) and cyclic guanosine monophosphate (cGMP). The subsequent modification of these cyclic nucleotides has been implicated in cell proliferation in other cell types (Rybalkin *et al.*, 2002). In relation to glioma, over-expression of PDE1C was first observed in the immortalised human glioblastoma cell lines SNB75 and SF295 (Vatter *et al.*, 2005). Whilst over-expressed PDE1C was detected, this did not produce any increases in cyclic nucleotide hydrolisation, therefore the authors concluded that PDE1C may not be an appropriate target for therapeutics. These results may have been caused by the glioblastoma cells being immortalised, resulting in genotypic changes and loss of functionality. In contrast, previously published data showed a 40% decrease in proliferation when short term cultures were treated with PDE1C siRNA and therefore, PDE1C may confer a potential therapeutic target (Rowther *et al.*, 2012). Additionally, a study using glioblastoma stem cell lines and data from the cancer genome atlas (TCGA) also

showed higher PDE1C expression correlated with shorter survival following surgery (Engstrom *et al.*, 2012).

1.1.4 Prognostic factors

Various factors impact whether a patient with glioma will successfully enter remission or relapse. Age, tumour grade and locale, treatment regime and the presence of certain molecular characteristics are all prognostically relevant. When taken in to account, these factors can be used to predict the outcome and probability of survival.

The chances of the patient surviving decreases as the grade of the tumour increases, because high grade tumours infiltrate surrounding tissue extensively making complete surgical resection difficult, acquire more mutations than lower grade glioma selective for cell survival and are more likely to develop resistance to treatment. For instance, patients with grade II diffuse astrocytomas have a 50% chance of surviving 5 years where as patients with grade IV glioblastoma have a 5% chance of surviving the same length of time (Ostrom *et al.*, 2013). Most survival rates decrease with the age of the patient, with the elderly having the worse prognosis (table 1.2) (Schwartzbaum *et al.*, 2006). This is most likely due to poor tolerance of therapy associated side effects compared to younger patients.

Table 1.2- Two year survival rates of glioma with respect to age of diagnosis and glioma-type, from 1973-2002.

Age of diagnosis (Years)	**Anaplastic astrocytoma** (Grade III)	**Astrocytoma (NOS)** (Grade I – II)	**Anaplastic oligodendroglioma** (Grade III)	**Oligodendroglioma** (Grade II)	**Glioblastoma** (Grade IV)	**Other (NOS)**
<20	59%	81.8%	N/A	88.8%	27.9%	53.1%
20-44	71.4%	76%	76.5%	92.3%	29.8%	68.6%
45-54	44%	41.3%	62.8%	83.7%	11.6%	38.6%
55-64	19.4%	20%	51.2%	67.1%	6%	26%
65-74	6.4%	9.1%	29.5%	50.9%	2.7%	12.7%
75+	4.1%	5.8%	4.9%	33.3%	1.4%	6.9%

NOS – Not otherwise specified. Adapted from Schwartzbaum, et al. (2006)

The location of the tumour also has an impact on the survival of the patient. Patients with glioma located in the parietal lobe are less likely to survive than those patients with glioma located in the frontal, temporal or occipital lobe of the brain (Ostrom *et*

al., 2013). Although the reasons for this are currently unknown, tumours within the parietal lobe are twice as likely to be malignant than benign and may represent a location where glioblastoma is more likely to occur (Sanai *et al.*, 2012).

Genetic alterations may also inform the clinician how the malignancy will respond to treatment. Promoter methylation of the O^6-methylguanine-DNA methyltransferase gene (*MGMT)* is a positive prognostic indicator during chemotherapy and radiotherapy. MGMT is responsible for DNA repair, reversing the alkylation of guanine at the 0^6 position. Methylation of the MGMT promoter silences the *MGMT* gene, preventing DNA repair, hence cytotoxicity and apoptosis is instigated in glioma patients administered alkylating agents, such as temozolomide (TMZ). Although promoter methylation is widely seen in grade II and grade III gliomas, hypermethylated 5`CpG islands are only observed in grade IV glioblastoma.

Other prognostic factors include the co-deletion of the p arm of chromosome 1 and q arm of chromosome 19 (1p/19q) and IDH1/2 function loss. Brandes *et al.,* studied TMZ chemotherapy, and in the presence of LOH 1p/19q, they found patients with grade II or III oligodendrogliomas and oligoastrocytomas to survive longer (Brandes *et al.*, 2006). This was further corroborated during another study, however both noted that the loss of one allele did not confer any survival advantage (Kouwenhoven *et al.*, 2006). IDH1 and 2 are enzymes important to the process of hydrolysing nicotinamide adenine dinucleotide phosphate (NADPH). In combination with glutathione, NADPH is used to remove reactive oxygen species (ROS) that can result in cellular toxicity (Rusyn *et al.*, 2004). Radiotherapy is much more effective in the presence of IDH 1/2 mutations (Okita *et al.*, 2012), as the ROS produced by ionising radiation is left to damage the cancerous cells and induce apoptosis. The IDH1 R132H mutation occurs most frequent, present in 93% of gliomas (Hartmann *et al.*, 2009); glioblastoma patients with this mutation survive 12 months longer than those with a functional IDH1 wild type gene (Lewandowska *et al.*, 2014).

1.1.5 Diagnosis

Glioma is suspected after a clinical history of seizures, limited vision and/or severe headaches that may induce vomiting (Weller, 2011). Diagnosis of a suspected case involves the collaboration of multiple disciplines, including radiology to confirm a suspected lesion, histology to determine cellularity and morphology and molecular analysis to determine the tumour grade.

Diagnosis begins with an MRI confirmed intracranial mass, which is biopsied and analysed histologically. Histological examination using haematoxylin and eosin (H&E) is routinely performed on all tissue sections; biopsied tissue sections displaying nuclear atypia, perinuclear halos and mitotic bodies are indicative of cells that are biologically immortal (Weller, 2011). Elucidated morphological characteristics are cross referenced with the WHO classification (table 1.1) to determine the tumour subtype. Immunohistochemistry (IHC) using antibodies specific to biomarkers present on the cell surface may also provide information towards diagnosis (Preusser *et al.*, 2008). Qualitative assessment of MGMT, EGFR and IDH1 expression using monoclonal antibodies may assist diagnoses. A R132H variation of IDH1 is seen in 93% of glioblastoma cases and is therefore an ideal target for IHC (Hartmann *et al.*, 2010). Although IHC can be effective inter-observer variability can be an issue, which is most likely due to variations in staining intensity.

In conjunction with histology, molecular analysis by fluorescence *in situ* hybridisation (FISH) and quantitative polymerase chain reaction (qPCR) may be performed (Masui *et al.*, 2012) to quantify genetic aberrations indicative of glioma sub-types, some of which were discussed in section 1.1.3.

1.1.6 Current treatment

Glioma treatment is tailored individually, as there are many factors that impact how the patient will respond. Treatment regimens include surgery, radiotherapy and chemotherapy with each modality tailored to tumour size, tumour location, patient age and molecular prognostic factors.

1.1.6.1 Surgery

Surgery is performed with the aim of debulking the tumour. Complete resection is usually not accomplishable because of the diffuse and invasive nature of glioblastoma. In a study of 416 patients who underwent glioblastoma resection, a significant survival advantage (median 13 months) was observed where ≥ 98% of the tumour was extracted compared to resections under 98% (median 8.8 months) (Lacroix *et al.*, 2001).

Brain surgery carries inherent risks as any degree of error can result in detrimental effects to autonomic and somatic processes. Although surgery decreases morbidity, surgery near areas of the brain responsible for autonomic processes is risky, especially when considering the invasiveness of the tumour to the surrounding tissue (Demuth and Berens, 2004). Surgery may not even be considered if the tumour has invaded certain areas, such as the brain stem or the corpus callosum. Only palliative care may be appropriate in these instances; however, targeted therapeutic approaches that are able to be delivered systematically may provide better outcomes.

1.1.6.2 Radiotherapy

Radiotherapy is the use of ionising radiation to damage DNA. DNA repair mechanisms initiate apoptosis when cellular toxicity is reached. Cells undergoing proliferation are more sensitive to radiation; causing the cancerous cells to incur irreversible DNA damage. The treatment is administered in small fractions (1.8-2 Gy) equating to a 60 Gy dose. Small doses give the surrounding healthy tissue adequate time to recover from any non-specific damage. The overall dose is reduced to 40 Gy when treating patients over 70 years old as it is better tolerated (Weller, 2011). Tumours exhibiting TP53 (loss of function) mutations are less sensitive to radiotherapy as programmed cell death is initiated less frequently (Yount *et al.*, 1996).

Radiotherapy following surgery has been shown to give patients a better chance of survival (Stupp *et al.*, 2005), however radiotherapy may cause adverse reactions, including secondary cancers and impaired memory loss amongst others (Newhauser and Durante, 2011, Surma-aho *et al.*, 2001). Cancerous cells are liable to

radioresistance, prompting glioma stem cells to express CD133 or Prominin-1 as a consequence of radiotherapy (Bao *et al.*, 2006). Upon radiation induced DNA damage, Prominin-1 will halt proliferation and repair any damage caused (Bao *et al.*, 2006). Wang *et al.,* showed that the Notch signalling pathway is needed for glioma radioresistance to occur. The pathway is needed for cell maintenance and cell-to-cell communication, and upon Notch inhibition, the cells were re-sensitised to radiation. The lack of selectivity produces inherent therapy associated side effects; moreover radiotherapy may leave residual cells behind that are resistant to ionising radiation.

1.1.6.3 Chemotherapy

As part of the National Institute for Health and Care Excellence (NICE) guidelines for glioma treatment, chemotherapy such as procarbazine, lomustine, vincristine (PCV), temozolomide (TMZ) and carmustine implants are implemented as an adjunct to radiotherapy (NICE, 2007). Chemotherapeutic agents, such as temozolomide, alkylate guanine nucleotides and upon cellular toxicity, apoptosis occurs (Wen and Kesari, 2008). Cancerous cells are more sensitive to chemotherapies because of their increased proliferative activity.

Carmustine wafers are biodegradable implants that are placed within the resected area of the brain following surgery. By directly placing the wafers within the resected cavity, the blood brain barrier (BBB) is bypassed and carmustine is directly released to target residual cancerous cells. Whilst the technology was approved for use in the UK, glioblastoma patients treated with carmustine implants did not exhibit a significant overall survival advantage when compared to the placebo group (NICE, 2007). Instead, a sub-group with 90% of the tumour excised, was identified with an overall survival gain of 4.2 months.

TMZ is an alkylating agent administered cyclically for 42 days with adjuvant radiotherapy. Higher doses are administered without radiotherapy for 5 days followed by a 23 day break. Six cycles are administered, during the second and subsequent cycles TMZ can be given at higher doses upto 200mg/m^2 (NICE, 2007). Using the treatment regime described, Athanassiou *et al.,* showed patients with glioblastoma

survived longer when treated using TMZ combined with radiotherapy (13.4 months), in contrast to radiotherapy alone (7.7 months) (Athanassiou *et al.*, 2005). In contrast, another study noted that > 60% patients do not gain any benefit from TMZ, although 20% develop significant toxicity (Chamberlain, 2010).

During tumour reoccurrence, combinatorial treatment PCV is part of the first line treatment. Whilst it is standard practise, the effectiveness of PCV has shown to be poor and does not confer any significant survival advantage (NICE, 2001). The same conclusion has been corroborated in subsequent studies, which also found haemotoxicity commonly occurred in 26% of patients (Kappelle *et al.*, 2001, Schmidt *et al.*, 2006). Subsequently, TMZ has been recommended as an alternative to PCV and has been shown to have better outcomes, with respective progression-free survival rates of 21% compared to 8% respectively (NICE, 2001).

All of the aforementioned drugs may cause unwanted side effects and could potentially make recurrent tumours more difficult to treat. Chemotherapeutics cause collateral damage as labile cells are more sensitive to these drugs. Rapidly dividing cells such as white and red blood cells, hair cells and skin cells are particularly susceptible to toxicity (Weller, 2011). Chemotherapeutic drugs have also been associated with multidrug-resistant proteins (MRPs) being over-expressed and TMZ therapy can result in *MGMT* promoter activation (Salmaggi *et al.*, 2006, Sarkaria *et al.*, 2008). Higher expression of MRPs have been found to occur in glioblastoma stem cells as a consequence of chemotherapy making reoccurring tumours harder to treat (Salmaggi *et al.*, 2006). TMZ may cause the *MGMT* promoter to be demethylated, resulting in increased production of the MGMT DNA repair protein. MGMT will remove alkyl groups from guanine nucleotides in response to TMZ and is thought to be a major protein involved in chemoresistance (Sarkaria *et al.*, 2008). Aptamers have been proposed as a targeting system that could deliver chemotherapeutic drugs specifically to cancerous cells, which would help reduce unwanted systemic side effects as well as reducing resistance if higher concentrations of drug could be delivered to the site of action.

1.2 Aptamers

1.2.1 History of Aptamers

During the 1980's, studies into the replication of HIV-1 and adenoviruses revealed short regulatory RNA sequences that interacted with specific proteins. For example, a 59 base sequence known as the trans-activation responsive (TAR) element precedes HIV-1 genes. TAR produces a tertiary structure that specifically interacts with the trans-activator (Tat) of HIV; a protein required for efficient transcription of HIV-1 genes and consequently, HIV-1 replication (Dollins *et al.*, 2008). These studies revealed that short sequences of nucleic acids could interact with and affect the function of proteins.

In 1990, the first organic aptamers were independently produced by two different groups, Ellington and Szostak, and Turk and Gold. Ellington and Szostak coined and defined the term aptamer, a short sequence of RNA or single-stranded DNA (ssDNA) selective to a target molecule (Ellington and Szostak, 1990). Ellington and Szostak selected RNA aptamers from a pool of 10^{13} unique sequences towards two chemically similar dyes. Although the dyes were similar in structure, they found that the sequences were specific towards the dye they were selected for and did not cross react. It was therefore demonstrated that aptamers were able to differentiate between similar targets. During Tuerk and Gold's study, RNA aptamers were selected from a pool of 65,000 unique sequences derived from a wild-type sequence already known to interact with the target. It was noted that selected sequences were structurally similar to the wild-type and the synthetic aptamers disassociation constant (K_d) was similar to the wild-type. As well as showing aptamers selected synthetically were just as good as those selected by nature, Tuerk and Gold pioneered the simple methodology which can be applied to select specific aptamers to a target. They coined this process Systematic Evolution of Ligands by Exponential Enrichment (SELEX) (Tuerk and Gold, 1990).

1.2.2 Structure and function

Aptamers have the ability to distinguish between proteins that are 96% similar and this allows for aptamers to be selected towards analogous proteins with high selectivity

and affinity. This trait is a consequence of the tertiary structure that the short nucleotide sequence conforms to (Fig 1.3). Secondary structures are defined by either Hoogsteen base pairing or Watson-Crick base pairing. Figure 1.3A shows the secondary structure of an RNA aptamer abiding by Watson-Crick complementation, where adenine pairs uracil (or thymine in DNA) and cytosine pairs guanine. Figure 1.3B shows the secondary and tertiary structure of a DNA thrombin binding aptamer (TBA), the secondary structure produced is a result of Hoogsteen complementation. Hoogsteen base pairing is the hydrogen bonding at the N^7 position of the purines; this is in contrast to the N^3 or N^4 position which occurs in Watson-Crick base pairing. The change in position means that very stable guanine-quadruplexes are able to form in sequences that are guanine-thymine rich.

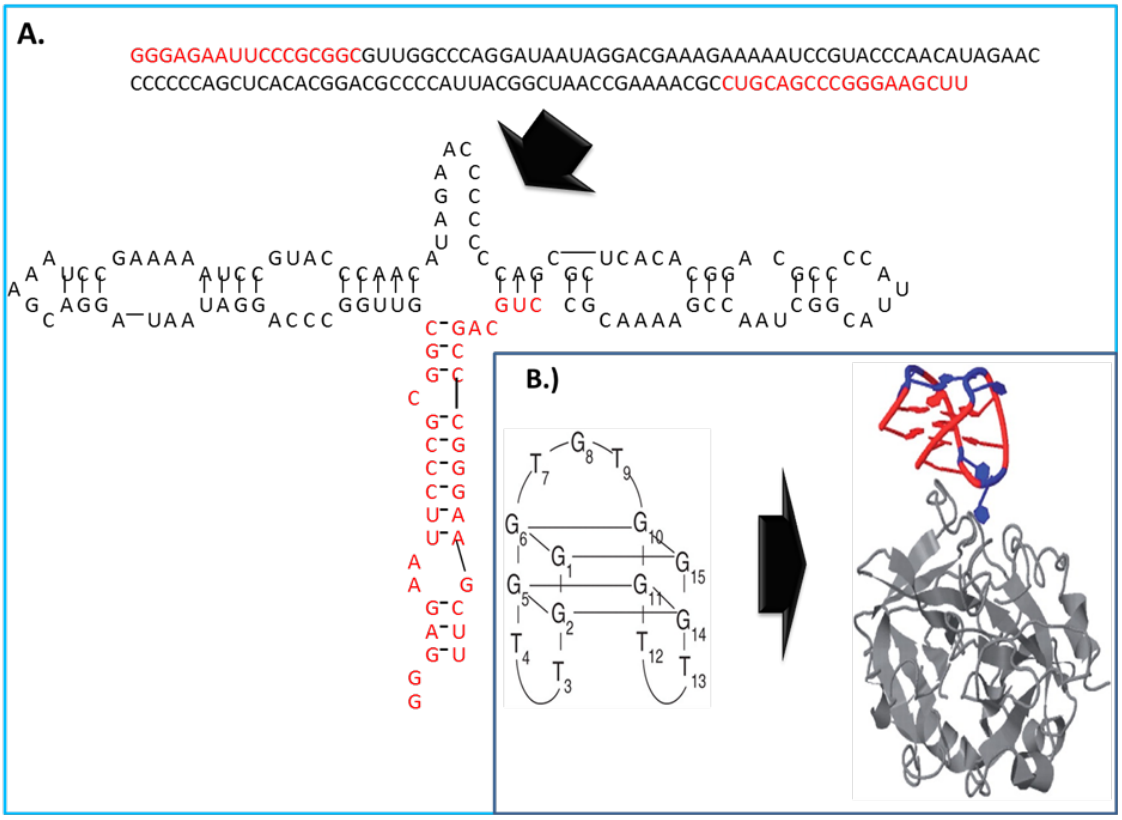

Figure 1.3 – The primary, secondary and tertiary structure of RNA and DNA aptamers. A: The primary and secondary structure of a 95mer RNA aptamer selected against Reactive Blue 4 dye. The secondary structure is created through Watson-Crick base pairing, primer regions are shown in red (Ellington and Szostak, 1990). B: The secondary and tertiary structure of a 15mer DNA aptamer selected against α-thrombin. The secondary structure is produced by Hoogsteen base pairing which subsequently fosters guanine-quadruplexes. The tertiary structure shows how the aptamer (red) interacts with the α-thrombin (grey). Figure adapted from Pasternak *et al,* (2011).

The tertiary structure of the aptamer is based on weak electrostatic interactions such as hydrogen bonding, Van der Waals forces and base stacking between adjacent aromatic residues (Mayer, 2009). Whilst many nucleotides will pair in any given aptamer sequence, those that are left unpaired produce stem loops containing potential binding sites (Duconge and Toulme, 1999). Hydrogen bonding and Van der Waal interactions are necessary for the aptamer binding to the target, which can only occur when stem loops containing unpaired nucleotides are present (Mayer, 2009). Protein targets with enzymatic functions bind substrates through weak electrostatic interactions. Consequently aptamers interact with the enzymatic active site through the same interactions in which the substrate would, blocking the substrate from binding, and hence are capable of inhibiting activity (Lin and Jayasena, 1997, Ikebukuro *et al.*, 2007, Townshend *et al.*, 2010, Simmons *et al.*, 2014).

The identification of specific DNA aptamers has been favoured over RNA aptamers, as they are more stable and cost-effective. As well as thymine being replaced by uracil, RNA has a 2' hydroxyl group as opposed to the 2' hydrogen molecule present in DNA. Consequently, the phosphoester bond between the ribose sugar and phosphate group may be degraded and cleaved internally. Despite being less stable, RNA aptamers are reported to produce more diverse and versatile shapes, although some RNA aptamers have been converted in to the DNA counterpart and still retained functionality (Mok and Li, 2008).

1.2.3 Aptamers *versus* antibodies

Cancer therapies, such as those discussed in Section 1.1.6, lack specificity and could potentially leave residual cancerous cells behind which could proliferate and become harder to treat. Chemotherapies conjugated to a targeting ligand, such as aptamers and antibodies, offer attractive solutions and could be exploited to produce a more targeted approach to therapy. There are many antibody alternatives including anticalins (Schlehuber and Skerra, 2005) and adhirons (Tiede *et al.*, 2014). Aptamers are widely acknowledged to be 'chemical antibodies', comparisons between the two targeting ligands have shown that they exhibit similar levels of affinity and selectivity to the chosen targets.

Monoclonal antibodies within cancer immunotherapy has been in use over the last 30 years and although an attractive solution, some challenges are still yet to be overcome. A challenge antibodies find difficult to overcome is bypassing the blood brain barrier. Antibodies are large multimeric proteins that are heavily glycosylated in order to retain stability, as a consequence of this the large molecular weight and the presence of efflux transporters within the BBB, such as P-glycoprotein, may prevent antibodies from crossing (Banks, 2009). An attractive candidate for cancer immunotherapy has been the cancer specific EGFRvIII mutation, present in 75% of glioblastoma exhibiting *EGFR* amplification. Using a murine model, a monoclonal antibody was isolated that specifically targeted EGFRvIII (Sampson *et al.*, 2000). The group noted that systematic treatment produced no overall survival advantage, whilst a significant increase was observed when the antibody was directly applied intracranially.

Antibodies are produced *in vivo* through an animal host, which are subsequently humanised or changed in to a chimeric antibody by substituting the Fc region. Whilst they are changed to prevent the administered antibody from potentiating an immune response, there is still a chance the immune system will recognise the antibody as foreign and could produce a life threatening allergic response. Whilst isolated anti-EGFRvIII monoclonal antibodies have thus far been made redundant, the targeting of the wild type EGFR has been moderately successful. Cetuximab, a chimeric anti-EGFR antibody, was shown to be potentially effective in treating glioblastoma when combined with chemotherapy and radiotherapy using mice models (Eller *et al.*, 2005). The effectiveness of cetuximab was trialled in humans more recently and a number of adverse events were recorded including grade 3 allergic responses to the skin, for which one patient needed plastic surgery (Hasselbalch *et al.*, 2010). In contrast to antibodies, aptamers are stable ligands that have been shown to cross the BBB and are not immunogenic (Cheng *et al.*, 2013, Foy *et al.*, 2007).

In comparison to antibodies, aptamers are relatively small and are able to penetrate the cell once bound to the target present on the cell surface, which would improve delivery of chemotherapeutic payloads. Whilst antibodies are the more commercially established targeting ligand, aptamers are identified through the *in vitro* process of SELEX and do not need the use of animals. As specific aptamers are isolated *in vitro*,

the process can be controlled and changed to suit the application for which it is meant for. Aptamers, unlike antibodies, are able to be counter selected against a compound that is analogous to the target (Sefah *et al.*, 2010b). This reduces the chances of the aptamer cross reacting and increases specificity to the target of choice.

NICE guidelines have reviewed an RNA aptamer, pegaptanib (branded Macugen, by Pfizer), and a monoclonal antibody, ranibizumab (branded Lucentis), for the treatment of neovascular or wet age-related macular degeneration (AMD) (Harding, 2008). Neovascular AMD arises due to abnormal angiogenesis, resulting in a build-up of exudates within the eye (Ishida *et al.*, 2003). NICE concluded that whilst both treatments were well tolerated, ranibizumab was more effective. Whilst ranibizumab is recommended as first line treatment, it should be noted that pegaptanib is cheaper and specifically targets the angiogenic VEGF-165, whereas the monoclonal antibody targeted all isoforms of VEGFα (Harding, 2008).

1.2.4 Identification of aptamers by SELEX

First described by Tuerk and Gold, SELEX is the basic process used to identify functional aptamers to an employed target (Tuerk and Gold, 1990). During SELEX, a starting pool of 10^{15} unique oligonucleotides is amplified and incubated with a counter selection, which is analogous to the target. Unbound sequences are then exposed to the target of choice (Jenison *et al.*, 1994). Aptamers bound to the target are eluted and amplified via polymerase chain reaction (PCR), utilising constant regions flanking either side of the randomised sequence. The amplified aptamers are then purified and concentrated in-order to control the reaction volume for the following round of selection. A summary of SELEX can be seen in Figure 1.4.

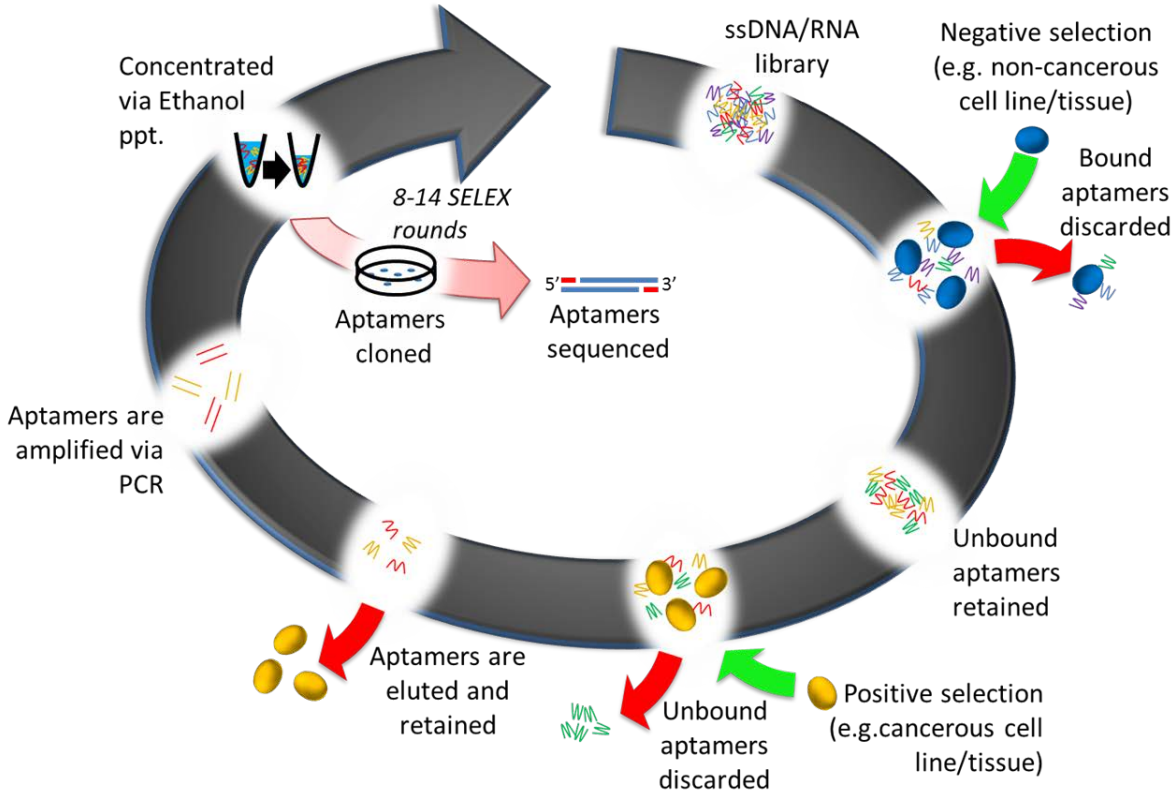

Figure 1.4 – Systematic Evolution of Ligands by Exponential Enrichment (SELEX). A nucleic library is incubated and filtered using a negative control and a positive selection. The aptamers eluted from the positive selection are amplified, concentrated and are used for further rounds of SELEX selection until a minority emerge. Figure adapted from Sefah, *et al.* (2010).

SELEX is produced in iterative cycles to evolve the starting naive library in to a pool of aptamers selective for the desired target. As rounds are produced, the competition for the epitope increases, however conditions can be made more stringent which impacts the aptamer affinity and K_d for the target. Over the last 20 years, the original SELEX process has been modified and updated to produce more than 25 different variations of the method (Aquino-Jarquin and Toscano-Garibay, 2011). Whilst the basic foundations of selection, elution, amplification and purification have stayed consistent, updated and less laborious technologies have been introduced producing aptamers of higher quality with better functionality. Some of the major advances are described in Table 1.3.

Table 1.3 – SELEX modifications to select aptamers more effectively or of higher quality

SELEX name	Modification	References
Capillary electrophoresis SELEX (CE-SELEX)	Capillary electrophoresis can be used to separated free and complexed molecules based on electrophoretic migration. CE incorporation leads to a high rate of enrichment which subsequently lowers the number of SELEX rounds needed to select aptamers with high affinity.	(Mendonsa and Bowser, 2004)
Spielgamer SELEX	DNA and RNA aptamers have short half-lives *in vivo*. Whilst the aptamers may be chemically altered to increase the half-life, spielgamer technology selects aptamers using a dextrorotatory aptamer library. The corresponding levorotatory sequence can be then used to prevent nuclease degredation; however this requires the target to have optical activity.	(Klussmann *et al.*, 1996)
FluMAG SELEX	FluMAG utilises a target immobilised to a magnetic bead in which fluorescently labelled aptamers are targeted to. Magnetic beads allow complexed aptamers to be separated efficiently, which are amplified using a fluorescently labelled primer.	(Stoltenburg *et al.*, 2005)

1.2.5 Review of aptamer applications

The SELEX process has been adapted to fit a wide range of targets, ranging from peptides to proteins and from viruses to whole cells, and hence a wide range of aptamer applications have been produced some of which, are described in the following sections.

1.2.5.1 Aptamers as therapeutic agents

The first Food and Drug Administration (FDA) approved aptamer was pegaptanib, for the treatment of neovascular age-related macular degeneration. Subsequently, Jellinek

et al. (1994) produced RNA aptamers that were 28 nucleotides long and specific to VEGF-165. The group showed that the aptamer blocked the angiogenic growth factor from interacting with the VEGF receptor in a dose-dependent manner, which exhibited a K_d in the 10-20 nM range.

VEGF-165 specific aptamers were modified and enhanced by Ruckman *et al.* (1998) by truncating to the minimal binding site consisting of 7 nucleotides. As these small ligands would have been liable to renal filtration if administered without any modifications, a 40kDa PEG moiety was added. The 7 nucleotides within the RNA aptamer were all modified with a 2'-O-methyl group to prevent internal degradation and external degradation via RNAses. The authors noted that the modified versions retained their affinity for the target VEGF-165, even though it was slightly reduced. One sequence out of the three modified, called pegaptanib, showed that it was a potent inhibitor of VEGF-induced vascular permeability (Ruckman *et al.*, 1998).

An anti-cancer aptamer called AS1411 has shown to be a promising therapeutic candidate for multiple cancer types, such as metastatic renal cell carcinoma (Rosenberg *et al.*, 2014), breast cancer (Soundararajan *et al.*, 2008) and glioma (Guo *et al.*, 2011). AS1411 is a DNA aptamer 26 nucleotides in length that targets nucleolin, a protein found on the surface of proliferating cells and is overexpressed on the surface of cancerous cells. Although the mechanism of action is not clear, it is proposed that the complex is internalised and destabilises mRNA encoded to produce B-cell lymphoma protein 2 (BCL-2); an anti-apoptotic protein (Chen, *et al*., 2008). AS1411 does not bind or affect nucleolin found on normal, healthy cells (Soundararajan *et al.*, 2009). During a recent phase II clinical trial, where 35 patients with metastatic renal cell carcinoma was enrolled, only one patient had a good response with the tumour shrinking by 84%. AS1411 was considered to be tolerated well, with one third of patients showing moderate adverse effects (Rosenberg *et al.*, 2014).

1.2.5.2 Aptamers for target identification

Aptamers are able to interact with certain biomarkers; however they may not have any therapeutic benefit once internalised. The *in vitro* identification of specific aptamers

means that they may be modified with various conjugates to add medicinal functionality (Ireson and Kelland, 2006). Therapeutic agents, such as chemotherapeutic drugs, interfering RNA and toxins, have been paired with aptamers, producing a targeted approach to therapy whilst sparing healthy tissue. One well studied aptamer in the delivery of functional conjugates is the prostate specific membrane antigen (PSMA) aptamer, A10 (Lupold *et al.*, 2002). The 40 nucleotide long RNA aptamer is internalised once complexed with its target and does not have any therapeutic effect. Prostate cancer therapy has been investigated using A10 conjugated to siRNA (Dassie *et al.*, 2009), toxins (Chu *et al.*, 2006), chemotherapeutic drugs (Bagalkot *et al.*, 2006) and nanoparticles (Dhar *et al.*, 2008).

Small interfering RNA (siRNA) hybridises messenger RNA (mRNA) normally translated to protein pivotal for cellular processes. Upon hybridisation, the mRNA is degraded and cytoplasmic levels of the protein for which it encoded is decreases. siRNA is an attractive treatment modality, however treatment efficacy is usually mitigated by poor selectivity. A10 conjugated to siRNA has shown to be effective in reducing Bcl-2 levels (Dassie *et al.*, 2009), which is over-expressed in prostate cancer and has anti-apoptotic effects.

Chemotherapeutic agents, such as cisplatin, have been encapsulated in nanoparticules in-order to improve targeted drug therapy (Dhar *et al.*, 2008). Cisplatin associated side effects, such as anaemia and nephrotoxicity may be mitigated utilising such aptamer bound vehicles. Liposomes, utilising aptamers modified with cholesterol, has also been implicated to improve drug delivery.

1.2.6 Use of aptamers in the targeting of glioma

Throughout the previous sections, the issues surrounding current treatment modalities for glioma have been reviewed whilst the versatility of aptamers as a targeting ligand have been outlined. Previous studies have produced aptamers that are specific to glioma. Cerchia *et al.,* and Kang *et al.,* selected aptamers towards the glioblastoma cells lines U87MG and U251 (Cerchia *et al.*, 2009, Kang *et al.*, 2012), using modified cell-SELEX procedures (Fitzwater and Polisky, 1996, Sefah *et al.*, 2010b).

Identified aptamers showed affinities towards the glioblastoma cells line, with minimal affinity to the negative selections used. The aptamers, GBM128 and GBM131, selected by kang *et al.,* also showed affinities for other glioma tissues, including anaplastic oligodendroglioma and pilocytic astrocytoma, implicating a common target (Kang *et al.*, 2012). Both groups showed that aptamers could be identified that are disease specific, which could be further utilised for medicinal applications.

1.3 Aims and objectives of study

The aim of this study was to identify novel DNA aptamers using cells from short term glioblastoma cultures. Whilst the slow growth of short term cultures may limit aptamer identification, a cell-SELEX protocol using minimal cell numbers was investigated in order to circumvent issues with slow growth. Furthermore, purified proteins that are known aberrations previously shown to be of importance in gliomagenesis, such as EGFRvIII and PDE1C were used for aptamer identification. Isolated aptamers were validated to determine whether the aptamers interacted with the protein target.

Chapter 2: Methods and materials

2.1 Cell culture and maintenance.

2.1.1 Cell lines and primary cell cultures

The cell lines SVGp12 and U87MG were used to optimise the cell-SELEX procedure. SVGp12 is a human foetal astroglia cell line that was used as the negative selection within SELEX selections and was obtained from the American Type Culture Collection (ATCC). U87MG is a human astroglia cell line representative of grade IV glioblastoma multiforme and was used as the positive selection within SELEX. U87MG was obtained from the European Collection of Cell Cultures (ECACC).

2.1.2 Cell Culture and Subculture

SVGp12 and U87MG were cultured in Eagles minimal essential medium (EMEM, Bio-Whittaker) supplemented with 10% foetal bovine serum (FBS, Bio-Sera), 1% non-essential amino acids (NEAA, Sigma UK), 2 mM L-Glutamine and 1 mM Sodium pyruvate (Sigma UK). Cell cultures were incubated at 37°C in a humidified 5% CO_2 environment and were subcultured to 80% confluency.

Once cell cultures reached confluency, the media was removed and cells were washed with phosphate buffered saline (PBS, pH 7.4) to remove residual media. Cells were removed from the flask through incubation at 37°C in 2ml of 1 x trypsin diluted in PBS, for 2 minutes. To inhibit the trypsin, EMEM was added at an equal volume and the cell suspension was centrifuged for 5 minutes at 200 x g. The supernatant was removed and the cell pellet was resuspended in fresh media. Appropriate dilutions were added to 10ml of EMEM (1:3 for SVGp12, 1:6 for U87MG) and incubated until required.

2.2.3 Cell Viability

Non-viable cells can bind aptamers non-selectively resulting in the loss of aptamers. The trypan blue exclusion assay was performed on cell cultures to determine cell viability. After trypsinisation, a homogenous cell suspension was aliquoted and trypan blue (Sigma UK) was added at a ratio of 1:1. The cells were checked for the

presence of non-viable blue cells and cell suspensions with ≥95% viability (non-viable/total cell count x 100) were used in SELEX selections.

2.3 Optimisation and establishment of an aptamer library.

2.3.1 The DNA aptamer library

Specific aptamers were selected from a large library of random oligonucleotides. In-order to create the library, 10^{15} potentially unique DNA aptamers were synthesised by Integrated DNA Technologies (IDT, UK) through machine mixed randomisation. All dNTPs were included at different ratios to avoid asymmetric binding efficiency and either side of the sequences were flanked by conserved regions. The aptamer template was as follows:

5`-ATCCTAATACGACTCACTATAGGGAGAGAATTC – N50 –

GAATTCTGCGGTAAACTCGAGGG-3`

The random region of 50 nucleotides (green) was flanked by a forward primer (red) and a reverse primer (blue), which was conserved throughout all sequences and were required for amplification by PCR.

2.3.2 Amplification of the DNA aptamer library

Inefficient amplification of DNA aptamers may result in the production of non-specific sequences, these sequences may compete with the specific sequence during SELEX selections, therefore reducing the efficiency of aptamers identification. In-order to reduce non-specific amplification, touchdown polymerase chain reaction (TD-PCR) was trialled as previously described by Korbie and Mattick (2008) and was validated in comparison with standard PCR. To compare the programmes, the optimal number of cycles for each programme was investigated. The annealing temperature of the forward and reverse primers (IDT, UK) was optimised previous to this study and was found to be optimal at 50°C (Table 2.1).

Table 2.1 – Primer sequences and properties

Primer Name	Sequence of primer	Melting temperature (T_m)	GC Content
AptForward	5`-ATCCTAATACGACTCACTAT-3`	46°C	35%
AptReverse	5`-CCCTCGAGTTTACCGCAGAATT-3`	57°C	50%

PCR reactions (Table 2.2) were amplified through TD-PCR and standard PCR programmes (Table 2.3). Control reactions were conducted in the absence of *Taq* polymerase. PCR products were aliquoted at increments of 5 cycles and were separated and visualised by agarose gel electrophoresis (see Section 2.2.3).

Table 2.2 – Reagents used for amplification of DNA aptamer library

Reagent	Final Concentration
5x PCR buffer	1x
Deoxynucleotide Solution	200µM
AptForward	0.5µM
AptReverse	0.5µM
Template DNA (Aptamer library)	10µg/µl
$MgCl_2$	1 mM
DNA Taq polymerase	0.02 U/ul

Table 2.3 – Touchdown and Standard PCR programmes used for the amplification of the DNA aptamer library.

Action	Time (Seconds)	Temperature (°C) TD-PCR	Temperature (°C) Standard PCR
Initial Denaturation	300	95	95
Phase One (10 Cycles)			
Denaturation	30	95	-
Annealing	30	60 (decreased 1°C/cycle)	-
Extension	30	72	-
Phase Two (30 Cycles)			
Denaturation	30	95	95
Annealing	30	50	50
Extension	30	72	72
Final Extension	420	72	72

2.3.3 Separation and visualisation of PCR products

Amplified PCR products were separated and visualised via agarose gel electrophoresis. PCR products were mixed with bromophenol blue (0.25% w/v bromophenol blue, 0.25% w/v xylene cyanol and 30% glycerol) at a ratio of 1:1 and separated on a 2% agarose gel (Fisher scientific, UK) prepared with 1 x TAE buffer (1.85 M Tris, 45 mM EDTA and 1M Glacial Acetic acid), containing 0.005% of SafeView nucleic acid stain (NBS Biologicals). After separation, the amplified PCR products were visualised under UV light.

2.3.4 Purification of DNA via ethanol precipitation

Dilute PCR products will lower stringency, decreasing the efficacy of SELEX selections, therefore the DNA aptamers were concentrated in-order to control the stringency of SELEX selections. A modified DNA precipitation procedure utilising the DNA carrier glycogen, as described by Fregal *et al.,* was compared with the standard

ethanol precipitation protocol. Furthermore, the temperature and concentration of glycogen used to facilitate precipitation was optimised.

A loading control was aliquoted from pooled PCR product (section 2.2.2) and the remaining DNA aptamers were distributed evenly between 6 precipitations (Table 4). For the standard procedure, $1/10^{th}$ volume of sodium acetate (3M) and 2 volumes of cold 100% ethanol (-20°C) was added to the PCR product. The mixture was incubated at the appropriate temperature for the allotted time, which was then centrifuged at 14,100 x *g* for 15 minutes at 4°C. The supernatant was discarded and the pellet was washed in cold 70% ethanol (-20°C) and centrifuged again. The supernatant was removed and the pellet was air dried for 5 minutes before being resuspended in dH_2O.

For the modified protocol, stock solutions of glycogen were prepared (50 mg/ml and 100 mg/ml) in 75 mM ammonium acetate. To the PCR product, $1/10^{th}$ volume of ammonium acetate (75 mM) with glycogen was added, as well as 2 volumes 100% cold ethanol (-20°C). The mixture was incubated at the appropriate temperature for the allotted time and before centrifugation. The supernatant was removed and the pellet was air dried for 5 minutes at room temperature before being resuspended in dH_2O.

Table 2.4 – The different precipitation protocols and varied temperatures and glycogen concentrations used to optimise DNA precipitation

Incubation at -80°C for 1 hour	Incubation at -20°C for 24 hour
Standard protocol	Standard protocol
Modified with Glycogen (5mg/ml)	Modified with Glycogen (5mg/ml)
Modified with Glycogen (10 mg/ml)	Modified with Glycogen (10mg/ml)

2.3.5 Preparation of ssDNA aptamers from concentrated PCR product

Following resuspension in an appropriate volume of dH_2O, amplified DNA aptamers were prepared as previously described by Sefah *et al.,*(2010). Binding buffer (25 mM glucose, 0.1% bovine serum albumin, 0.25 mM $MgCl_2$ and 1 x PBS) was added to the DNA aptamers and heated to 95°C for 5 minutes. Following denaturation, the ssDNA was snap-cooled on ice for 5 minutes and kept on ice or stored at 4°C until required.

2.4 Systematic evolution of ligands by exponential enrichment using cell lines (cell-SELEX).

2.4.1 Negative Selections of amplified library against SVGp12 cell line

To ensure selected aptamers were specific to the positive selection, snap-cooled ssDNA aptamers were exposed to a negative selection of the non-cancerous SVGp12 astrocyte cell line. Subcultured SVGp12 were trypsinised (section 2.1.3) and viability was assessed (Section 2.1.4). Cells were washed with washing buffer (25mM glucose, 0.25mM $MgCl_2$ and 1X PBS) and centrifuged at 200 x *g* for 5 minutes to remove excess media. Cells were resuspended in binding buffer and the ssDNA aptamers were added (total volume 700µl). SVGp12 cells were then incubated at 4°C for 1 hour with shaking. After incubation the cells were centrifuged at 200 x *g* for 5 minutes and the supernatant was retained for use in the positive selection.

2.4.2 Positive selections against U87MG cell line

Aptamers which did not bind to the negative selection were carried forward in to a positive selection against U87MG. Cells were prepared as described previously (section 2.4.1) and the aptamers retained from the negative selection was added to the U87MG cells. The mixture was incubated at 4°C for 1 hour with shaking. After incubation the cells were centrifuged and the cells were washed with washing buffer three times to remove any unbound aptamers. Cells were resuspended in dH_2O and heated to 95°C for 10 minutes to elute any bound aptamers. The cells were centrifuged at 14,100 x g for 1 minute and the supernatant was retained.

Eluted aptamers were then amplified via PCR (section 2.2.2), concentrated by ethanol precipitation (section 2.2.4), quantified by gel electrophoresis (section 2.2.3), snap-cooled on ice (section 2.2.5) and reapplied in to iterative rounds of SELEX.

2.4.3 Minimum number of cells required to return specific aptamers

In-order to establish the minimum number of cells which would return selective aptamers, a round of SELEX was performed using SVGp12 (section 2.3.1) and U87MG (section 2.3.2). The aptamer library was applied to cell numbers of $1000x10^3$, $500x10^3$, $250x10^3$, $125x10^3$, $62.5x10^3$, $32x10^3$, $16x10^3$, $8x10^3$, $4x10^3$, $2x10^3$, $1x10^3$, $0.5x10^3$, $0.25x10^3$ and $0.1x10^3$. Cell numbers were constant through negative and positive selections.

The minimal cell number that returned sufficient bound aptamers was put through 5 rounds of SELEX to confirm the cell number could be used for the identification of aptamers. After each round of selection, the number of PCR programme cycles was optimised to determine the number of cycles that returned the optimal yield of aptamers, but with maximum specificity. This was performed as in section 2.2.2 and amplified DNA aptamers were concentrated by the optimised ethanol precipitation procedure and visualised by agarose gel electrophoresis.

2.5 Primary cell SELEX

Two glioblastoma short-term cell cultures, BTNW390 and BTNW914, were obtained from the Brain Tumour North West tissue bank located at Royal Preston hospital, UK. BNTW390 primary cells were extracted from an 80 year old male and BTNW914 primary cells were biopsied from a 64 year old female. Normal human astrocytes (NHA) were cultured in AGM Astrocyte Growth Bulletkit (Lonza). Short-term patient samples were cultured in F10 HAM (Sigma, UK) supplemented with 10% FBS of (LifeTechnologies, Australia). Cultures were incubated at 37˚C in a humidified CO_2 environment.

To harvest cultured NHA cells, the cells were washed with dulbeccos phosphate buffered saline (DPBS). Following washes, the cells were removed by incubating at 37˚C in trypsin EDTA for 2 minutes. Astrocyte media was added at equal amounts to inhibit the trypsin and cells were centrifuged 200 x g, and washed three times to remove residual media and trypsin before being entered in to SELEX selections. Short-term cell cultures were washed with PBS and subsequently harvested by incubating for 4 minutes at 37˚C in 2x trypsin. F10 HAM was added at an equal concentration to inhibit the trypsin, before being centrifuged at 200 x g. Cells were washed three times before being entered in to SELEX selections.

Five rounds of SELEX from the short-term cultures were produced. ssDNA aptamer libraries (prepared as in Section 2.3.5) were incubated with NHA cells for 60 minutes at 4˚C on a rocker shaker. Following incubation, cells were pelleted by centrifugation at 200 x g and the supernatant, containing unbound aptamers, underwent positive selection. Unbound aptamers were incubated with the short term cultures for 60 minutes at 4˚C with shaking. Following incubation, the cells were pelleted by centrifugation at 200 x g and the cells were washed with washing buffer three times, before the aptamers were eluted in dH_2O by heating to 95˚C for 5 minutes. The cell-SELEX selections for both short term cultures were produced separately and after five rounds of selection, aptamers still present were cloned and sequenced.

2.6 Identification of DNA aptamers towards purified biomarkers via Counter-SELEX

2.6.1 Counter-SELEX against Phosphodiesterase 1C (PDE1C)

To produce aptamers specific to PDE1C, one negative selection against glutathione S-transferase (GST) and one negative selection against agarose resin were performed. The resulting pool of filtered aptamers were positively selected against GST tagged PDE1C during 6 rounds of positive selection.

2.6.1.1 Expression of glutathione S-transferase (GST)

pGEX-KG vector (fig 2.1) was added to chemically competent BL21 *E.coli* cells (genotype: *BF–dcm ompT hsdS(rB–mB–)gal*) and incubated on ice for 30 minutes. Cells were heat shocked at 42˚C for 90 seconds before being snap cooled on ice for 2 minutes. Transformed cells were spread on to pre-warmed LB agar plates containing 25µg/µl ampicillin and were incubated overnight at 37˚C. Control plates were produced by substituting pGEX-KG vector with dH_2O.

Transformed BL21 *E.coli* cells were inoculated in to LB broth and incubated at 37 ˚C with shaking. The optical density (abs 600nm) of the culture was monitored. When the culture reached an OD_{600nm} of 0.6, 1mM isopropyl β-D-1-thiogalactopyranoside (IPTG) was added to the culture to induce GST expression. The induced culture was left for 210 minutes at 37 ˚C with shaking at 180rpm.

Cells were harvested via centrifugation at 16,000 x g for 10 minutes at 4 ˚C, the supernatant was discarded and the cells were washed with dH_2O. Following centrifugation and removal of the supernatant, cells were resuspended in 1x PBS before sonication. BL21 cells expressing GST were lysed by intermittent cycles of sonication of 30 seconds, at an amplitude of 14. Cellular fragments were pelleted by centrifugation at 16,000 x *g* and the supernatant, containing soluble intracellular proteins, was retained.

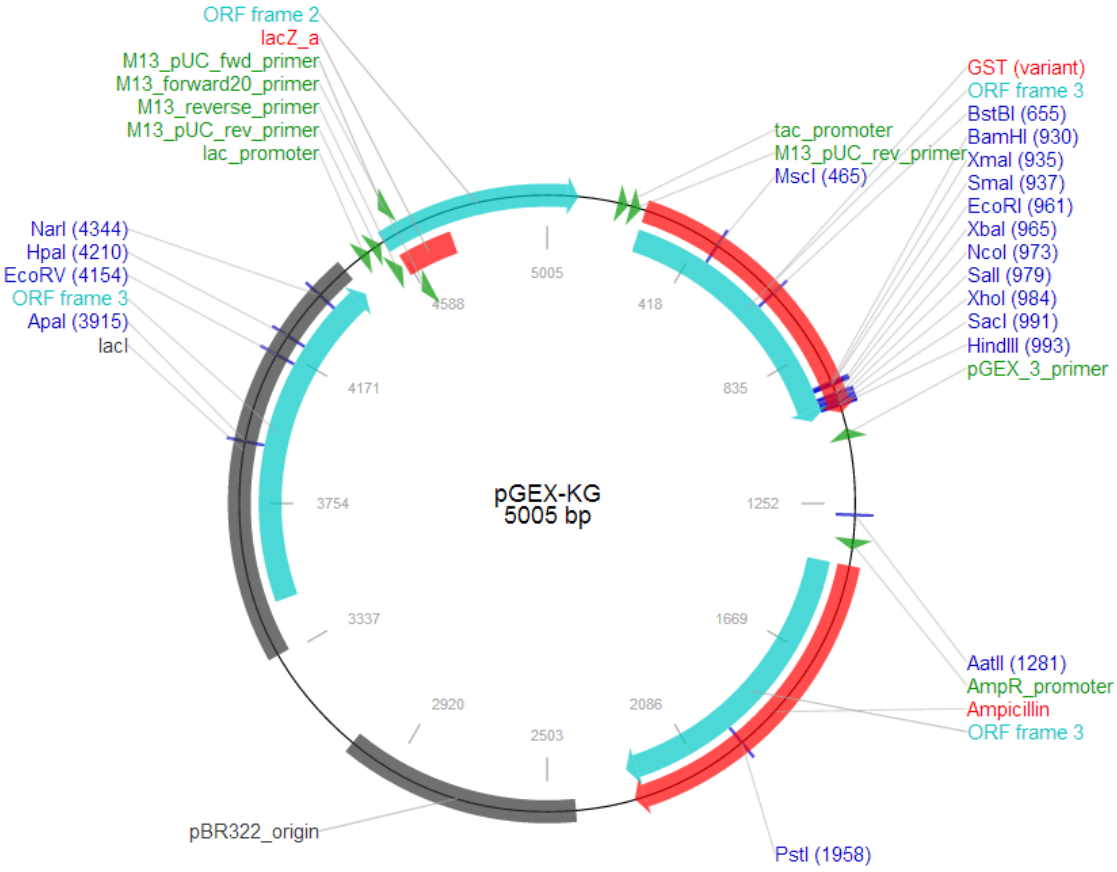

Figure 2.1 – Map of the pGEX-KG vector transformed in to chemically competent BL21 *E.coli* for the expression of GST.

SDS-PAGE gel electrophoresis was performed to confirm successful expression of GST. BL21 *E. coli* before and after induction of GST expression were heated to 95˚C for 5 minutes in 1x Laemelli buffer (65mM Tris-HCl pH 6.8, 10% glycerol, 1% SDS, 0.0025% bromophenol blue). Samples were loaded on to a 4-20% gradient mini-protean gel (BioRad, UK) and were run in the presence of 1x running buffer (3.5mM SDS, 25mM Tris and 0.2M glycine). The gel was visualised using coomassie blue stain (0.1% coomassie brilliant blue R-250, 50% methanol and 10% glacial acetic acid).

2.6.1.2 Immobilisation and negative selection against GST

Glutathione sepharose 4B beads (Pierce, UK) were centrifuged at 400 x g for 2 minutes and washed with ddH_2O three times to remove any ethanol present. To purify GST the beads were incubated with the BL21 cell lysate for 60 minutes with

shaking at 4˚C. Sepharose beads were centrifuged again and the supernatant was removed, before undergoing 3 washes with PBS.

An amplified aptamer library was negatively selected against GST using the GST immobilised sepharose beads. DNA aptamers were prepared as described in section 2.3.5 and were added to the GST beads, supplemented with selection buffer (1x PBS, 5mM $MgCl_2$, 10mM KCl and 0.01% v/v Tween-20) to a final volume of 1ml. The mixture was then incubated for 60 minutes at room temperature with shaking, before being centrifuged at 1000 x *g* for 2 minutes; the supernatant was retained and kept ready for the positive selection.

2.6.1.3 Positive selection against immobilised PDE1C

Purified GST tagged PDE1C, obtained from Genscript (US) was reconstituted in 1x PBS (made with ddH_2O) to a final concentration of 20µg/ml. N-hydroxysuccinimide (NHS) activated dry agarose resin (Thermo Scientific Pierce) was added to PDE1C (0.1667g/ml swell volume) and was left to couple at room temperature for 60 minutes on a rotary shaker. The resin was washed with PBS and centrifuged at 500 x g, the supernatant was removed before undergoing two more washes. The agarose resin was then blocked in 1M Tris for 30 minutes at room temperature on a rotary shaker. The agarose resin coupled with PDE1C was washed three times and resuspended in selection buffer. Supernatant from the negative selection was added to the resin and incubated on a rotary shaker for 30 minutes at room temperature.

Following positive selection, the beads were washed with PBS before being resuspended in dH_2O and heated to 95˚C for 5 minutes to elute any aptamers. The eluted aptamers were then incorporated in to a PCR mastermix, of which 4 aliquots (2 reactions and 2 controls) were used to optimise the number of TD-PCR cycles as previously described. Once the optimal number of TD-PCR cycles was elucidated, the remaining mastermix was amplified before being purified via ethanol precipitation. Six rounds of counter-SELEX were performed, initial concentrations of

0.02 µg/µl of protein were used, however concentrations were decreased by 0.005 µg/µl every other round to increase stringency.

2.6.2 Counter-SELEX against EGFRvIII peptide

DNA aptamers were identified towards the mutated region exclusive to EGFRvIII. Negative selections were produced using EGFR wild type (EGFRwt) protein obtained from Life Technologies and aptamers were identified through positive selections towards the EGFRvIII peptide (amino acids 6-19; Leu, Glu, Glu, Lys, Lys, Gly, Asn, Tyr, Val, Val, Thr, Asp, His, Cys), obtained from Genscript.

The EGFRwt protein and the EGFRvIII peptide were immobilised as described in section 2.5.1.3 using NHS-activated dry agarose resin. For negative selections, an amplified DNA aptamer library was incubated with immobilised EGFRwt for 30 minutes at room temperature on a rotary shaker. The agarose resin was centrifuged at 500 x g and the supernatant containing unbound aptamers was administered to a positive selection with immobilised EGFRvIII peptide. Following incubation for 30 minutes at room temperature on a rotary shaker, bound aptamers were eluted by heating the resin to 95˚C for 5 minutes. Eluted aptamers were incorporated in to a PCR mastermix which was used to determine the optimal number of TD-PCR cycles, before the remaining PCR mastermix was used to amplify eluted aptamers. Amplified PCR products was purified via ethanol precipitation and entered back in to subsequent rounds of selection. Five rounds of counter-SELEX were performed, initial concentrations of 0.02 µg/µl of protein were used, however concentrations were decreased by 0.005 µg/µl every other round to increase stringency.

2.7 Establishing aptamer sequences

2.7.1 Transformation and cloning of identified DNA aptamers

Once DNA aptamers were selected they were transformed in to chemically competent DH5α *Escherichia coli* (genotype: F- ϕ80(*lac*Z)ΔM15 Δ*lac*X74 *hsd*R(rk-, mk+) Δ*rec*A1398 *end*A1 *ton*A) using a TOPO pCR 2.1 cloning kit (Invitrogen) as per manufacturer's instructions (Fig 2.2). Controls lacked any PCR product within the

ligation reaction. Ligated plasmids were added to chemically competent DH5α, following incubation for 60 minutes on ice the cells were then heat shocked at 42˚C for 90 seconds prior to being snap-cooled on ice for 120 seconds. Transformants were spread on to selective LB (63.5mM tryptone, 0.171M NaCl, 0.5% yeast extract agar and 10% agar) plates containing 25µg/µl ampicillin, before being incubated overnight at 37˚C.

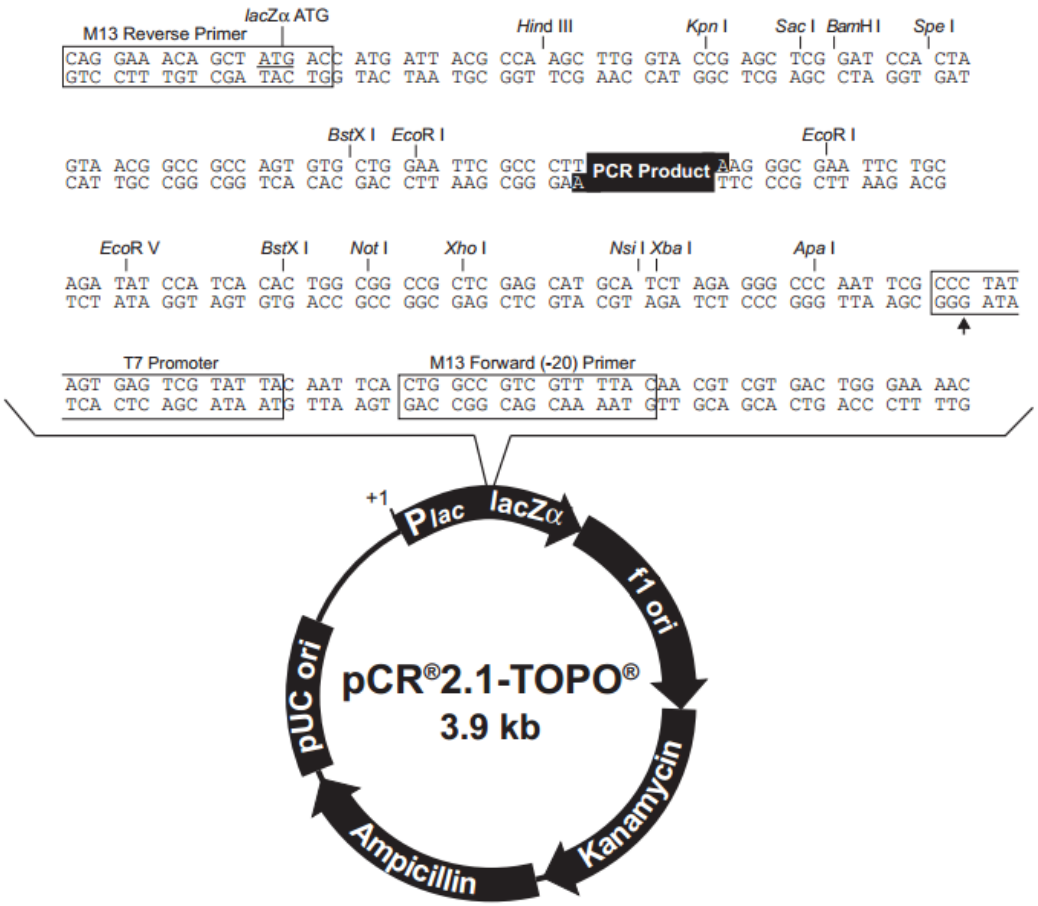

Figure 2.2 – A map of the pCR 2.1 TOPO vector used to ligate aptamers in to, which were subsequently transformed in to chemically competent DH5α *E.coli* and cloned.

Single colonies were selected and resuspended in dH_2O, which was utilised as template in a PCR reaction containing M13 primers for colony screening. The PCR programme was as depicted in Table 2.5 and PCR products were visualised on a 2% agarose gel. Positive transformants were inoculated into LB media containing ampicillin before being incubated overnight at 37˚C with shaking. The DH5α *E.coli* cells were harvested by centrifugation at 1000 x g and cloned plasmid was purified

using a GeneJET Plasmid Miniprep kit (Thermo Scientific) as per manufacturer's instructions.

Table 2.5 – Colony PCR programme used to screen for positive aptamer insert.

Action	Time (Seconds)	Temperature (°C)
Initial denaturation	300	95
Denaturation	30	95
Annealing	30	45
Extension	30	72
Final extension	420	72

2.7.2 Identifying novel aptamer sequences

Plasmids positive for insert were sequenced by Sanger by Source Biosciences (Nottingham, UK) using the M13 primer sites, sequencing used a quality score of 20. Aptamer sequences were deduced based on the presence of aptamer primer sites (Table 2.3),. Unedited aptamer sequences were analysed by Clustal Omega (available: http://www.ebi.ac.uk/Tools/msa/clustalo/) to determine closely related sequences based on homology. Families of sequences were re-entered in to Clustal Omega to elucidate homologous sequences. Secondary structures of the ssDNA aptamers were predicted using MFold software (available: http://mfold.rna.albany.edu/?q=mfold/DNA-Folding-Form). The conditions that entered in to MFold were dependent on the type of SELEX performed.

2.8 Validation of aptamer-target specificity

Aptamers identified through counter-SELEX, towards EGFRvIII and PDE1C, and cell-SELEX, towards primary cell cultures were validated through varied methods. Aptamers were biotinylated and utilised in a variety of methods, including denaturing and non-denaturing western blots, oligohistochemistry and aptoprecipitation assays to determine whether the aptamers recognised and bound any proteins.

2.8.1 Preparation of biotinylated ssDNA aptamers for validation studies

Plasmids, containing required aptamer were used to amplify specific aptamer sequences via TD-PCR. The TD-PCR programme used was as in table 3, with 10 phase two cycles. The aptamers were biotinylated through substituting the forward primer within the PCR reaction with a biotinylated forward primer. PCR products were pooled and concentrations were determined using a nanodrop 1000, at a wavelength of 260nm. Amplified aptamers were denatured by heating at 95˚C for 5 minutes, before being snap-cooled on ice for 10 minutes to produce ssDNA aptamers. The ssDNA aptamers were diluted to 100nM using buffers dependent on the validation study.

2.8.2 Denaturing and non-denaturing Western blot

For the denaturing Western blot, SVGp12 and U87MG cells were resuspended in cold RIPA buffer at 4˚C. The cells were incubated at 4˚C for 60 minutes with shaking, before being centrifuged at 16,000 x g for 10 minutes. The supernatant was boiled in Laemmli buffer (60 mM Tris, pH 6.8, 10% glycerol, 2% w/v SDS and 0.01% bromophenol blue) at 95˚C for 5 minutes. Boiled cell lysates were then run on a 4-20% gradient Mini-PROTEAN TGX gel (BioRad) in the presence of running buffer (25 mM Tris, 192 mM glycine and 0.1% SDS). Separated proteins were transferred on to polyvinylidene fluoride (PVDF) membrane in the presence of transfer buffer (25 mM Tris, 192 mM glycine and 10% methanol). The PVDF membrane was blocked in TBST buffer (50 mM Tris, 150 mM NaCl and 0.05% v/v Tween-20) containing 10% marvel milk powder. Following blocking, the membrane was washed three times in TBST for 5 minutes per wash, before being incubated with 100 mM aptamer in TBST for 60 minutes at room temperature with shaking. The membrane was washed three times, before incubation with Vectastain ABC system as per manufacturer instructions. Following another three washes with TBST, aptamer-protein interaction was visualised using 3,3’-Diaminobenzidine (DAB) peroxidase substrate solution (Dako, UK).

Non-denaturing Western blot was performed on cell lines as above with the following modifications. SVGp12 and U87MG cells were gently lysed using 0.1% Triton X100 in PBS; cells were incubated for 60 minutes with shaking at 4˚C. Following incubation, the cells were centrifuged at 16,000 x g at 4˚C, before the supernatant was boiled in Laemlli buffer not containing SDS. Proteins within the lysate were separated via PAGE in the presence of running buffer without SDS. Non-denaturing Western blots were also produced for five glioblastoma tissue samples, kindly provided by Royal Preston hospital. The tissue samples were already shown to be positive for *EGFR* amplification through the use of the mouse monoclonal EGFR antibody (Leica). Tissue samples were homogenised prior to being incubated in 0.1% Triton X100 for 60 minutes with shaking at 4˚C. The samples were centrifuged at 16,000 x g and the cell lysates were decanted ready for native Western blot analysis as previously described.

2.8.3 Oligohistochemistry

Paraffin embedded glioblastoma tissue sections were kindly provided by Royal Preston hospital, UK. Tissue sections were immersed in Histoclear for 15 minutes to deparaffinise the tissue. The tissue was then rehydrated through graded washes of ethanol (100%, 90% and 70%) for 5 minutes each wash. Antigen retrieval was performed by immersing the tissue in to 0.01M citric acid (pH 6.0) and heated for 20 minutes at 97˚C. The tissue sections were allowed to cool by standing at room temperature for 30 minutes, before the tissue was incubated with 100nM biotinylated aptamer in PBS for 60 minutes at room temperature. The Vectastain ABC kit was used to detect aptamer-protein interaction as per manufacturer's instructions. Following three washes with PBS, ABC system was visualised using DAB peroxidase substrate solution for 10 minutes. Following three PBS washes, the tissue sections were dehydrates through gradual washes of ethanol (70%, 90% and 100%) before being mounted using DPX mounting media (Sigma, UK). Microscopy was produce using a Nikon light microscope.

2.8.4 Aptoprecipitation (AP) assay

SVGp12 and U87MG cells were gently lysed using 0.1% Triton X100 as previously described (Section 2.8.2). Streptavidin agarose beads were blocked through 2 hour incubation at 4˚C with 0.1% bovine serum albumin (BSA) in PBS, with shaking. Biotinylated aptamers (100nM) were added to the native cell lysates, which was incubated at 4˚C for 60 minutes with shaking. Once blocked, the beads were washed three times with cold PBS (4˚C), before being added to the cell lysate, which was incubated for 60 minutes at 4˚C with shaking. Following incubation, the streptavidin agarose beads were allowed to settle gravimetrically without any centrifuging. The supernatant (input) was removed, and the beads were washed three times with cold PBS, each time the beads were allowed to settle gravimetrically. Following washes, the streptavidin agarose beads (output) was boiled in Laemmli buffer at 95˚C for 5 minutes, the same was produced for the input, before the samples were analysed by SDS-PAGE as previously described. The SDS-PAGE gel was stained using coomassie blue.

Chapter 3: Results and analysis

3.0 Results

3.1 Optimisation of DNA aptamer amplification and purification

The amplification and purification of aptamers, through PCR and ethanol precipitation respectively, are important independent procedures within SELEX. Non-specific sequences may hinder SELEX selections and reduce the amplification of DNA aptamers (Bell and DeMarini, 1991). In-order to increase the specificity of aptamer amplification, the PCR protocol was optimised. Inefficient purification of the resulting amplified aptamers may lead to the loss of sequences; therefore the purification protocol was enhanced to determine the conditions that would precipitate DNA aptamers most effectively, which was measured by agarose gel electrophoresis.

3.1.1 Optimisation of DNA aptamer amplification via polymerase chain reaction (PCR)

As minimal biological material was available for SELEX selections, it was important that the PCR programme was sensitive and specific enough to amplify the respectively small amounts of aptamers that would be eluted. For these reasons, touch-down PCR (TD-PCR) was trialled, as it has been previously shown to be more specific and sensitive than the standard PCR programme (Korbie and Mattick, 2008). A touch-down phase (phase one, see table 3.1) was added to the traditional PCR programme (phase two), which was optimised and compared with the standard PCR programme to validate the additional steps. The standard PCR did not utilise the touch-down phase and therefore, only consisted of a total of 30 cycles, where as TD-PCR totalled 40 cycles. The phase two cycle was optimised to see the number of cycles required without amplifying non-specific sequences. The bands produced at different cycle numbers by different PCR programmes were visualised by agarose gel electrophoresis and compared to determine which programme amplified aptamers most effectively (Fig 3.1).

Table 3.1 – The TD-PCR and standard PCR programmes. The TD-PCR consisted of an extra 10 phase one cycles in which the annealing temperature was gradually reduced 1˚C per cycle. The standard PCR did not utilise any phase one cycles and only underwent the phase two cycles.

Action	Temperature (°C) TD-PCR	Temperature (°C) Standard PCR
Initial Denaturation	95	95
Phase One (10 Cycles)		
Denaturation	95	-
Annealing	60 (decreased 1°C/cycle)	-
Extension	72	-
Phase Two (30 Cycles)		
Denaturation	95	95
Annealing	50	50
Extension	72	72
Final Extension	72	72

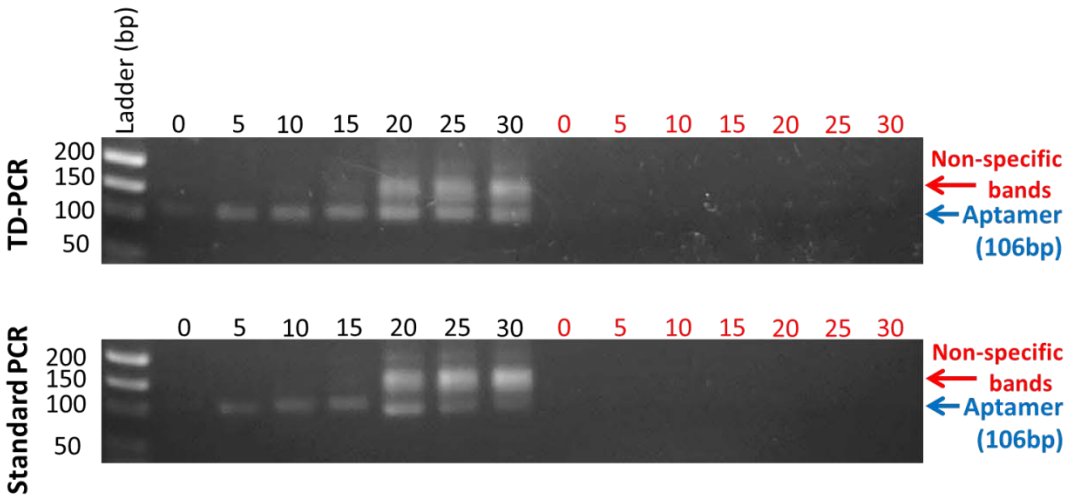

Figure 3.1 – Comparison of TD-PCR vs. Standard PCR programme and optimising the number of phase two cycles. The optimal number of cycles for the standard PCR programme was 15 and 10 for the touch-down programme. The band at 10 cycles of TD-PCR was sufficiently bright such that the number of cycles may be reduced therefore potentially reducing amplification of non-specific sequences. Both gels were pictured using the same exposure time and the touch-down stage (phase one, see table 2.3) was not shown. Controls (in red) were negative for any amplification.

Agarose gels, shown in Fig 3.1, were visualised using the same UV exposure so that comparisons could be made. Aptamers, 106bps in length, were amplified after 5 cycles of both PCR programmes. Non-specific sequences, 150 bps in length, were present following 20 cycles of either PCR programme. The intensity of the bands corresponds to the amount of DNA that is present, therefore with increased amplification there should be an increase in band intensity. The bands with the highest intensity were produced by TD-PCR, indicating an increase in aptamer amplification using this programme. Based on the agarose gels, 15 cycles of phase two amplification was optimal for the standard PCR programme, as further cycles would result in the amplification of non-specific sequences. Aptamers were amplified following 5 phase two cycles using TD-PCR; however non-specific sequences were not seen until 20 cycles. Ten cycles were identified as optimal for TD-PCR.

Comparisons between the two agarose gels were investigated further by densitometry analysis using ImageJ software. The density of the 106bp aptamer band was determined for each cycle number across both PCR programmes. By comparing values generated from ImageJ, ratio change for TD-PCR was calculated. A number above 1 showed that there was an increase in aptamer amplification using TD-PCR, where as a value below 1 indicated an increase in aptamer amplification using the standard PCR programme (Fig 3.2).

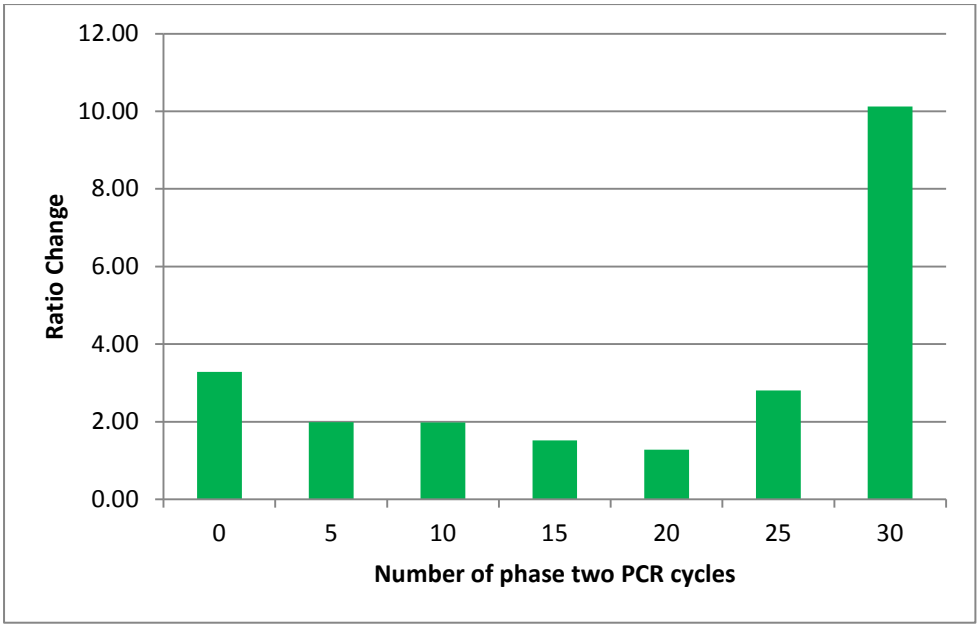

Figure 3.2 – Ratio change of aptamer amplification, using TD-PCR across varied numbers of phase two cycles, in comparison to the standard PCR programme. Values generated by ImageJ, based on the density of specific bands at 106 bps, were used to calculate the fold change for TD-PCR**.**

Values produced by ImageJ showed that TD-PCR produced higher rates of aptamer amplification (Fig 3.2), especially between 25 and 30 cycles of amplification. A 2 fold increase was observed using 10 phase two cycles, a slight decrease in ratio change was observed using 15 cycles. As 15 cycles did not increase aptamer amplification significantly and further cycling would result in the production of non-specific sequences (Fig 3.3), 10 cycles was determined to be optimal. In accordance with these results, the TD-PCR programme was utilised for aptamer amplification and 10 phase two cycles was used for the initial amplification of the DNA aptamer library.

3.1.2 Optimisation of DNA aptamer purification via ethanol precipitation

DNA is insoluble in high concentrations of ethanol, therefore it is commonly used as an inexpensive method to precipitate and purify DNA. Commercially available DNA purification kits are expensive and may not be efficient when purifying small sequences. In order to maximise the amount of DNA aptamer purified from PCR products during SELEX, a modified ethanol precipitation method was trialled and compared to the standard method. Modifications of the method included varying

the concentration of glycogen and incubation conditions (Table 2.4), as well as substituting sodium acetate for ammonium acetate. DNA aptamers were amplified by TD-PCR and subsequently pooled, before being aliquoted and purified by the aforementioned ethanol precipitation procedures. The resulting pellets of DNA were resuspended in the same volume of dH_2O and analysed by agarose gel electrophoresis (Fig 3.3).

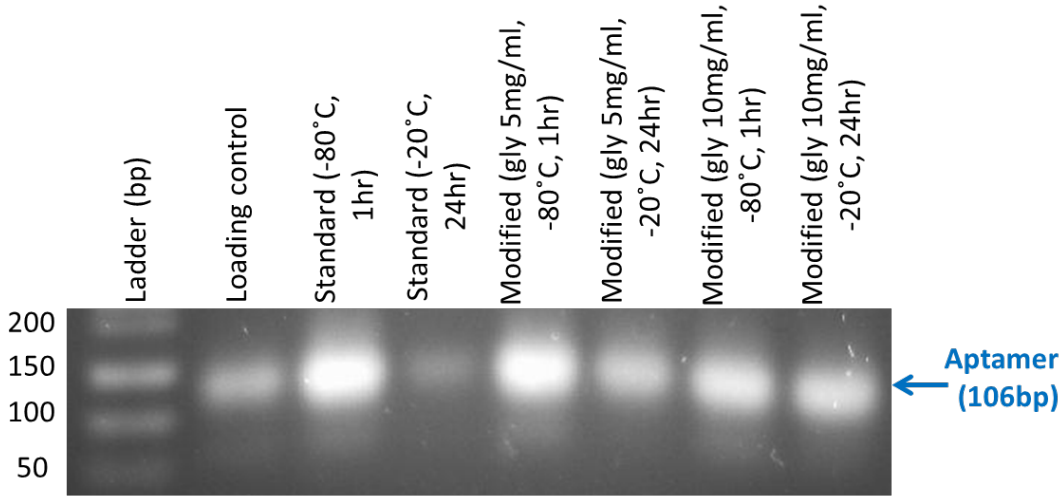

Figure 3.3 – Comparison of the standard ethanol precipitation protocol with the modified protocol and optimisation of the incubation conditions. Optimal incubation conditions were -80 ˚C for 1 hour across both methods of aptamer purification. The optimal glycogen concentration was 5 mg/ml showing higher band intensity than that of 10 mg/ml; however the standard protocol lacking any glycogen inferred the best method of purification with a brighter band.

A control sample was taken from the pooled PCR products that did not undergo any purification; this was taken to determine the level of amplified DNA without purification. The majority of the purification methods were sufficient to produce bands with higher intensity than that of the loading control, suggesting that DNA was purified and concentrated through each method. The exception was the standard method with incubation conditions of -20˚C for 24 hours, which showed reduced levels of DNA compared to the control suggesting loss of aptamers. The modified ethanol method, using a glycogen concentration of 5 mg/ml, with incubation conditions of -80 ˚C for 1 hour showed optimal aptamer purification. The standard procedure, involved incubation of PCR products at -80˚C for 1 hour and

showed a band with similar intensity to that of the optimal improved procedure, which utilised 5 mg/ml glycogen and incubation conditions of -80˚C for 1 hour. These bands were further analysed using ImageJ software. Values for the varied DNA purification methods were taken and compared to that of the loading control (Fig 3.4). A ratio change above 1 indicated that the sample was purified and concentrated, where as a value below 1 indicated that aptamers were lost.

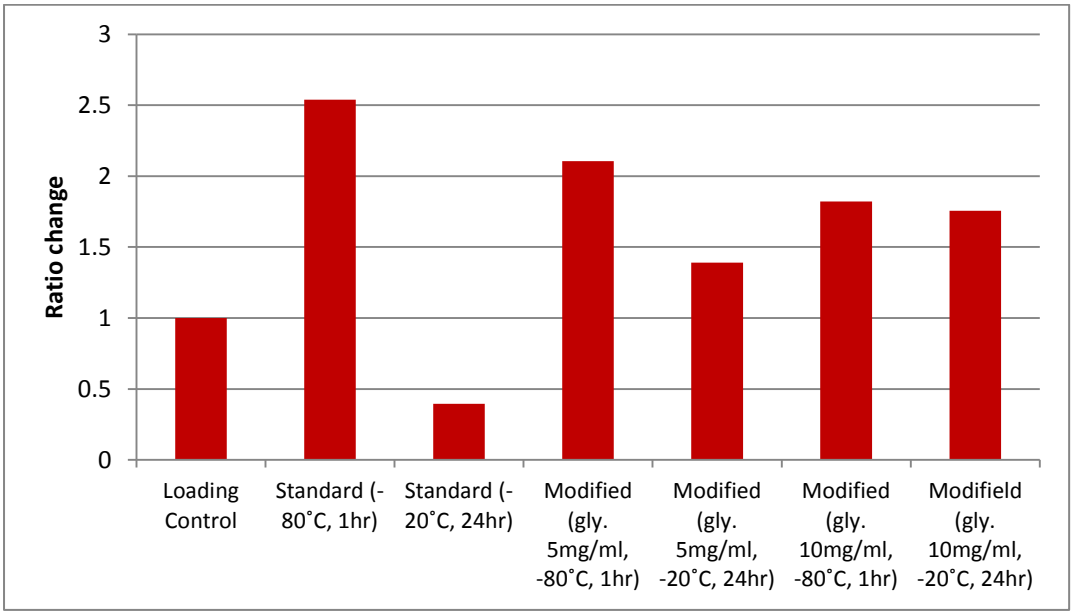

Figure 3.4 – Comparison of DNA purification by the standard procedure and the modified procedure, all with varied conditions. Most of the methods tested were successful in purifying and concentrating the DNA aptamers, with the exception of the standard protocol using glycogen at a concentration of 5mg/ml with incubation conditions of -20˚C for 24 hours. The standard procedure, with incubation at -80˚C for 1 hour purified the DNA aptamers most effectively, with a ratio change of over 2.5.

Values from ImageJ confirmed the results observed on the agarose gel. The standard procedure, where the DNA was incubated at -20˚C for 24 hours resulted in two-thirds of the aptamers being lost. All other DNA purification methods were able to concentrate the aptamers, with the most effective method being the standard protocol, with an incubation at -80˚C for 1 hour, which concentrated the aptamers to 2.5 x in comparison to the loading control. The standard procedure, incubating at -80 ˚C for 1 hour, was taken forward to maintain the integrity of SELEX selections.

3.2 Optimisation of cell-SELEX for use on primary cells

A feature of cell-SELEX is the ability to target a ligand towards biomarkers indicative of disease, present on the cell surface. Cell-SELEX is commonly performed on cell lines; however some novel biomarkers that exist within primary tissues may not be present within cell lines. SELEX selection using whole cells could elucidate novel biomarkers whilst also producing a targeting ligand, however the number of cells used to select specific aptamers is usually in the hundreds of thousands to millions range. If using primary cells, this number of cells may not be available, as short-term cultures reach confluence slowly, in comparison to cell lines. A cell-SELEX procedure that could be used to identify aptamers using small numbers of cells was investigated. The cell-SELEX protocol was optimised using cell lines to determine the lowest cell number that would return bound aptamers, which could be amplified sufficiently. The smallest cell number was then taken through 5 iterative rounds of cell-SELEX. The amplification stage, via TD-PCR, was optimised during each round by determining the optimal number of TD-PCR phase two cycles. The cycle number which amplified aptamers without amplifying non-specific sequences dictated the optimal number of phase two TD-PCR cycles.

3.2.1 Minimum cell number to return bound DNA aptamers

Identification of aptamers using a small number of cells would circumvent limitations incurred by small amounts of biological material. One round of cell-SELEX was undertaken using the cell lines SVGp12 and U87MG, eluted aptamers were then amplified using the optimised TD-PCR programme (see Section 3.1.2). Initially cell-SELEX was performed on a range of cell numbers between $500x10^3$ to $32x10^3$ cells, and it was shown that aptamers could be amplified through all cell numbers tested (data not shown). This was taken further and tested on smaller cell numbers, using $32x10^3$ down to $0.1x10^3$ cells (Fig 3.5).

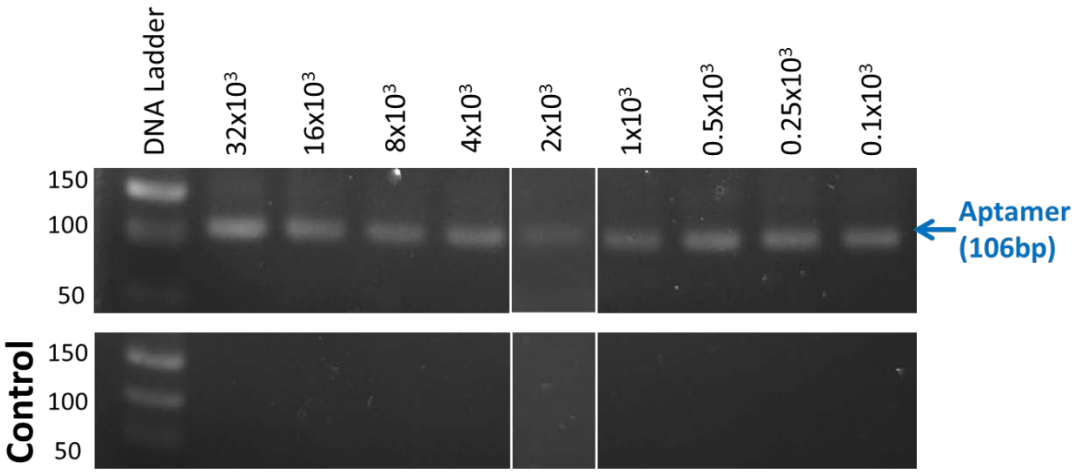

Figure 3.5 – Determination of the lowest cell number to return bound aptamer through the use of cell lines. Bands were visible across all cell numbers near 100bps, with the exception of $2x10^3$ cells. No bands were present within the controls. Increases in band intensity can be seen when using $32x10^3$ cells; however saturation occurs throughout the bands present thereafter.

Aptamers were successfully eluted and amplified following one round of selection using each cell number. Similar levels of amplification was seen between $16x10^3$ and $0.1x10^3$ cells, which showed that similar amounts of aptamers were eluted from these cell numbers. Aptamers were successfully eluted and amplified from 100 cells, showing that aptamers may be identifiable using this small number of cells.

3.2.2 Optimisation of amplification during each round of Cell-SELEX using minimal cell number.

Aptamers that are not specific to the target are mainly lost during the first one or two rounds of selection, thereby reducing the amount of aptamers that would be eluted and entered in to amplification. As template concentration has an effect on amplification, 100 cells were used through 5 iterative rounds of cell-SELEX to ensure sufficient amounts of aptamer could still be eluted and amplified. The amplification stage was optimised during each round of selection, by determining the optimal number of TD-PCR phase two cycles; this step was added to maintain the specificity of the TD-PCR programme when amplifying small amounts of eluted aptamer (Fig 3.6).

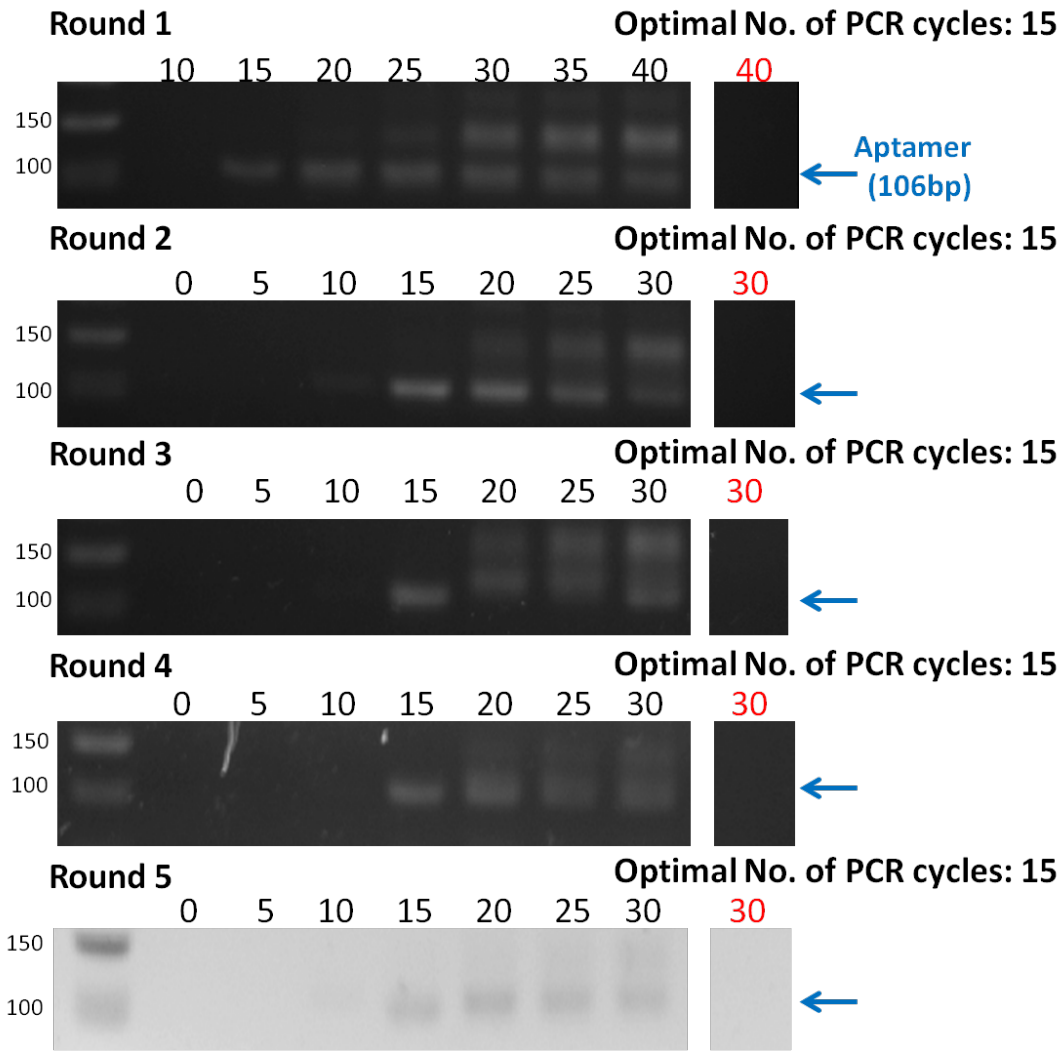

Figure 3.6 – Optimisation of TD-PCR cycle number during 5 iterative rounds of Cell-SELEX using 100 cells. The 2 % agarose gels showed 15 cycles of TD-PCR to be universally optimal across Cell-SELEX selections, with non-specific bands presenting with increased amplification. Phase one cycles were during 0-10 cycles, and phase two cycles were during 15-40 cycles. The agarose gel for round 5 was inverted to make the bands more visible**.**

Figure 3.6 shows 2% agarose gels, used to visualise amplified DNA aptamers from five iterative rounds of SELEX using 100 cells. Fifteen phase two cycles of TD-PCR were universally optimal, showing one band 106bps in length throughout all 5 rounds of cell-SELEX selection. Non-specific bands appeared at 150bps with 20 cycles or more. The agarose gels verified that aptamers could be amplified throughout 5 rounds of cell-SELEX using 100 cells.

3.2.3 Novel DNA aptamer sequences

Following five rounds of optimised cell-SELEX using 100 cells, DNA aptamers were cloned in to pCR 2.1 TOPO plasmids and positive inserts were checked by colony PCR. PCR products were separated on a 2% agarose gel and visualised to determine whether positive aptamer inserts were present (Fig 3.7).

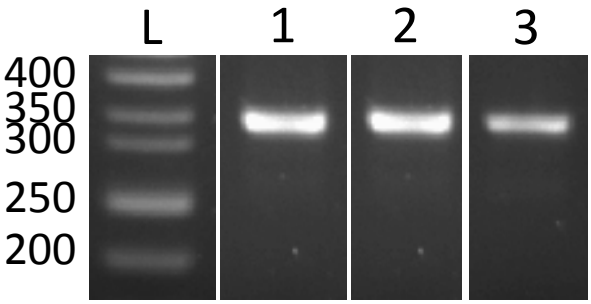

Figure 3.7 – Colony screening for positive aptamer insert into pCR 2.1 plasmids. Visible colonies were entered in to colony PCR to check for positive aptamer insert. Three colonies were positive for aptamer insert, displaying a bright band at 308 bps in length, which corresponds to the 106 bp aptamer and 202 bps between the M13 primer sites.

Following visualisation, three colonies were positive for aptamer insert (Fig 3.8). The positive clones were purified by a commercially available kit, and novel DNA aptamer sequences were elucidated by Sanger sequencing. Aptamer sequences were determined by the presence of the aptamer primer sites or the complementary aptamer primer sites (Table 3.2).

Table 3.2 – Aptamer primer sequences and their respective complementary sequence.

	Aptamer primers (5' - 3')	Complementary aptamers primers (3' – 5')
Forward sequence	ATCCTAATACGACTCACTAT	ATAGTGAGTCGTATTAGGAT
Reverse sequence	AATTCTGCGGTAAACTCGAGGG	CCCTCGAGTTTACCGCAGAATT

Before SELEX selection, the aptamers are present as double stranded DNA prior to being denatured in to single stranded DNA; therefore, for each unique aptamer within the starting pool, a complementary aptamer sequence also existed. Consequently, whether the 'sense' aptamer (5`-3`) or the complementary 'anti-

sense' aptamer (3'-5') was the specific sequence that interacted with the target was unknown until validation studies were carried out. Only the M13 forward read was sequenced during Sanger sequencing. The assumption that the unknown sequence would complement the forward read via Watson-Crick base pairing was taken in-order to elucidate the M13 reverse sequence (Table 3.3).

Table 3.3 – Aptamer and complementary aptamer sequences selected towards the primary cell cultures U87MG. Primer sites are highlighted in dark red (forward) and light blue (reverse), as are the complementary primer sequences which are highlighted in red (forward) and blue (reverse). Sequences in bold were elucidated by Sanger sequencing, those that are not in bold were elucidated based on complementation to the sequenced sense or anti-sense strand**.**

Sequence name	Aptamer sequence (Sense sequence, 5'-3')	Complementary aptamer sequence (Anti-sense sequence, 3'-5')
U87CLL1	**ATCCTAATACGACTCACTAT**AGG GAGAGAATTCGTGTGTGTTGCTT CGGTTTTGGCAAAAGGTTGGAGC GAAGGGTTGGGCCAG**AATTCTGC GGTAAACTCGAGGG**	**CCCTCGAGTTTACCGCAGAATTCTG GCCCAACCCTTCGCTCCAACCTTTTG CCAAAACCGAAGCAACACACACGA ATTCTCTCCCTATAGTGAGTCGTATT AGGAT**

Three clones were shown to be positive for aptamer insert, however only one sequence was able to be sequenced (Table 3.3). As there were no other sequences for comparison, Clustal Omega analyses were not performed.

3.2.4 Structural determination of aptamer sequences.

Both sense and anti-sense aptamer sequences were entered in to MFold to predict secondary structures that the aptamers may conform to. The varied conditions entered into the MFold programme were matched to how aptamer selections were produced. Prior to selection, the aptamers were denatured and snap-cooled on ice to produce single-stranded DNA (ssDNA) aptamers. It was during this step that the aptamers folded into three-dimensional structure based on the sequences; therefore a temperature of 4˚C was inputted into MFold to match the temperature of the snap-cooling process. During the denaturing process, the aptamers were contained in a selection buffer containing ions that could impact the aptamer

structure. To match the buffer conditions, Mg^{2+} and Na^{+} concentrations of 1 mM and 5 mM were also inputted in to Mfold. The predicted structures could help determine whether aptamers have similar shapes (Fig 3.8).

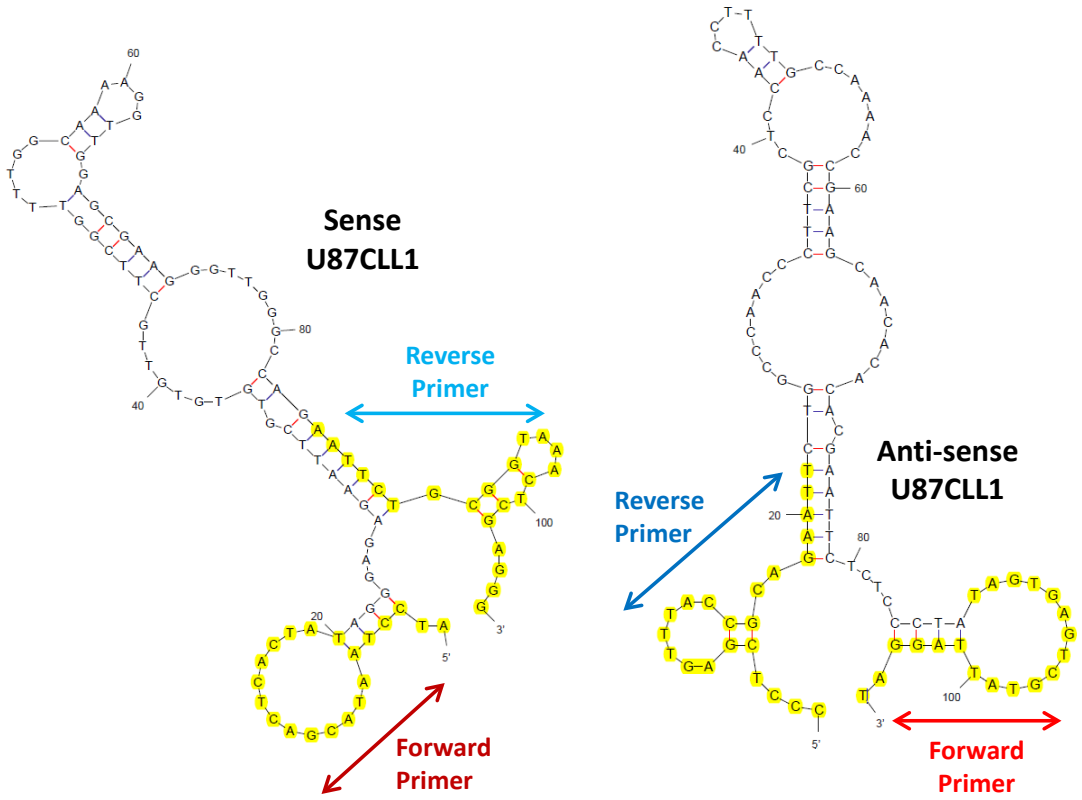

Figure 3.8 – Predicted secondary structure of novel DNA aptamer sequences selected towards U87MG, determined by MFold software. Primer sites are highlighted, with arrows depicting the location of the forward (red) and reverse (blue) primers**.**

3.3 Identification of DNA aptamers towards primary cells using tailored cell-SELEX procedure.

With the cell-SELEX protocol fully optimised for 100 cells, the methodology was applied to primary cultures. Aptamers were negatively selected towards normal human astrocyte (NHA) cells and positively selected towards two short-term cell cultures, BTNW390 and BTNW914.

3.3.1 DNA aptamer recovery during each round of Cell-SELEX towards primary cultures.

The aptamer library was amplified before being negatively selected against NHA cells; the supernatant was then positively selected towards either BTNW390 or BTNW914 glioblastoma short-term cultures. The cell-SELEX procedure was performed as previously optimised (Fig 3.6). TD-PCR products were visualised after each round of selection to confirm amplification of the aptamer sequences (Fig 3.9).

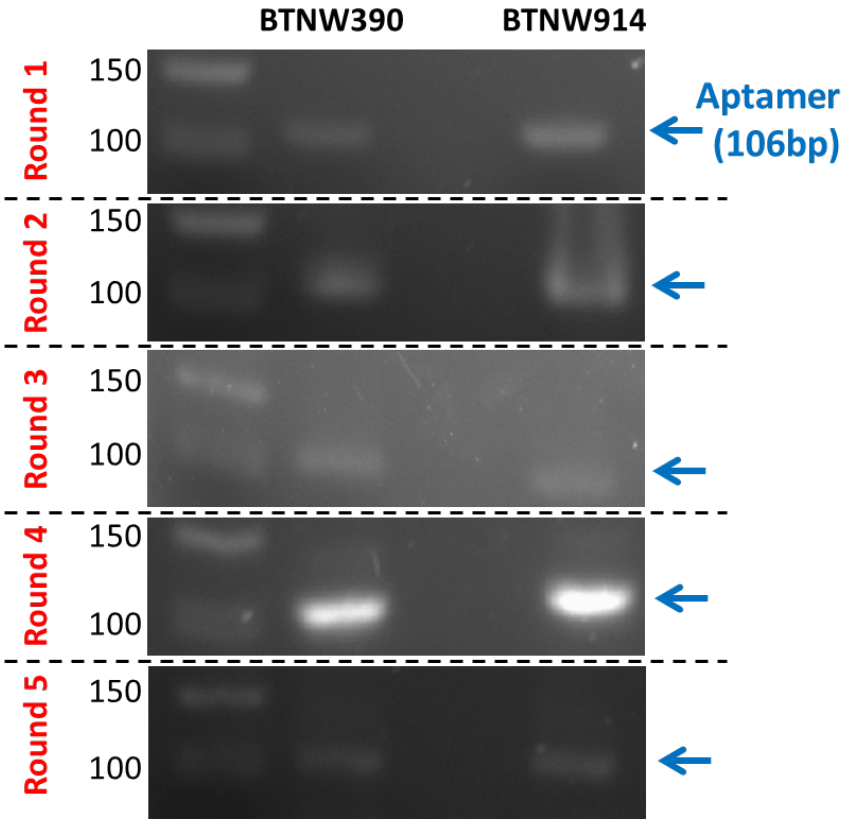

Figure 3.9 – DNA aptamers following recovery and amplification after each round of Cell-SELEX selection. Aptamers were eluted and amplified via TD-PCR after each round of selection, which was visualised to check aptamers were still present. Round 4 was an exception were the aptamers were visualised after purification and not after amplification. Bands are present at 106bps throughout each round of selection; however primer dimers at 50 bps are visible after round 5.

Following visualisation by gel electrophoresis, amplified DNA aptamers were still present after each round of cell-SELEX selection (Fig 3.9). Amplified aptamers eluted from the primary cells after round 5 of cell-SELEX were not purified by ethanol precipitation. This was to ensure the DNA aptamers retained the polyA tail, added by *Taq* polymerase, required for cloning into a pCR 2.1 vector.

Selected aptamers were ligated in to a pCR 2.1 vector and transformed into chemically competent DH5α *E.coli*, before selection on LB agar containing

ampicillin. Colonies were subsequently utilised in a PCR reaction to check for positive aptamer inserts. PCR products were separated and visualised on a 2% agarose gel (Fig 3.10).

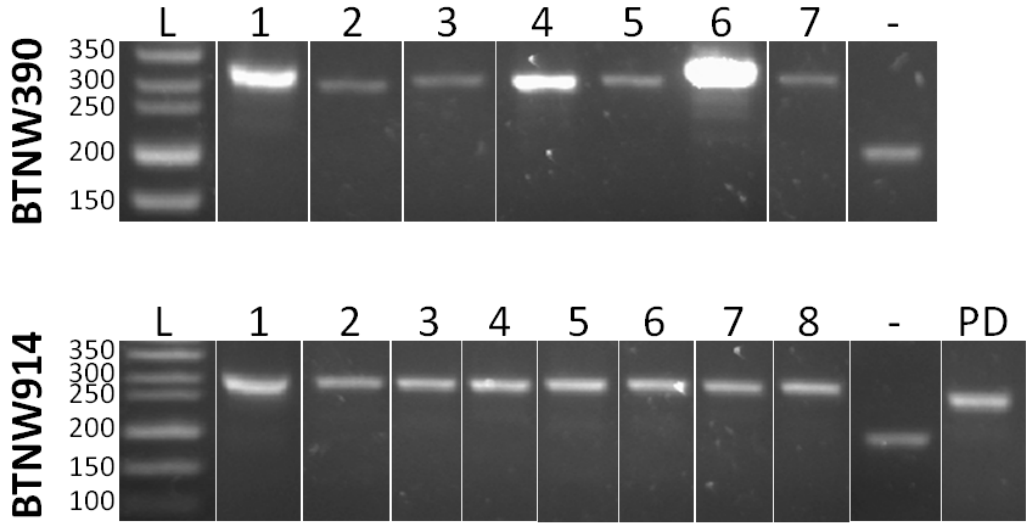

Figure 3.10 – Colony screening for positive aptamer insertion into pCR 2.1 plasmid. Transformants were checked for positive aptamer insertion into the pCR 2.1 plasmid via colony PCR. PCR products were separated and visualised on a 2% agarose gel. Seven colonies for aptamers derived against BTNW390 and eight colonies for aptamers derived against BTNW914 tested positive for aptamer insertion, displaying a band 308 bps in length. Negative colonies (-) for aptamer insertion were observed with bands corresponding to the bases between the primer sites within the plasmid at 202bps in length. One plasmid displaying a 50bp insertion was shown, this was likely to be a primer-dimer (PD) produced during amplification within the last round of cell-SELEX.

Seven colonies tested positive for the aptamer insert, which were isolated from cell-SELEX selections using BTNW390 primary cells. Bright bands at 308bps in length were observed for these colonies, which was indicative of the length between the M13 primer sites (202bps) with the addition of the 106bp aptamer. Eight colonies tested positive for the aptamer insert by displaying a band 308bps in length, which was isolated through cell-SELEX using BTNW914 short-term cultures. Colonies negative (-) for insert (202bps) was observed whilst screening for positive aptamer insert isolated against both short-term cell cultures, whilst one plasmid with a 50bp insert was only found for BTNW914.

3.3.3 Novel DNA aptamer sequences

The plasmids were sequenced via Sanger sequencing using the M13 forward primer. The identified sequences are shown in Table 3.4. Aptamers that were identified through the M13 forward read are highlighted in bold and the assumed sequences are not in bold. From 7 of the positive plasmids containing aptamers derived against BTNW390, one failed to be sequenced. One aptamer, CLL001(U), was observed in 57% of isolated plasmids, which were positive for inserted aptamers selected towards BNTW390. The same aptamer was also present in 38% of positive plasmids containing aptamers selected towards BTNW914. Another aptamer, CLL002(U), was found once in plasmids containing aptamers selected towards both BTNW390 and BTNW914. Overall one unique aptamer was identified towards BTNW390 and four unique aptamers was identified towards BTNW914. Two universal aptamers were identified that may be specific to a target found within both short-term cultures.

The sense sequences were put through the Clustal Omega sequence alignment software (available: http://www.ebi.ac.uk/Tools/msa/clustalo/) to determine similarities between the sequences. The anti-sense sequences were not used for Clustal as these sequences are complementary and would reiterate the same information. Using information derived from Clustal, possible binding sites and positions of importance could be implicated which may allow the aptamer to be modified with confidence that the binding would not be impaired. Phylogenetic analysis grouped the sequences based on homology, the resulting families of sequences were separately analysed by Clustal Omega to elucidate similar positions. Sequence alignments were determined using the whole aptamer sequence, as possible binding sites may utilise the constant regions for stability. Although the primer sites were included with the sequences for analysis, they were removed from the diagrams for clarity.

Table 3.4 – Aptamer sequences and complementary sequences selected towards the primary cell cultures BTNW390 and BTNW914. Primer sites are highlighted in dark red (forward) and light blue (reverse), as are the complementary primer sequences which are highlighted in red (forward) and blue (reverse). Sequences in bold were elucidated by Sanger sequencing, those that are not in bold were elucidated based on complementation to the sequenced sense or anti-sense strand.

Sequence Name	Primary culture used for Cell-SELEX selections.	Aptamer sequence (Sense sequence, 5' – 3')	Complementary aptamer sequence (Anti-sense, 3' – 5')
CLL001(U)	BTNW390, BTNW914	**ATCCTAATACGACTCACTATAGGGAGAGAATTCCACGG CAGTGTCGTACGGATGAGGAAGTGAAGACGGGGAGGG AAGGAGTGGAATTCTGCGGTAAACTCGAGGG**	**CCCTCGAGTTTACCGCAGAATTCCACTCCTTCCCTCC CCGTCTTCACTTCCTCATCCGTACGACACTGCCGTGG AATTCTCTCCCTATAGTGAGTCGTATTAGGAT**
CLL002(U)	BTNW390, BTNW914	**ATCCTAATACGACTCACTATAGGGAGAGAATTCTCATCC CCGCGGAAATGACAAAGGACACCGATAACTAGACACCG TACTCTGAATTCTGCGGTAAACTCGAGGG**	**CCCTCGAGTTTACCGCAGAATTCAGAGTACGGTGTC TAGTTATCGGTGTCCTTTGTCATTTCCGCGGGGATG AGAATTCTCTCCCTATAGTGAGTCGTATTAGGAT**
CLL003	BTNW390	ATCCTAATACGACTCACTATAGGGAGAGAATTCAGTCAG GTCACTTATGGTGGGCATAGCTTATTAACATGGTCAAGT GGTATGAATTCTGCGGTAAACTCGAGGG	**CCCTCGAGTTTACCGCAGAATTCATACCACTTGACC ATGTTAATAAGCTATGCCCACCATAAGTGACCTGAC TGAATTCTCTCCCTATAGTGAGTCGTATTAGGAT**
CLL004	BTNW914	ATCCTAATACGACTCACTATAGGGAGAGAATTCAACAGG GGAGACTAGGATGTGAAATATTGCTGACTAAATGAAAA GGACCGGAATTCTGCGGTAAACTCGAGGG	**CCCTCGAGTTTACCGCAGAATTCCGGTCCTTTTCATT TAGTCAGCAATATTTCACATCCTAGTCTCCCCTGTTG AATTCTCTCCCTATAGTGAGTCGTATTAGGAT**
CLL005	BTNW914	ATCCTAATACGACTCACTATAGGGAGAGAATTCAGTCGG GTCACTTATGGTGGGCATAGCTTATTAACATGGTCAAGT GGTATGAATTCTGCGGTAAACTCGAGGG	**CCCTCGAGTTTACCGCAGAATTCATACCACTTGACC ATGTTAATAAGCTATGCCCACCATAAGTGACCCGAC TGAATTCTCTCCCTATAGTGAGTCGTATTAGGAT**
CLL006	BTNW914	**ATCCTAATACGACTCACTATAGGGAGAGAATTCCCGGT**	CCCTCGAGTTTACCGCAGAATTCCTGCGATCCCCCTC

		GGTGGGAAAGTGCTCGGGAGGTGGATTGGGGGAGGG GGATCGCAGGAATTCTGCGGTAAACTCGAGGG	CCCCAATCCACCTCCCGAGCACTTTCCCACCGGGAAT TCTCTCCCTATAGTGAGTCGTATTAGGAT
CLL007	BTNW914	ATCCTAATACGACTCACTATAGGGAGAGAATTCGGTGGT CCGGAAAAAGCAAGCAAACATGCACGTAAAGAGAAGGA GCTGCCGAATTCTGCGGTAAACTCGAGGG	**CCCTCGAGTTTACCGCAGAATTCGGCAGCTCCTTCTC TTTACGTGCATGTTTGCTTGCTTTTTCCGGACCACCG AATTCTCTCCCTATAGTGAGTCGTATTAGGAT**

Figure 3.11 – A phylogram of identified aptamers selected towards BTNW390 and BTNW914 short-term cultures, by Clustal Omega software. Clustal omega identified three different groups based on similarities between the sequences. Aptamers CLL002(U), CLL003 and CLL005 may share the same target or targets with similar protein configurations; the same applies to aptamers CLL001(U) and CLL004. The aptamers CLL006 and CLL007, selected against BTNW914, were separated in to their own groups potentially indicating different and unique targets compared to the rest of the aptamers.

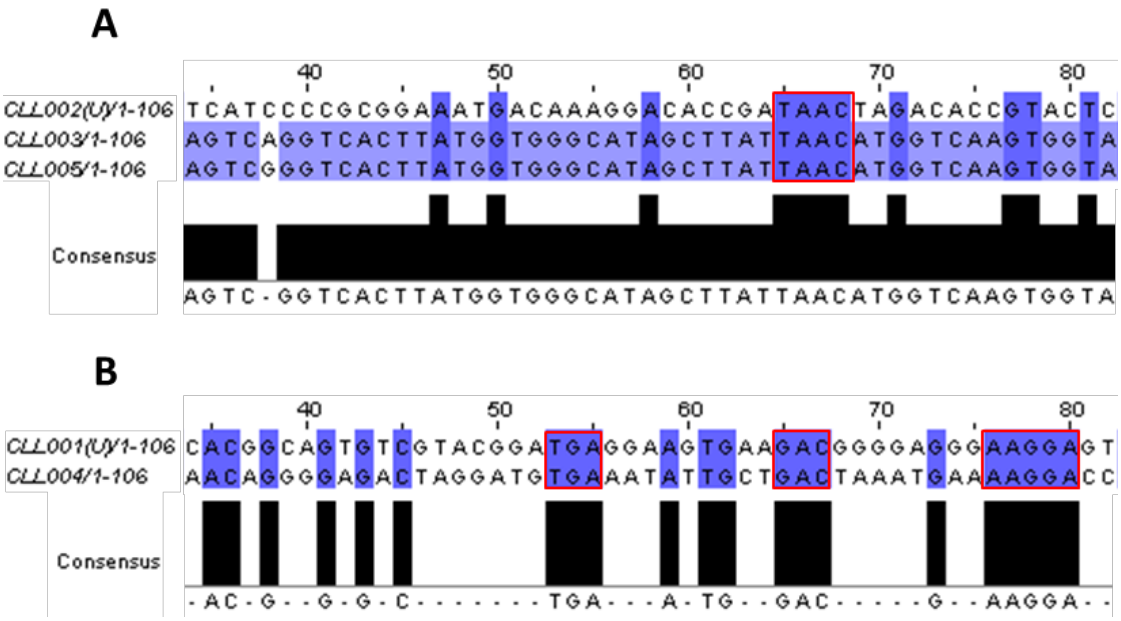

Figure 3.12 – Consensus sequences displaying similar bases within familial sequences identified towards short-term cultures, as determined by Clustal Omega software. Following phylogenetic analysis where sequences were grouped into families, the sequences were further analysed to determine where similarities are within each family. The first family of sequences (A), containing the aptamers CLL002(U), CLL003 and CLL005, several positions were conserved throughout the group including a TAAC sequence located at position 65 to position 68. The second family (B), consisting of the aptamers CLL001(U) and CLL004, showed 21 positions with

identical nucleotides, including a large AAGGA cluster located at position 76 to position 80.

The Clustal Omega software grouped the novel DNA aptamers in to three different families, of which one contained two sub-groups (Fig 3.11). Familial sequences were analysed within their sub-group to highlight where similar nucleotides are present. Aptamers CLL003 and CLL005 are 99.06% similar (Fig 3.12A), with the only difference being a 38G>A single base change within the CLL003 aptamer. CLL002(U) was the remaining member of the family and was isolated from cell-SELEX selections from both primary cultures. The nucleotide sequence TAAC can be seen from position 65 to position 68 within all three aptamer sequences. CLL001(U) shares multiple sites of homology with CLL004 (Fig 3.12B), and was isolated from individual selections from both primary cell cultures. Similarly to CLL002(U) and homologous aptamers CLL003 and 005, the aptamers CLL001(U) and CLL004 may bind a common target present on the cell surface of both primary cell cultures. CLL006 and CLL007 do not show a significant degree of homology with any of the aforementioned aptamers.

3.3.4 Structural determination of aptamer sequences

The sense and anti-sense aptamer sequences were entered in to MFold to predict secondary structures that the aptamers may produce. The varied conditions entered into the MFold programme were matched to how aptamer selections were produced. The predicted structures could help determine whether aptamers have similar shapes, and therefore determine which share common or unique targets. Combined with information from the Clustal Omega sequence alignment software, binding sites could also be predicted (Fig 3.13).

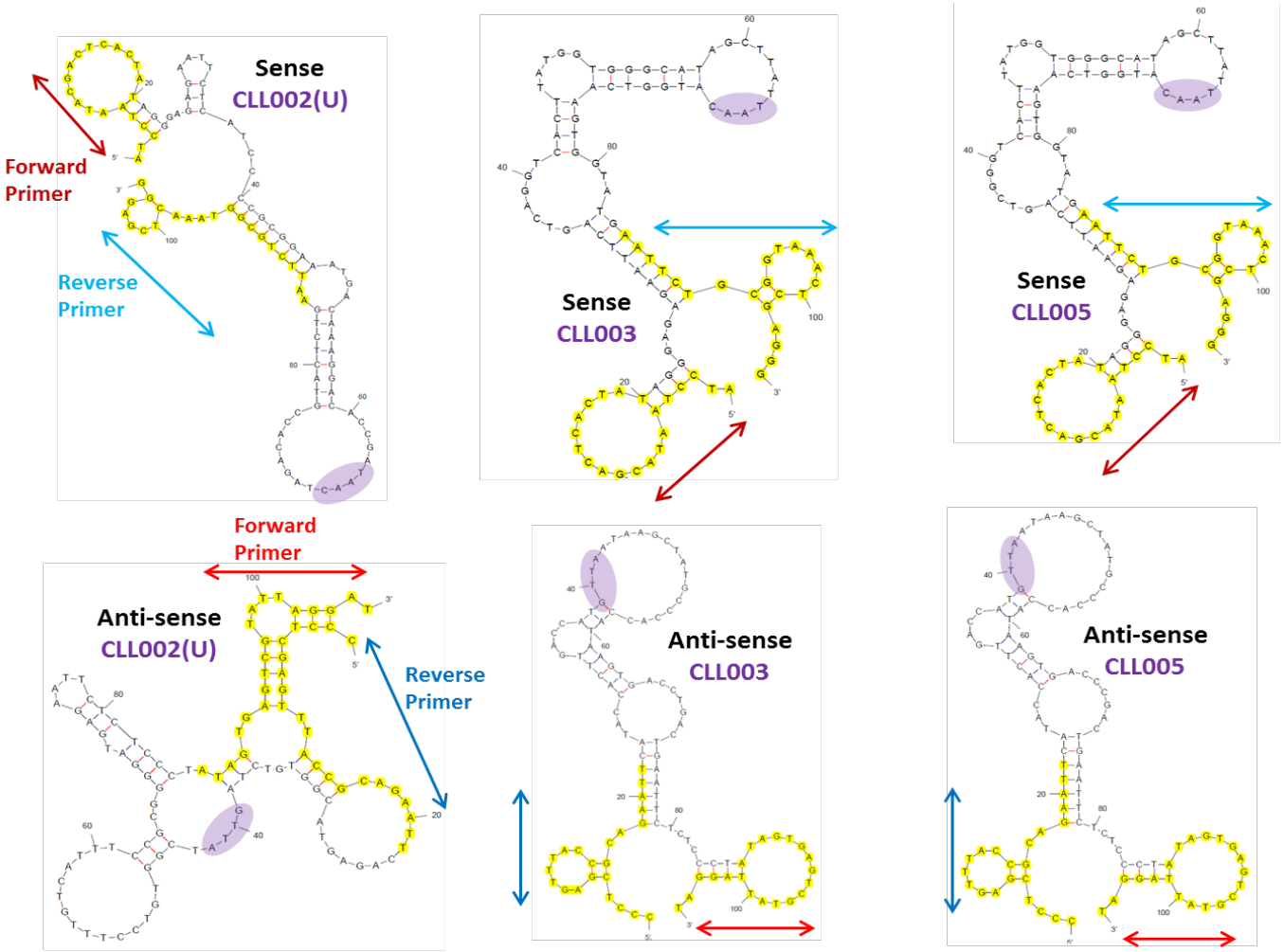

Figure 3.13 – Predicted secondary structure of novel DNA aptamer sequences selected towards short-term cell cultures and determined by MFold software. Points of similarity are highlighted (purple) within the sequences, which was determined using Clustal Omega software. Primer sites are highlighted, with arrows depicting the location of the forward (red) and reverse (blue) primers.

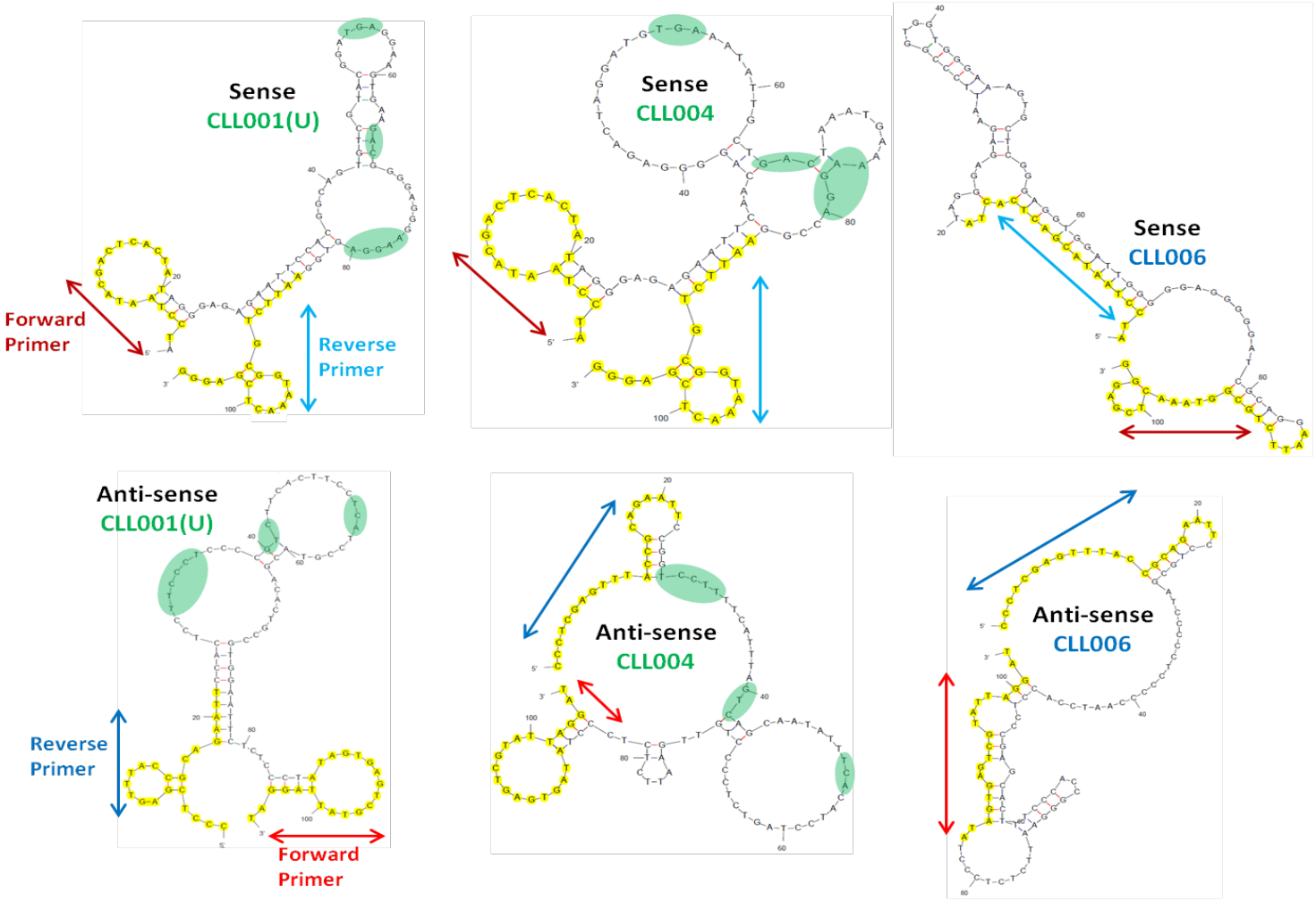

Figure 3.13 – Predicted secondary structure of novel DNA aptamer sequences, selected towards short-term cell cultures and determined by MFold software. Points of similarity are highlighted (green only) within the sequences, which was determined using Clustal Omega software. Primer sites are highlighted, with arrows depicting the location of the forward (red) and reverse (blue) primers.

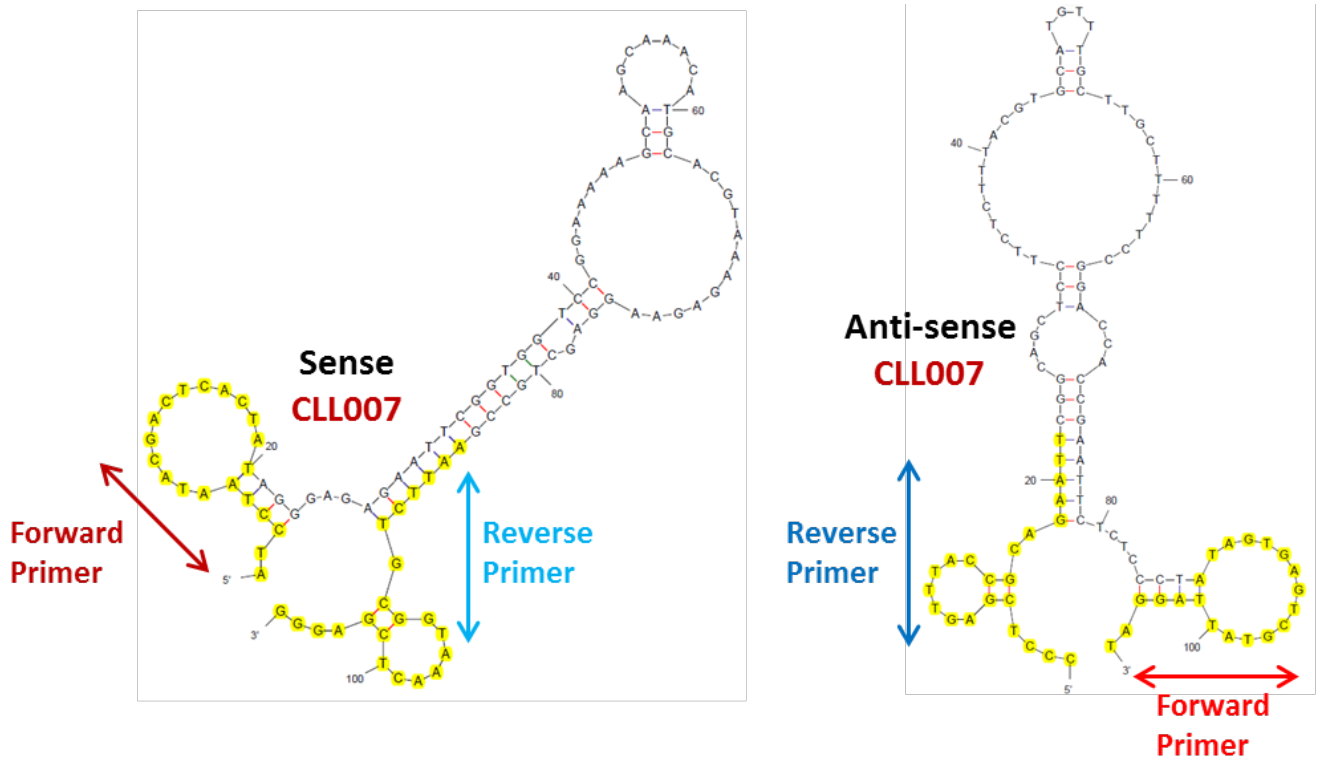

Figure 3.13 – Predicted secondary structure of novel DNA aptamer sequences, selected towards primary cell cultures and determined by MFold software. Primer sites are highlighted, with arrows depicting the location of the forward (red) and reverse (blue) primers.

3.3.5 Validating identified aptamers against primary cells

From the seven aptamers sequenced, two were chosen to be taken forward into validation studies. CLL001(U) and CLL002(U) were picked because these sequences were isolated towards both BTNW390 and 914. The aptamers were biotinylated so that the ABC system could be utilised to detect aptamer-protein interactions.

Native cell lysate was prepared from five glioblastoma tissue samples, which was analysed by Western blot. The biotinylated aptamers were used to probe the PVDF membrane to deduce whether the aptamers interacted with any proteins (Fig 3.14).

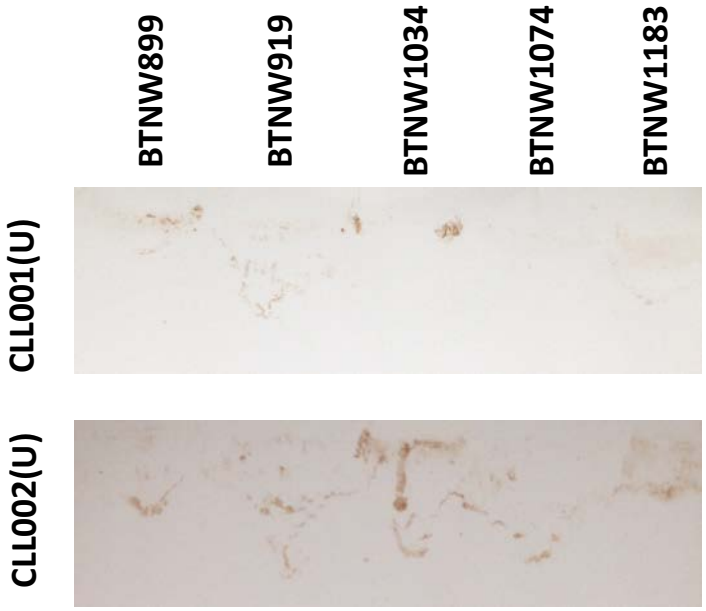

Figure 3.14 – Western blot analysis of native cell lysate from five glioblastoma tissue samples, using biotinylated CLL001(U) and CLL002(U) aptamers. Native cell lysate from five glioblastoma tissue samples were analysed by Western blot and probed with biotinylated aptamer to determine aptamer-protein interactions. No specific bands were present for either western blot and instead, non-specific staining was observed.

Following Western blot analysis, no specific interactions were observed for either aptamer tested. In contrast, non-specific staining of DAB was observed for both Western blots. Further analysis of these aptamers was produced by oligohistochemistry using tissue sections of BTNW390 and 914 (Fig 3.15). As these were the tissues used to identify the aptamers, they may be specific to a target only found on the cell surface of these tissues.

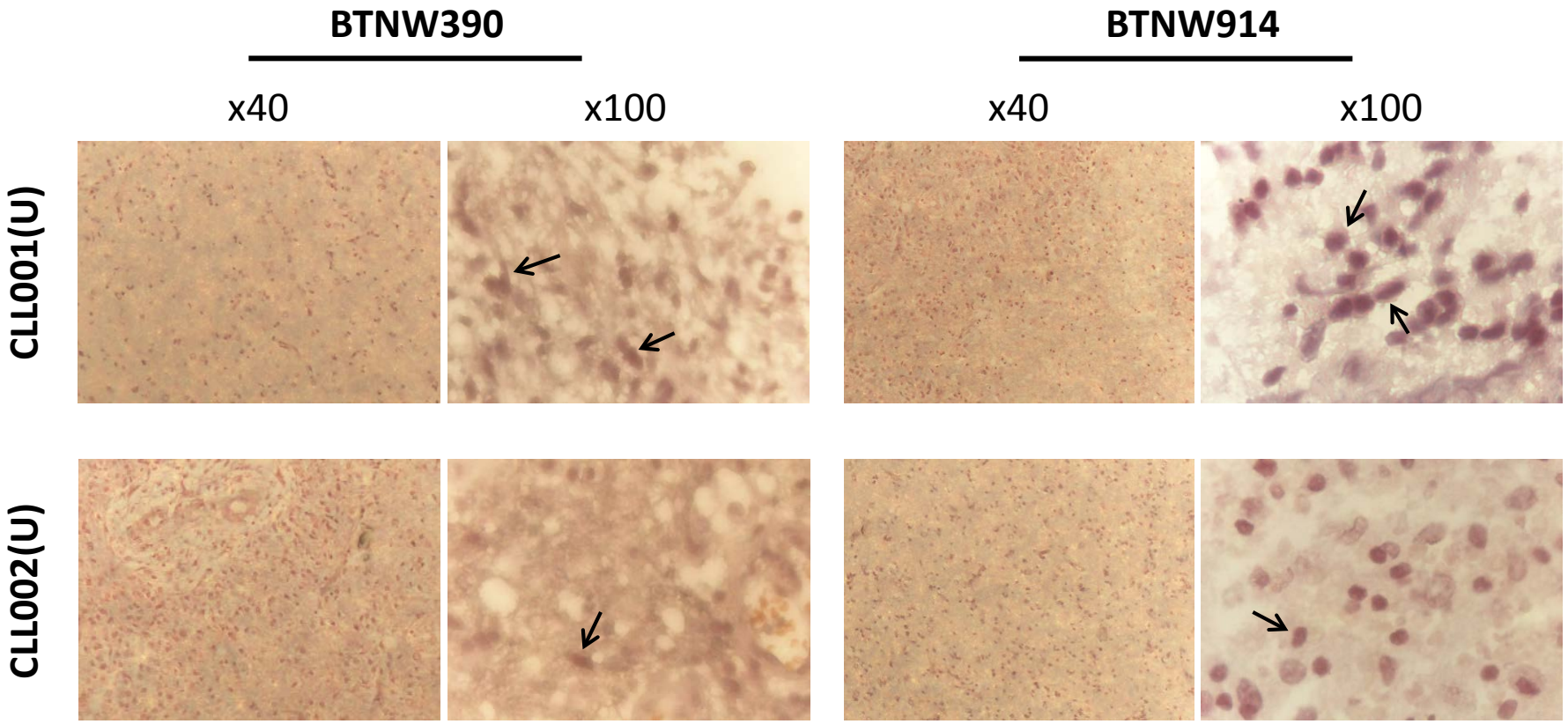

Figure 3.15 – Oligohistochemistry using the biotinylated CLL001(U) and CLL002(U) aptamers to detect aptamer-protein interactions within BTNW390 and BTNW914 tissue sections. BTNW390 and BTNW914 tissue sections were deparaffinised and probed with biotinylated aptamers derived from SELEX selections using short term cultures. Upon visualisation, cells can be seen throughout the tissue samples with brown cell surfaces (arrows), implicating aptamer-protein interactions.

The tissue sections indicated that the aptamers interacted with a protein on the cell surface of cells within the tissue sections. Facilitated by nuclei counterstaining, cellular membranes were seen to be more strongly stained brown by DAB, implicating aptamer-protein interaction on the cell surfaces.

3.4 Identification of DNA aptamers towards EGFRvIII peptide through tailored counter-SELEX.

Approximately 44% of glioblastoma cases exhibit *EGFR* amplification. Three-quarters of those with EGFRwt over-expressed co-express a truncated EGFR mutant that is constitutively active, known as EGFRvIII (Kancha *et al.*, 2013). As the mutation is cancer specific, aptamers targeted to the EGFRvIII may offer better therapeutic approaches. To identify aptamers specific to EGFRvIII, DNA aptamers were positively selected towards and identified against an immobilised EGFRvIII peptide. The counter-SELEX procedure was optimised during each round and selected aptamers were cloned, before being sequenced and their secondary structures predicted.

3.4.1 Optimisation of DNA amplification via TD-PCR during 6 rounds of Counter-SELEX

DNA aptamers were negatively selected against an immobilised full length EGFRwt protein; this was performed to produce aptamers that would specifically recognise EGFRvIII by filtering out aptamers that could bind EGFRwt. The remaining aptamers that did not bind EGFRwt were positively selected towards immobilised EGFRvIII peptide. The peptide can be found between the positions 6-19 within the whole EGFRvIII protein and signifies the points at which the 267 amino acid deletion occurs, along with a novel glycine insertion. During each round of selection, a small fraction of the eluted aptamers was used to optimise the number of TD-PCR phase two cycles and determine whether the aptamers were still present. Following optimisation of the TD-PCR programme, the remaining eluted aptamers underwent amplification and were visualised on a 2 % agarose gel (Fig 3.16).

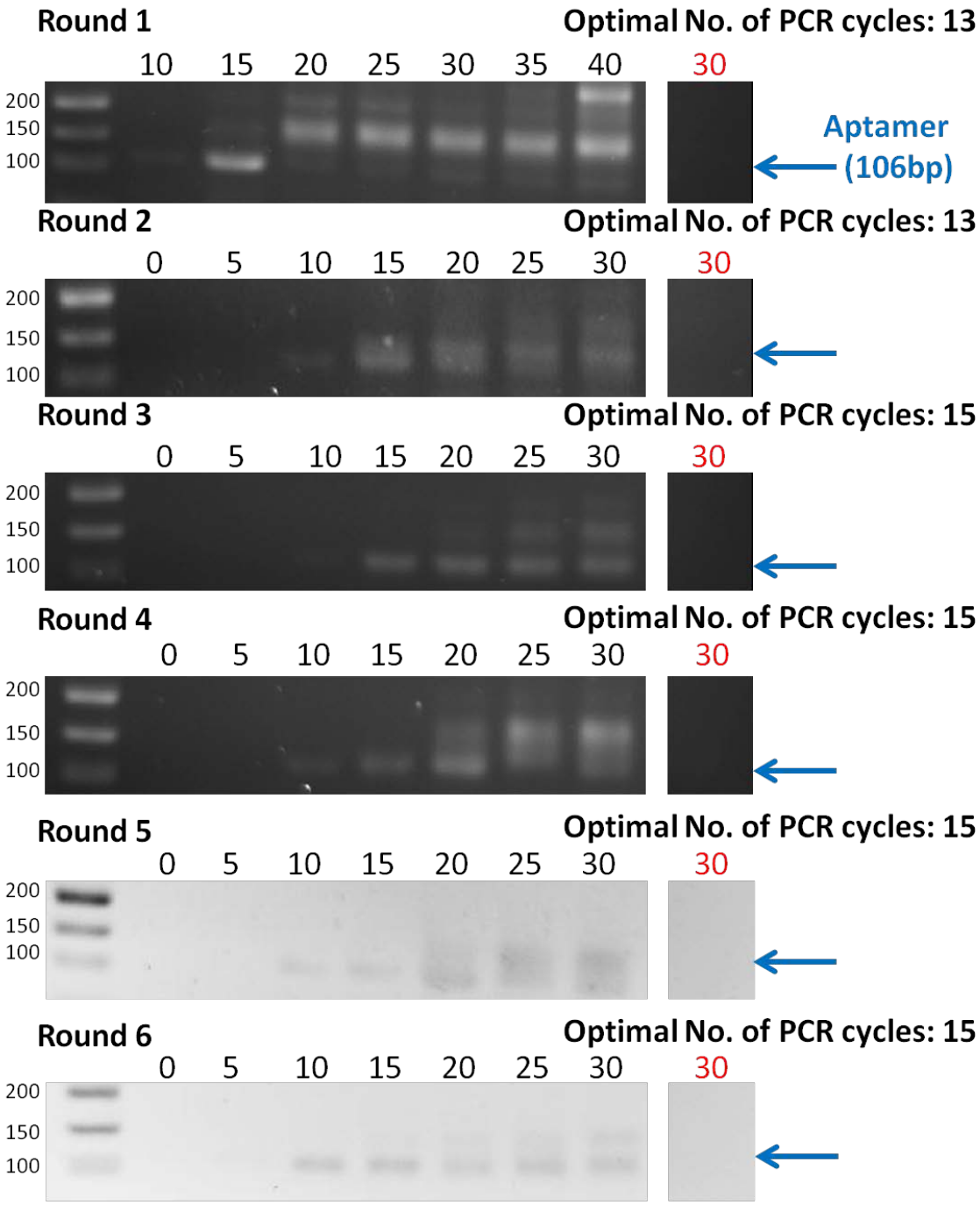

Figure 3.16 – Optimisation of the number of TD-PCR phase two cycles following EGFRvIII peptide selection. Amplification was optimal after 13 phase two cycles of TD-PCR during rounds 1 and 2, and 15 cycles for rounds of selection thereafter. Amplification of non-specific bands was detected after 15 cycles for rounds 1 and 2, whereas non-specific bands were seen after round 20 for rounds 3, 4, 5 and 6 of EGFRvIII peptide selection. No bands were visible in any control lanes; therefore data is shown only for 30 cycles (in red) for clarity. Agarose gels for rounds 5 and 6 were inverted to see the bands more clearly.

Following each round of counter-SELEX, the number of phase two cycles were optimised to produce specific sequences 106bps in length, required for enriching

the next round (Fig 3.13). After round 6 of counter-SELEX selection, amplified DNA aptamers were ligated in to a pCR 2.1 plasmid and transformed in to chemically competent DH5α *E.coli*. Visible colonies on selection plates were screened to identify colonies positive for insert. Colonies were picked and utilised in a standard PCR reaction, containing M13 sequencing primers, and visualised on a 2% agarose gel.

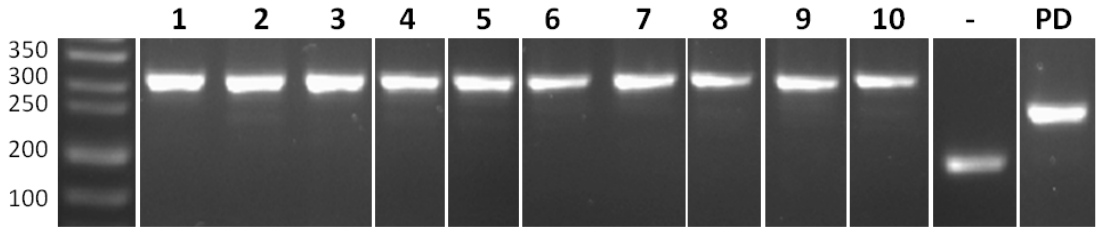

Figure 3. 17 – Colony PCR screening of chemically competent DH5α *E.coli* transformants for positive aptamer inserts. The agarose gel shows 10 pCR 2.1 plasmids positive for aptamer insert, 1 plasmid containing a 50bp primer dimer (PD) and 1 plasmid negative for any insert (-). The plasmids positive for aptamer insert corresponds to 308 bases, with the aptamer at 106 bases and the distance between the M13 primer sites being 202 base pairs long.

Ten colonies screened positive for aptamer insert, displaying a band at 308 base pairs (Fig 3.17). The bands correspond to the length of the aptamers, 106bps, and the sequences in between the M13 primer sites, 202bps. Two negative bands are present, one of which may be the result of a primer-dimer being ligated instead of aptamers and one where nothing was ligated into the plasmid, indicated by the 202bp band.

3.4.2 Identified novel DNA aptamer sequences, selected towards EGFRvIII

The plasmids positive for aptamer insert were purified through a commercially available kit and the sequences were elucidated through the M13 forward primer by Sanger sequencing. Sequences were determined by the presence of the aptamer primer sites and the complementary aptamers primer sites (Table 3.1).

The sequences identified by the M13 forward read was used to determine the complementary aptamer sequences, based on the assumption that they conformed to Watson-Crick base pairing. The sequences are listed in Table 3.3, with the

sequences identified through Sanger sequencing in bold. Sense aptamer sequences were put through Clustal Omega sequence alignment software to determine if there was any similarity between the sequences.

Table 3.5 – Identified novel DNA aptamer sequences selected towards EGFRvIII peptide following 6 rounds of Counter-SELEX. Primer sites are highlighted in dark red (forward) and light blue (reverse), as are the complementary primer sequences which are highlighted in red (forward) and blue (reverse). Sequences in bold were elucidated by Sanger sequencing, those that are not in bold were elucidated based on the sequenced sense or anti-sense strand.

Sequence	Aptamer sequence (5'-3')	Complementary aptamer sequence (3'-5')
EGFRvIII1	ATCCTAATACGACTCACTATAGG GAGAGAATTCATAGAATGGGGTC ACGAACGGCACCACACGACACAC AACATGAATTAAAAGAATTCTGC GGTAAACTCGAGGG	**CCCTCGAGTTTACCGCAGAATTCTTTTA ATTCATGTTGTGTGTCGTGTGGTGCCG TTCGTGACCCCATTCTATGAATTCTCTC CCTATAGTGAGTCGTATTAGGAT**
EGFRvIII2	**ATCCTAATACGACTCACTATAGG GAGAGAATTCAAGAAATTAAAC GACGGATAGACACAAGAAAGGA TCGAAACTATTTCTCAGAATTCTG CGGTAAACTCGAGGG**	CCCTCGAGTTTACCGCAGAATTCTGAGA AATAGTTTCGATCCTTTCTTGTGTCTATC CGTCGTTTAATTTCTTGAATTCTCTCCCT ATAGTGAGTCGTATTAGGAT
EGFRvIII3	ATCCTAATACGACTCACTATAGG GAGAGAATTCCAGGAAGGAAAA CAGTAGCGACCTCTAGGAAGGCG CAGCTAACGCCTACTGAATTCTGC GGTAAACTCGAGGG	**CCCTCGAGTTTACCGCAGAATTCAGTA GGCGTTAGCTGCGCCTTCCTAGAGGTC GCTACTGTTTTCCTTCCTGGAATTCTCTC CCTATAGTGAGTCGTATTAGGAT**
EGFRvIII4	**ATCCTAATACGACTCACTATAGG GAGAGAATTCGATACATACCAGC GCGACTGCAGAGACGAAGGGAA GGGAACGAAAGCTATGAATTCT GCGGTAAACTCGAGGG**	CCCTCGAGTTTACCGCAGAATTCATAGC TTTCGTTCCCTTCCCTTCGTCTCTGAAGT CGCGCTGGTATGTATCGAATTCTCTCCC TATAGTGAGTCGTATTAGGAT
EGFRvIII5	ATCCTAATACGACTCACTATAGG GAGAGAATTCGGTGGTCCGGAA	**CCCTCGAGTTTACCGCAGAATTCGGCA GCTCCTTCTCTTTACGTGCATGTTTGCTT**

	AAAGCAAGCAAACATGCACGTAA AGAGAAGGAGCTGCCGAATTCTG CGGTAAACTCGAGGG	**GCTTTTTCCGGACCACCGAATTCTCTCC CTATAGTGAGTCGTATTAGGAT**
EGFRvIII6	**ATCCTAATACGACTCACTATAGG GAGAGAATTCTCATCCCCGCGGA AATGACAAAGGACACCGATAAC TAGACACCGTACTCTGAATTCTG CGGTAAACTCGAGGG**	CCCTCGAGTTTACCGCAGAATTCAGAGT ACGGTGTCTAGTTATCGGTGTCCTTTGT CATTTCCGCGGGGATGAGAATTCTCTCC CTATAGTGAGTGGTATTAGGAT
EGFRvIII7	ATCCTAATACGACTCACTATAGG GAGAGAATTCAGAATGAGGAAAT AGGTAATCGCAATACGGAATAGG CCAGATATGACAGGGAATTCTGC GGTAAACTCGAGGG	**CCCTCGAGTTTACCGCAGAATTCCCTGT CATATCTGGCCTATTCCGTATTGCGATT ACCTATTTCCTCATTCTGAATTCTCTCCC TATAGTGAGTCGTATTAGGAT**
EGFRvIII8	**ATCCTAATACGACTCACTATAGG GAGAGAATTCGACGCAACGAAA CGGGGCAGGTATGGTCCGACCG AGGGACAGAAAAGCAAGAATTC TGCGGTAAACTCGAGGG**	CCCTCGAGTTTACCGCAGAATTCTTGAT TTTCTGTACCTCGGTCGGACCATACCTG CCCCGTTTCGTTGCGTCGAATTCTCTCCC TATAGTGAGTCGTATTAGGAT
EGFRvIII9	ATCCTAATACGACTCACTATAGG GAGAGAATTCAGAAGACAAAGG ACATAAGAGCTAACCAAGGGTAA ACGAAGAGGCACAGTGAATTCTG CGGTAAACTCGAGGG	**CCCTCGAGTTTACCGCAGAATTCACTGT GCCTCTTCGTTTACCCTTGGTTAGCTCTT ATGTCCTTTGTCTTCTGAATTCTCTCCCT ATAGTGAGTCGTATTAGGAT**
EGFRvIII10	ATCCTAATACGACTCACTATAGG GAGAGAATTCGAGCGGCTGAATA AACAAGGAAGCGCTACAAATTTA AATGAAGACTGCATGAATTCTGC GGTAAACTCGAGGG	**CCCTCGAGTTTACCGCAGAATTCATGC AGTCTTCATTTAAATTTGTAGCGCTTCC TTGTTTATTCAGCCGCTCGAATTCTCTC CCTATAGTGAGTCGTATTAGGAT**

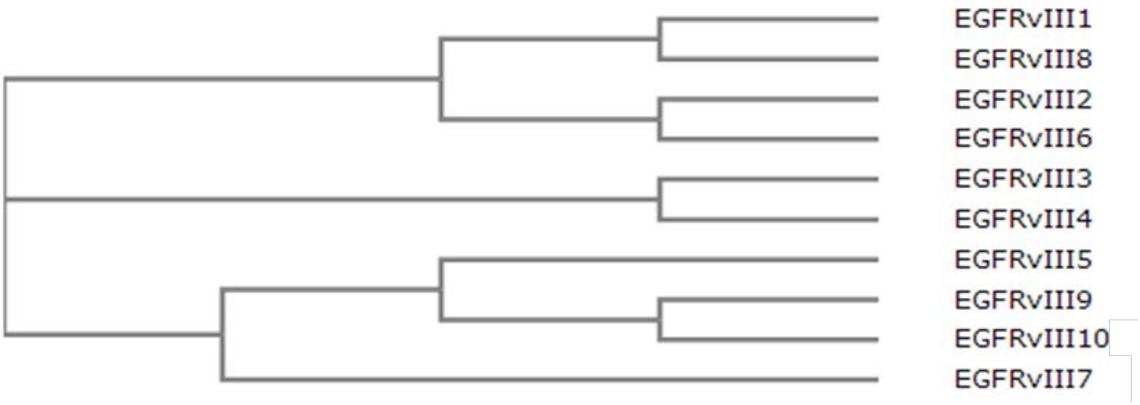

Figure 3.18 – Phylogram of identified novel aptamer sequences selected towards EGFRvIII peptide, determined by Clustal Omega. Clustal omega grouped the aptamers into three separate families with some containing sub-groups. Families and sub-groups were produced based on similarities between the sequences.

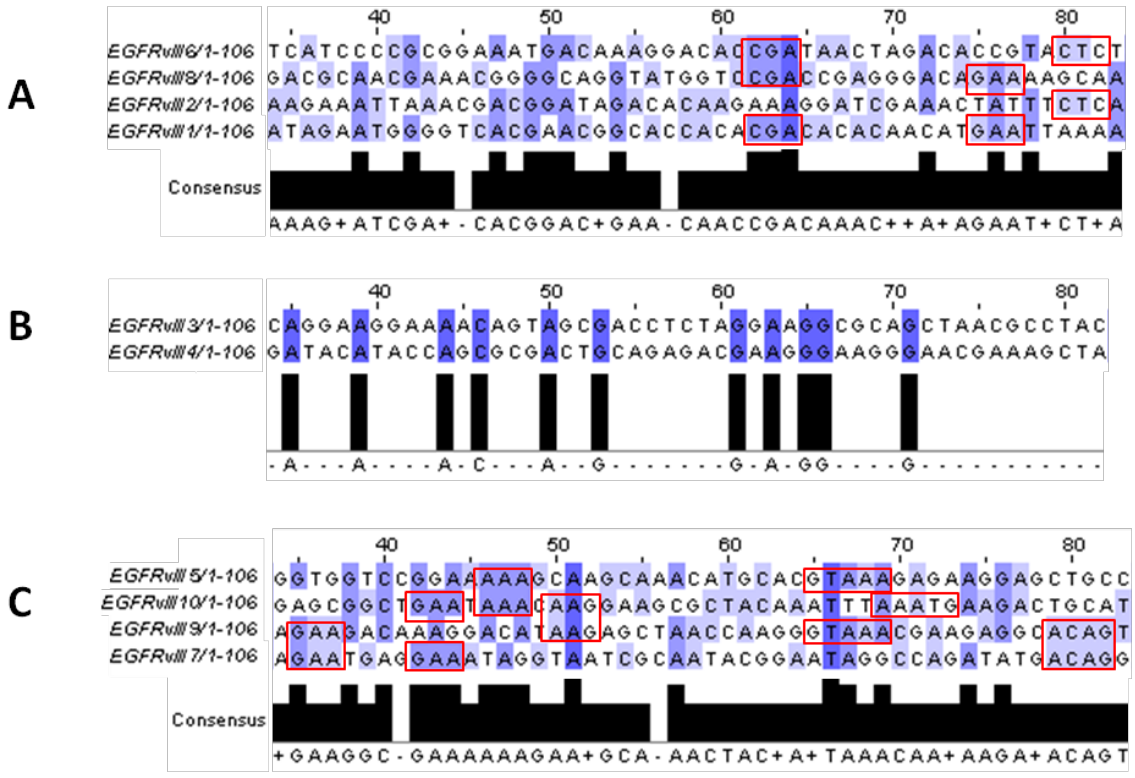

Figure 3.19 – Consensus sequences displaying similar bases within familial sequences identified towards primary cultures, as determined by Clustal Omega software. Clustal omega highlighted multiple sites of homology within family A. There was no similar sequence that was present within all sequences; therefore a possible binding site could not be suggested. There were small similarities between the two aptamers within family B and a possible binding site may be located between nucleotides 61 to 66. Multiple sites of homology are present within family C, including a GAA sequence present in all aptamers however was located at different positions in some sequences.

Clustal Omega grouped the sequences in to three different families (Fig 3.18); families A and C contained further sub-groups. These groups were based on nucleotide similarities within the aptamer sequences, as seen in Fig 3.19. Family A consisted of four aptamers, from two sub-groups. Similar sequences were seen throughout all novel aptamers, including CGA, GAA and CTC segments located at similar positions. Although these similarities were seen throughout the family of aptamers, no homologous sequence was seen in all aptamers. Family B did not present with large segments of similarity, but instead showed multiple positions where one or two nucleotides were similar. The largest family, family C, presented with many sites of similarity. A GAA was present in all sequences in exact positions, with some exceptions, and may represent a sequence of importance. The GAA segment within the EGFRvIII5 aptamer was one place out of position, at position 43 to 45 instead of 42 to 44. The segment was mirrored within the EGFRvIII9 sequence with the nucleotide sequence of AAG instead of GAA, as GAA and AAG segments were present multiple times for some aptamers. A large segment of GTAAA was found in both EGFRvIII5 and EGFRvIII9. This sequence was not present within EGFRvIII7; however the mirrored sequence, AAATG, was observed at a similar position in the aptamer EGFRvIII10.

3.4.4 Structural determination of aptamers identified towards EGFRvIII peptide

The sense and anti-sense aptamer sequences were put through Mfold to predict the secondary structures the aptamers may conform to (Fig. 3.20). The conditions entered in to MFold were as described in section 3.3.4.

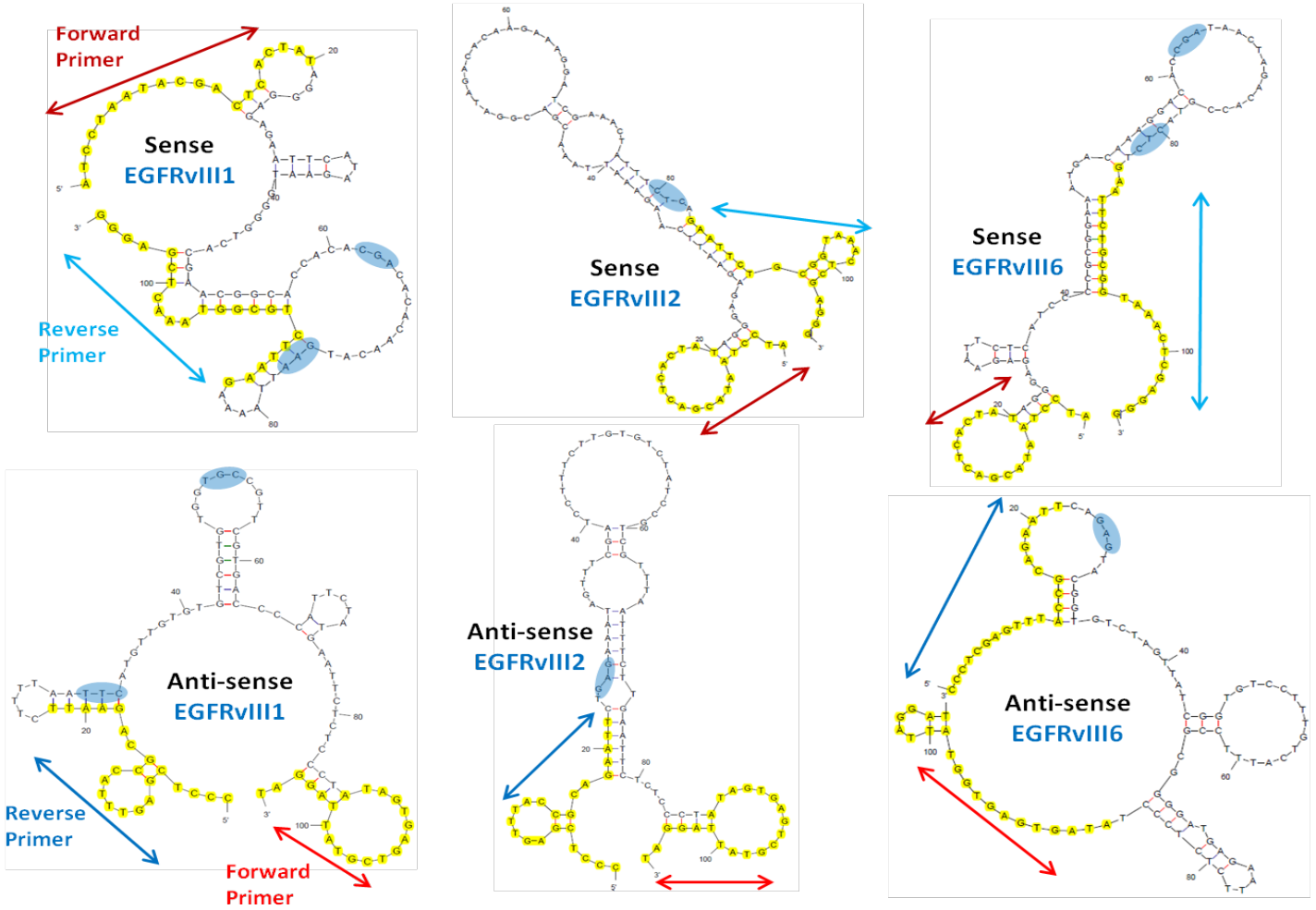

Figure 3.20 – Predicted secondary structure of novel DNA aptamer sense sequences, selected towards an EGFRvIII peptide and determined by MFold software. Points of similarity are highlighted (blue) within the sequences, which was determined using Clustal Omega software. Primer sites are highlighted, with arrows depicting the location of the forward (red) and reverse (blue) primers.

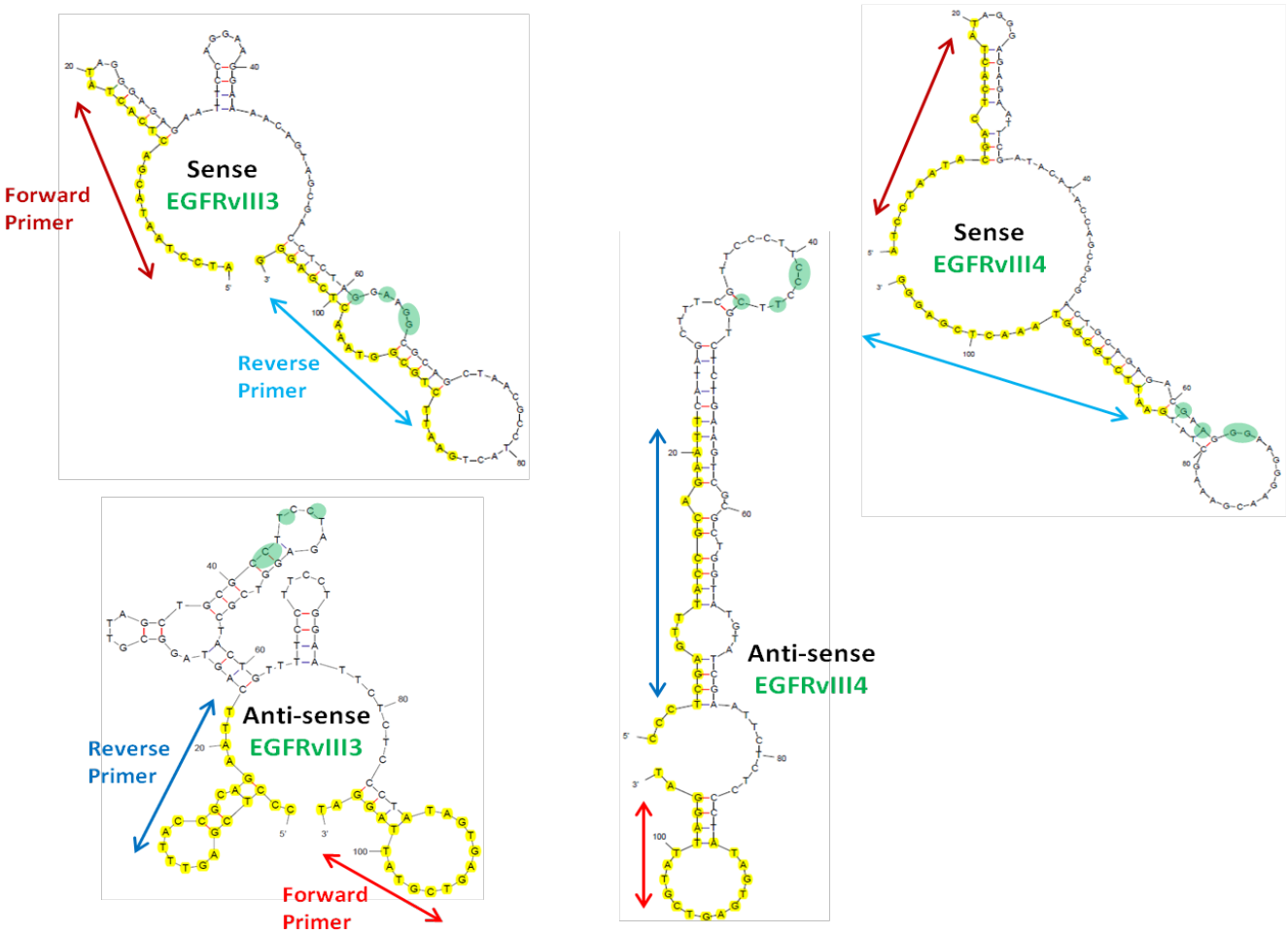

Figure 3.20 – Predicted secondary structure of novel DNA aptamer sense sequences, selected towards an EGFRvIII peptide and determined by MFold software. Points of similarity are highlighted (green) within the sequences, which was determined using Clustal Omega software. Primer sites are highlighted, with arrows depicting the location of the forward (red) and reverse (blue) primers**.**

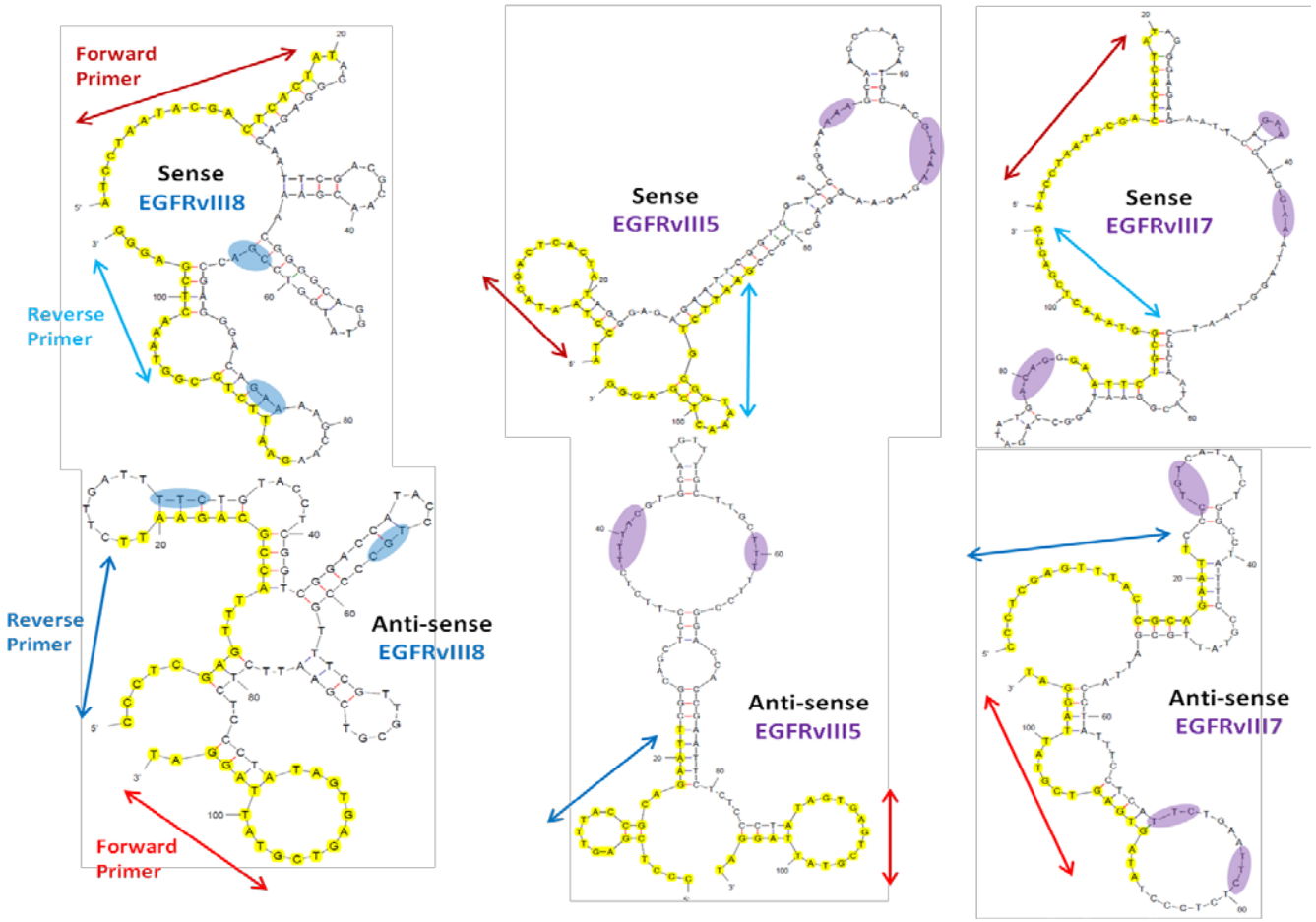

Figure 3.20 – Predicted secondary structure of novel DNA aptamer anti-sense sequences, selected towards an EGFRvIII peptide and determined by MFold software. Points of similarity are highlighted (blue and purple) within the sequences, which was determined using Clustal Omega software. Primer sites are highlighted, with arrows depicting the location of the forward (red) and reverse (blue) primers**.**

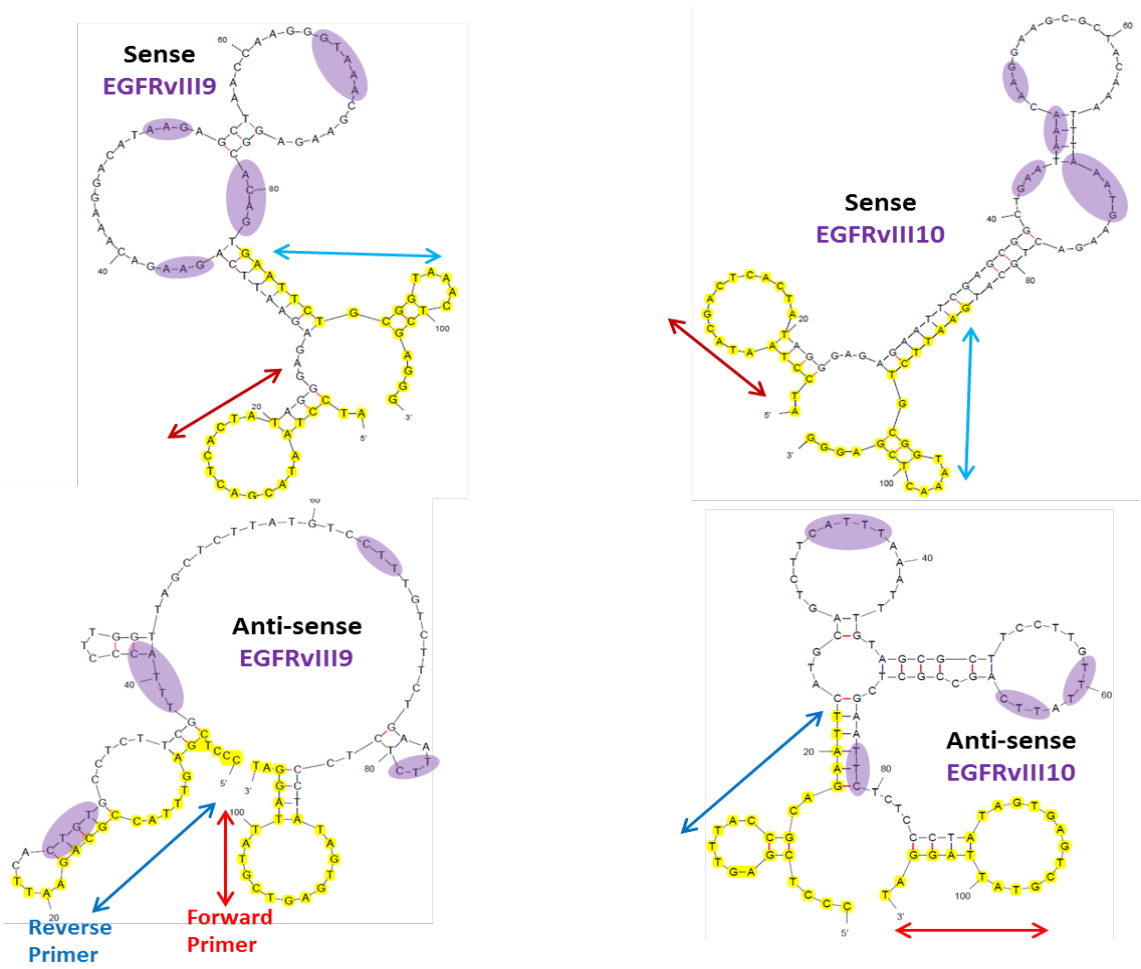

Figure 3.20 – Predicted secondary structure of novel DNA aptamer sequences, selected towards an EGFRvIII peptide and determined by MFold software. Points of similarity are highlighted (purple) within the sequences, which was determined using Clustal Omega software. Primer sites are highlighted, with arrows depicting the location of the forward (red) and reverse (blue) primers.

3.4.5 Validation of novel DNA aptamers, targeted towards an EGFRvIII peptide

Four aptamers from ten were chosen based on dissimilarities and GT content. The isolated aptamers, EGFRvIII3, 6, 7 and 8 were biotinylated and further utilised in Western blot analyses to determine whether the aptamers interacted with a target. Native cell lysate was derived from five glioblastoma tissue samples, all of which were positive for *EGFR* amplification. Whether these samples were EGFRvIII positive or not, was unknown. Native cell lysates were analysed by Western blotting and the biotinlyated aptamers were used to probe the PVDF membranes (Fig 3.21).

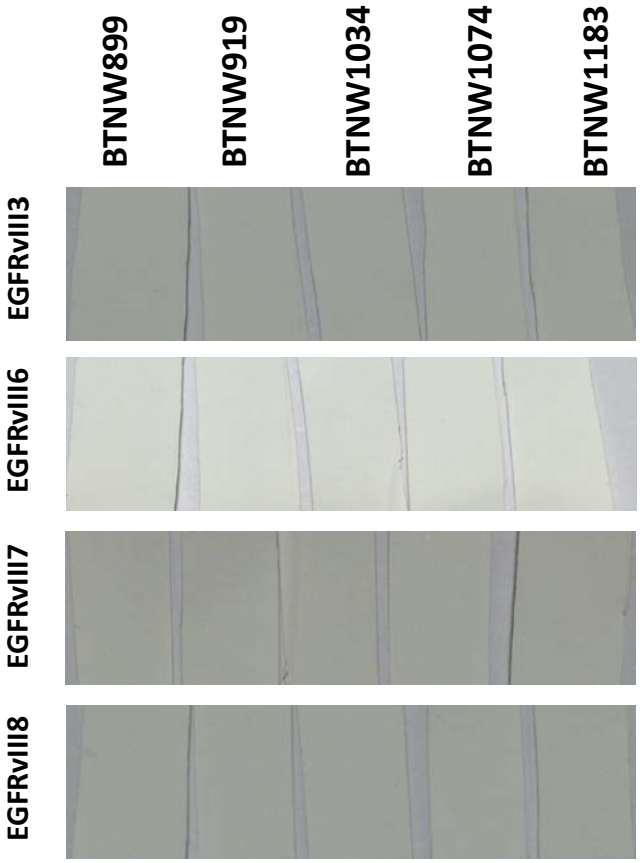

Figure 3.21 – Western blot analyses of native cell lysate from five *EGFR* amplification positive glioblastoma tissue samples. Native cell lysates from glioblastoma tissue were analysed by Western blot. Tissues were *EGFR* amplification positive, consequently the PVDF membrane was probed with EGFRvIII aptamers varying in sequence, to determine whether the aptamers would interact with any protein.

Native cell lysate from five patients were probed using EGFRvIII different in sequence to not only deduce whether the aptamers interacted with a protein, but to also determine whether the tissue samples co-expressed the EGFRvIII mutation. Western blots using the four EGFRvIII aptamers were all negative, which showed the aptamer did not interact with any proteins.

3.5 Identification of DNA aptamers towards PDE1C through tailored counter-SELEX

DNA aptamers were selected towards purified GST-tagged PDE1C. To prevent cross reactivity, negative selections against purified GST and NHS-activated agarose resin was produced. PDE1C is not truncated in glioblastoma, but has been shown to be over-expressed instead. A negative selection towards a PDE1C analogue was therefore deemed unnecessary.

Identified novel DNA aptamers were biotinylated and used to validate aptamer-PDE1C binding. Denaturing and native Western blots were performed using SVGp12 and U87MG cell lysate. Further validation was produced via an aptoprecipitation assay, which pulled the aptamer bound target out of the cell lysate for subsequent detection.

3.5.1 Optimisation of DNA amplification via TD-PCR during 6 rounds of Counter-SELEX

An amplified DNA aptamer library was utilised in 6 rounds of Counter-SELEX to identify aptamers specific to PDE1C. To circumvent DNA aptamers targeting the GST tag bound to the PDE1C, a negative selection against GST immobilised on sepharose 4b beads was produced. As the NHS-activated agarose resin was used to immobilise the PDE1C, negative selections were produced against the resin to prevent the aptamers cross reacting with the resin.

To produce the GST needed for the negative selection, a pGEX-KG vector was transformed in to BL21 *E. coli.* Following GST induction, the cells were harvested

and sonicated to produce cell lysate containing the expressed GST. BL21 *E. coli* cells, taken before and after protein expression, were boiled in laemmli buffer and was analysed by SDS-PAGE to confirm the presence of expressed GST (Fig 3.22).

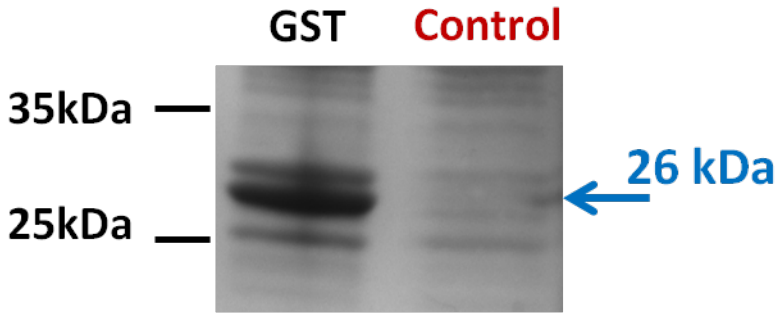

Figure 3.22 – SDS-PAGE of BL21 *E. coli* cells before and after GST induction. BL21 *E.coli* was transformed with a pGEX-KG plasmid to produce GST that would be used for the negative selection to select aptamer specific to PDE1C. Cells were aliquoted before and after GST expression was induced through 100 mM IPTG. The SDS gel showed a surplus of a protein, 26 kDa in size, being produced following protein induction, whilst no increase of this protein was seen in the control.

Sepharose 4b beads were used to isolate the GST from the cell lysate and the subsequent sepharose-GST beads were used for the negative selection of aptamers. Unbound aptamers from the negative selection underwent positive selection using PDE1C immobilised to NHS-activated agarose resin. Following each round of selection, the eluted aptamers were entered in to a PCR mastermix. A portion of the mastermix was used to optimise the number of phase two TD-PCR cycles. Aliquoted PCR products were separated on a 2% gel and visualised using UV light (Fig. 3.23). The remaining mastermix containing eluted DNA aptamers were amplified using the optimal number of cycles.

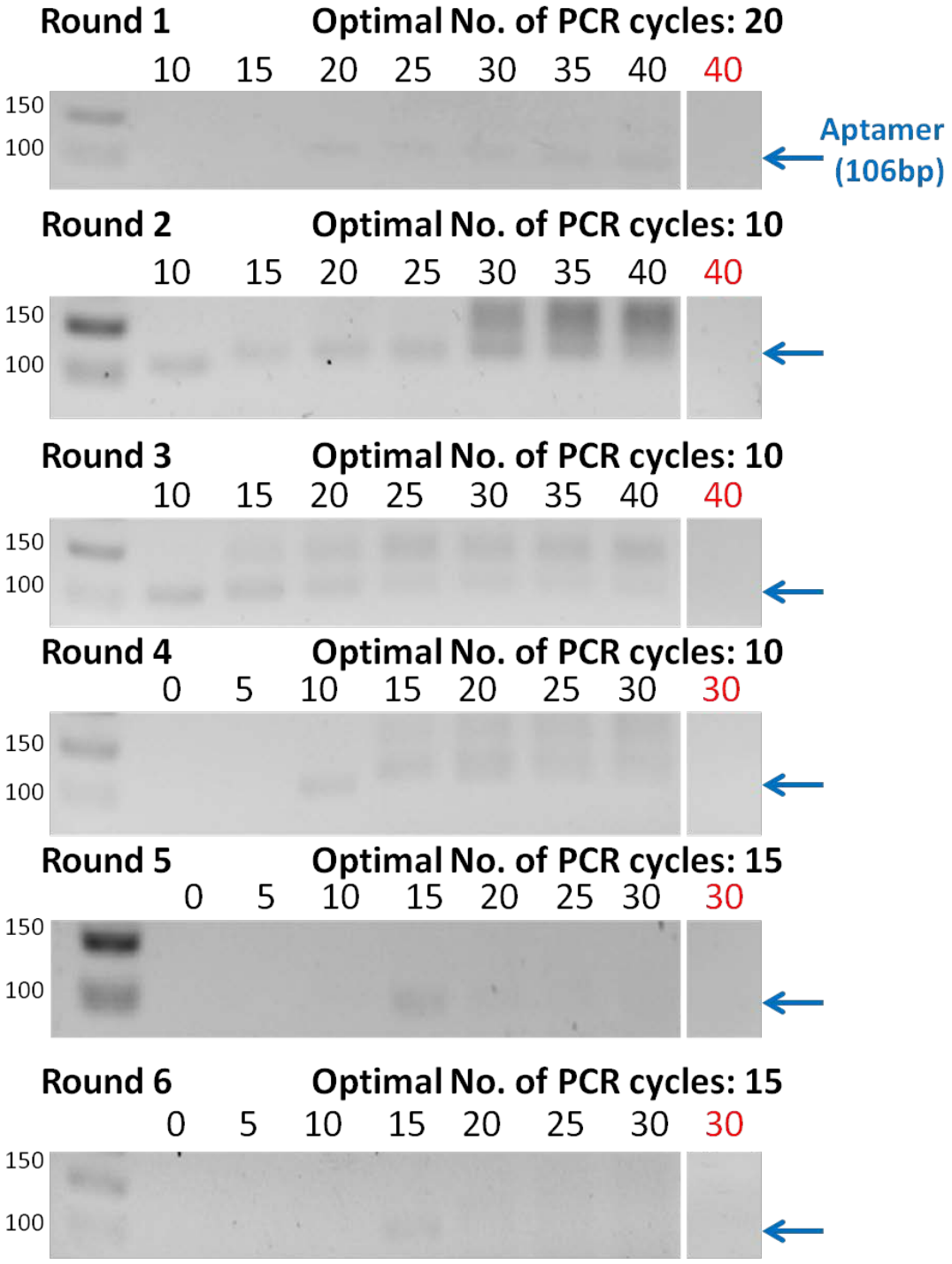

Figure 3.23 – Optimisation of the number of TD-PCR phase two cycles following PDE1C selection. Amplification was optimal after 20 cycles of TD-PCR during round 1, 10 cycles for rounds 2, 3 and 4 and 15 cycles for rounds 5 and 6. Non-specific bands can be seen after 15 cycles for rounds 2, 3 and 4. Bands were also seen after 20 cycles for rounds 5 and 6, but with less intensity than the specific band shown during optimal amplification. No bands were visible in any control lanes (in red). All gels were inverted to increase the visibility of present bands.

Following round 1, the optimal number of phase two cycles was shown to be 20 cycles. For rounds 2, 3 and 4 the optimal number of cycles decreased to 10 cycles of TD-PCR. Non-specific bands 150bps in length appeared after further cycling at 15 cycles and upwards. After rounds 5 and 6, the optimal number of cycles increased to 15 cycles with increased cycling showing non-specific bands and decreased specific aptamer at 106 base pairs in length.

After the last round of counter SELEX, the amplified aptamers were not ethanol precipitated and were instead purified using a commercially available PCR clean up kit. Aptamers were ligated in to a pCR2.1 TOPO vector, before subsequent transformation in to DH5α *E. coli* and grown overnight on selection. Visible colonies were entered in to colony screening via PCR, amplified products were separated and visualised via agarose gel electrophoresis (Fig 3.24).

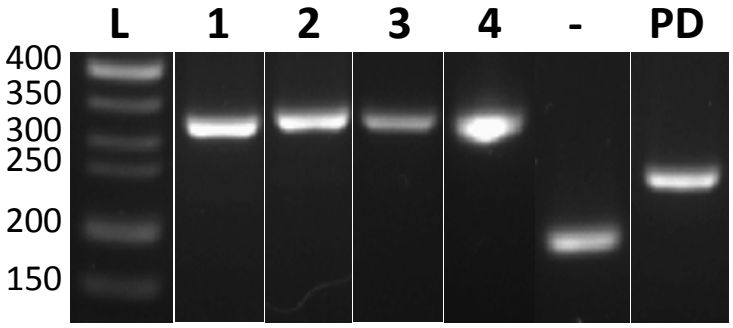

Figure 3. 24 – Colony PCR screening of chemically competent DH5α *E.coli* transformants for positive aptamer inserts. The agarose gel shows four pCR 2.1 plasmids positive for aptamer insert, 1 plasmid containing a 50bp primer dimer (PD) and 1 plasmid negative for any insert (-). The plasmids positive for aptamer insert corresponds to 308 bases, with the aptamer at 106 bases and the distance between the M13 primer sites being 202 base pairs long.

A total of 17 colonies were shown to be positive for an insert, however only four were later shown by Sanger sequencing to have a 106 bp aptamer insert with the remaining positive plasmids having non-specific sequences inserted in to the vector (see section 3.5.2). Lanes 1 - 4 showed a band indicative of positive aptamer insert, at 308 bps long, which corresponded to the 202bps between the M13 primer sites and the 106 bp aptamer insert. The insertion of a sequence 50bps in length was seen, which was most likely due to the insertion of primer dimers (PD).

3.5.2 Identified novel DNA aptamer sequences, selected towards PDE1C

Plasmids positive for inserts were purified from the chemically competent DH5α *E.coli*. The novel DNA aptamers within the pCR 2.1 vector was then elucidated by Sanger sequencing. A M13 forward read and a M13 reverse read was produced for all positive plasmids. Some sequences identified through Sanger sequencing were not 106 bps in length. These non-specific sequences can be found in Appendix 1 and were not taken further, however the specific aptamer sequences of 106 bps can be found in Table 3.6.

Table 3.6 – Novel DNA aptamer sequences selected towards PDE1C. Primer sites are highlighted in dark red (forward) and light blue (reverse), as are the complementary primer sequences which are highlighted in red (forward) and blue (reverse). Sequences in bold were elucidated by Sanger sequencing, those that are not bolded were elucidated based on complementation to the sequenced sense or anti-sense strand.

Sequence	M13 reverse read	M13 forward read
XApt001	**CCCTCGAGTTTACCGCAGAATTCCT GCGATCCCCCTCCCCCAATCCACCT CCCGAGCACTTTCCCACCACCGGG AATTCTCTCCCTATAGTGAGTCGTA TTAGGAT**	**ATCCTAATACGACTCACTATAGGGAG AGAATTCCCGGTGGTGGNNNNNNGC TCGGGAGGTGGATTGGGGGAGGGG GATCGCAGGAATTCTGCGGTAAACTC GAGGG**
XApt002	**CCCTCGAGTTTACCGCAGAATTCA TACCACTTGACCATGTTAATAAGC TATGCCCACCATAAGTGACCTGAC TGAATTCTCTCCCTATAGTGAGTCG TATTAGGAT**	ATCCTAATACGACTCACTATAGGGAG AGAATTCAGTCAGGTCACTTATGGTG GGCATAGCTTATTAACATGGTCAAGT GGTATGAATTCTGCGGTAAACTCGAG GG
XApt003	**CCCTCGAGTTTACCGCAGAATTCT GGCCCAACCCTTCGCTCCAACCTTT TGCCAAAACCGAAGCAACACACAC GAATTCTCTCCCTATAGTGAGTCGT ATTAGGAT**	**ATCCTAATACGACTCACTATAGGGAG AGAATTCGTGTGTGTTGCTTCGGTTTT GGCAAAAGGTTGGAGCGAAGGGTTG GGCCAGAATTCTGCGGTAAACTCGAG GG**
XApt004	**CCCTCGAGTTTACCGCAGAATTCC ACTCCTTCCCTCCCCGTCTTCACTTC CTCATCCGTACGACACTGCCGTGG AATTCTCTCCCTATAGTGAGTCGTA TTAGGAT**	**ATCCTAATACGACTCACTATAGGGAG AGAATTCCACGGCAGTGTCGTACGGA TGAGGAAGTGAAGACGGGGAGGGA AGGAGTGGAATTCTGCGGTAAACTC GAGGG**

The aptamer sequences were analysed by Clustal Omega to determine any similarity between the sequences. The sequences were grouped in to families through phylogenetic analysis to determine which sequences were most alike (Fig

3.25). Clustal Omega was also used to determine if there were similar nucleotides at similar positions (Fig 3.26), which could help implicate potential binding sites or positions of importance. Primer sites were included during Clustal Omega analysis but were removed from the diagrams for clarity.

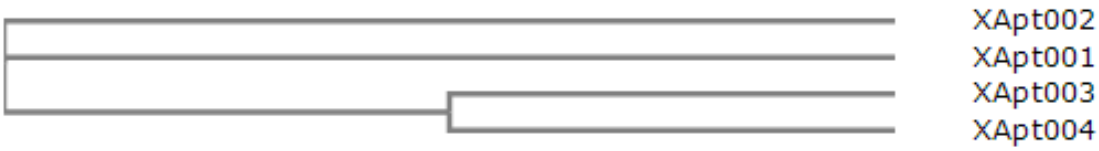

Figure 3.25 – Phylogram of identified novel aptamer sequences selected towards EGFRvIII peptide, determined by Clustal Omega. Clustal omega grouped the aptamers in to three separate families. XApt001 and 002 were isolated within their own family showing that they are not similar to the other sequences. XApt003 and 004 make up the only family with more than one member, displaying some homology between the two sequences.

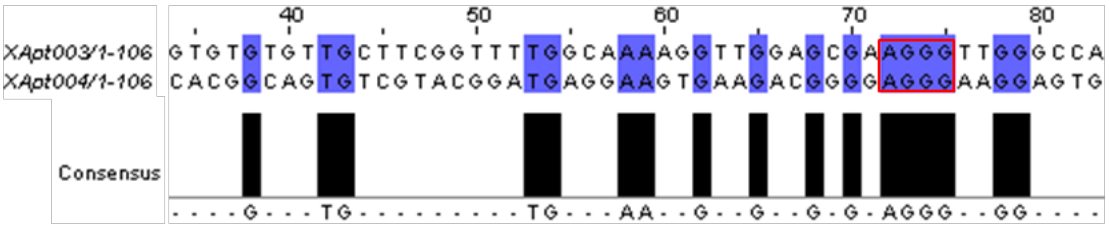

Figure 3.26 – Consensus sequences displaying similar bases within familial sequences identified towards primary cultures, as determined by Clustal Omega software. Clustal Omega analysis showed that there were multiple positions of similarity, including a 4 nucleotide sequence of AGGG which could potentially be a binding site.

Clustal Omega grouped the sequences in to three separate families, two families contained one member each (XApt001 and XApt002) and the remaining family consisted of two members (XApt003 and XApt004). XApt1 and 2 were not similar to the other sequences because they were put in their own separate families. The remaining two aptamers were grouped with one another showing they exhibited some similarities, which were further investigated through consensus alignment profile. There were several regions of similarity between the two DNA aptamers, including a four nucleotide sequence of AGGG at position 72 to position 75. These positions may represent sites of importance, such as a potential binding site.

3.5.3 Structural determination of aptamer sequences, selected towards PDE1C

The identified DNA aptamer sequences were entered in to MFold (Section 3.3.4) to predict secondary structures of the aptamers may conform to (Fig 3.27). Nucleotides existing in a loop were not usually bound to a complementary base and therefore contained positions at which hydrogen bonding with the target may occur. The secondary structures for the complementary anti-sense aptamer sequences were not predicted.

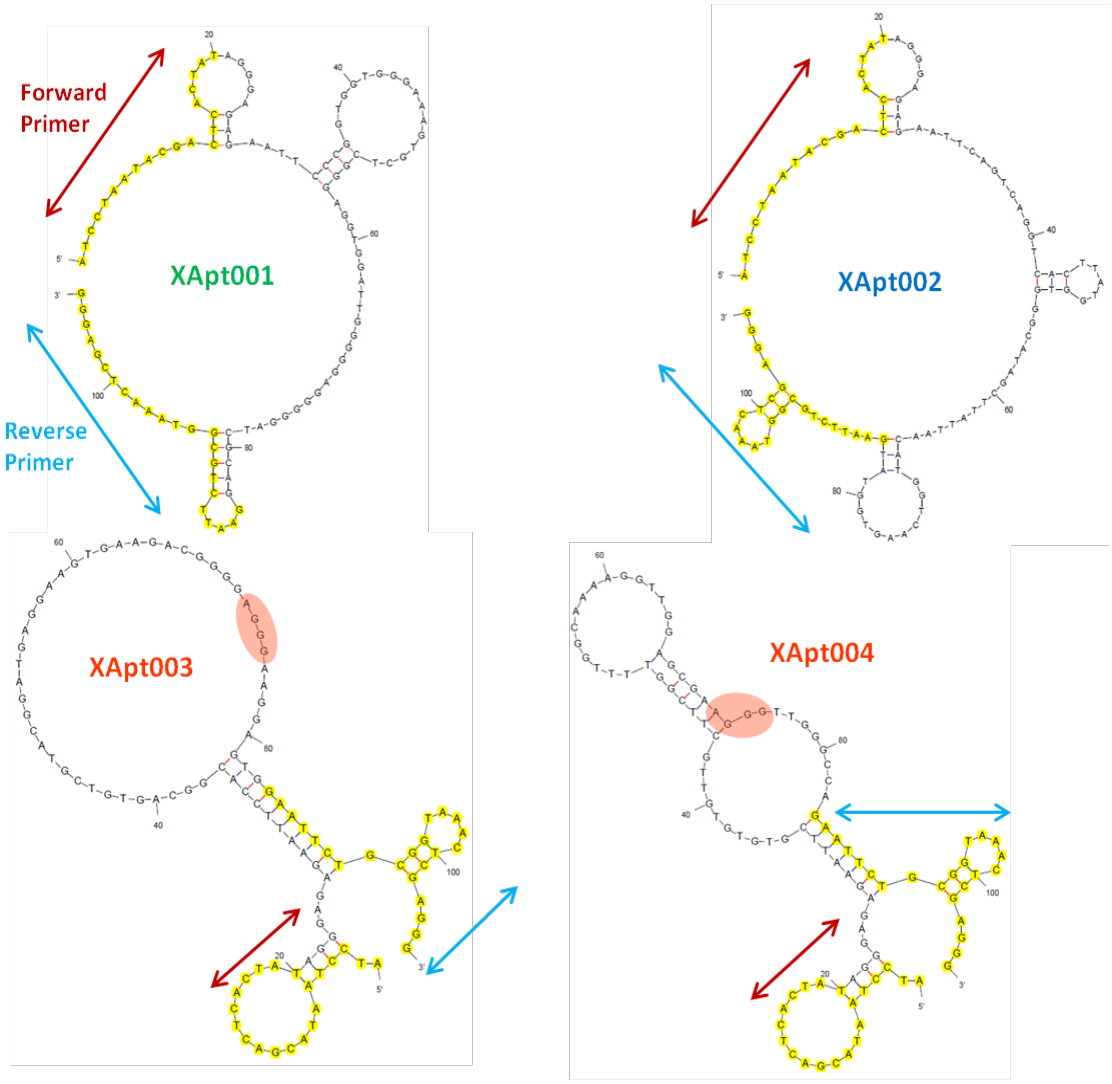

Figure 3. 27 – Predicted secondary structure of novel DNA aptamer sequences, selected towards PDE1C and determined by MFold software. Points of similarity are highlighted (orange) within the sequences, which was determined using Clustal Omega software. Primer sites are highlighted, with arrows depicting the location of the forward (red) and reverse (blue) primers.

3.5.4 Validation of novel DNA aptamers, targeted towards PDE1C

Identified aptamer sequences were biotinylated and were utilised in an avidin-biotin complex (ABC) system for detection. The ABC system contained a biotin-horse radish peroxidase (HRP) complex, which allowed detection through the substrate 3,3'-diaminobenzidine (DAB).

SVGp12 and U87MG cell lysate containing PDE1C was prepared and utilised on a Western blot to determine whether the aptamers would bind a protein with a

similar molecular weight to that of PDE1C. Biotinylated aptamers were used to probe the PVDF membrane to determine whether the aptamer interacted with PDE1C, however, only one aptamer (XApt004) showed visible binding (Fig. 3.28).

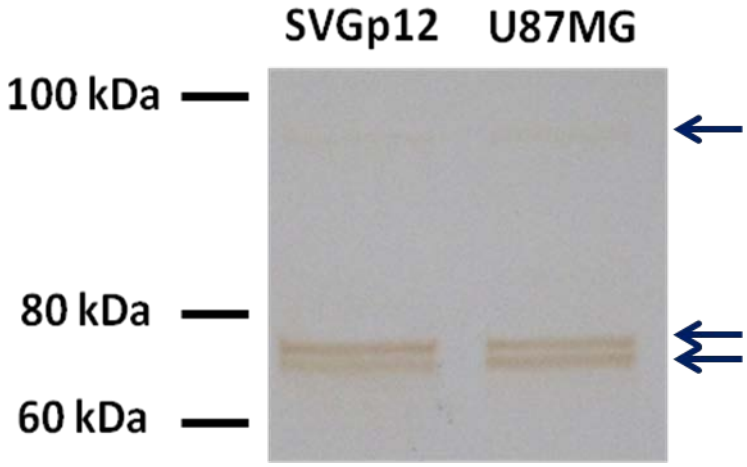

Figure 3.28 – Western blot analysis of cell lysate from SVGp12 and U87MG cell lines, using biotinylated XApt004 aptamer. SVGp12 and U87MG were analysed by Western blot, as both cell lines contain PDE1C. The PVDF membrane was probed with biotinylated aptamers, however only one aptamer (XApt004) was successful in detecting any protein. Two bands, 70 kDa in size was detected and may be indicative of PDE1C. The higher band may be the acetylated active version of PDE1C, whilst the lower band is left unmodified. A faint band, 90 kDa in size, was also detected and can be explained by the PDE1C isoform 3, also present in both cells.

Figure 3.28 showed that the aptamer Xapt004 detected proteins from both cell lysates. The two bands around 70kDa suggested detection of PDE1C. The lower band of the two is likely to be the inactive form of PDE1C, were as the higher band may be the acetylated active PDE1C. A faint band showing the detection of protein around 90kDa was seen. This may be an isoform of PDE1C known as PDE1C3, which is also present in astrocyte cells.

Three aptamers did not bind any protein within the cell lysates during Western blotting. SELEX selections were performed with a PDE1C protein in native conformation; therefore the aptamers were designed to target a native protein and not a denatured one. With these considerations in mind, a native Western blot was

produced to determine whether the aptamers detected any proteins in their native state (Fig 3.29).

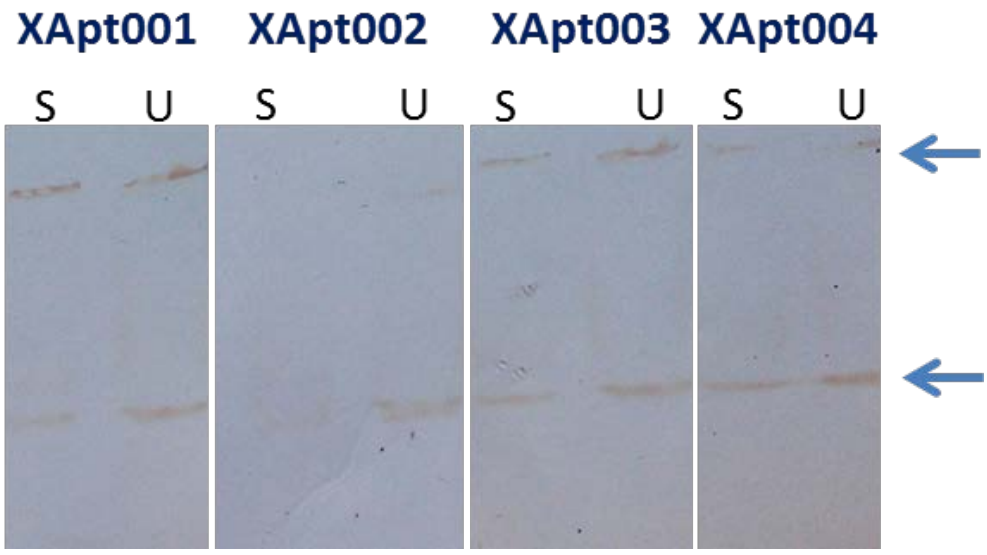

Figure 3.29 – A native Western blot, using cell lysate from SVGp12 (S) and U87MG (U) to show any aptamer-protein binding. Native cell lysate extracted from two cell lines were analysed by Western blot and probed using biotinylated aptamer. Most aptamers recognised protein from cell lysates, with the exception being XApt002 which did not detect protein extracted from XApt002. As XApt004 detected proteins similar to various forms of PDE1C, it was considered as a positive control. XApt004 detected two proteins from the lysates, which were also detected by other biotinylated PDE1C aptamers, therefore all aptamers bound a protein similar to PDE1C but only XApt001-003 could bind the native conformation.

By using native conditions for cell lysate preparation, most aptamers were able to bind to proteins on the Western blot, as shown by the two brown bands. XApt002 showed limited aptamer-protein interaction within the SVGp12 cell lysate and minimal interaction with the U87MG cell lysate lane when compared to the other aptamers used. Some aptamers showed increased staining in the higher band than the lower band and vice versa. For instance, XApt001 and XApt003 had an increase in staining intensity for the higher band than the lower band. Conversely, XApt004 showed an increase in staining intensity for lower band than the higher band.

Whilst the aptamers have shown they interact with a protein from the cell lysates, the molecular weight is unknown because of the absence of SDS.

The biotinylated aptamers were further used in a procedure known as aptoprecipitation (AP). During this protocol, the aptamer binds to the target and the complex is pulled out of the protein lysate by utilising the biotin tag, which subsequently isolates the aptamer and the bound target. Streptavidin-agarose beads facilitated the process, by binding the biotin tag attached to the 5’ end of the aptamer. The isolated proteins were then denatured and separated based on molecular weight via SDS-PAGE and visualised using coomassie blue (Fig 3.30)

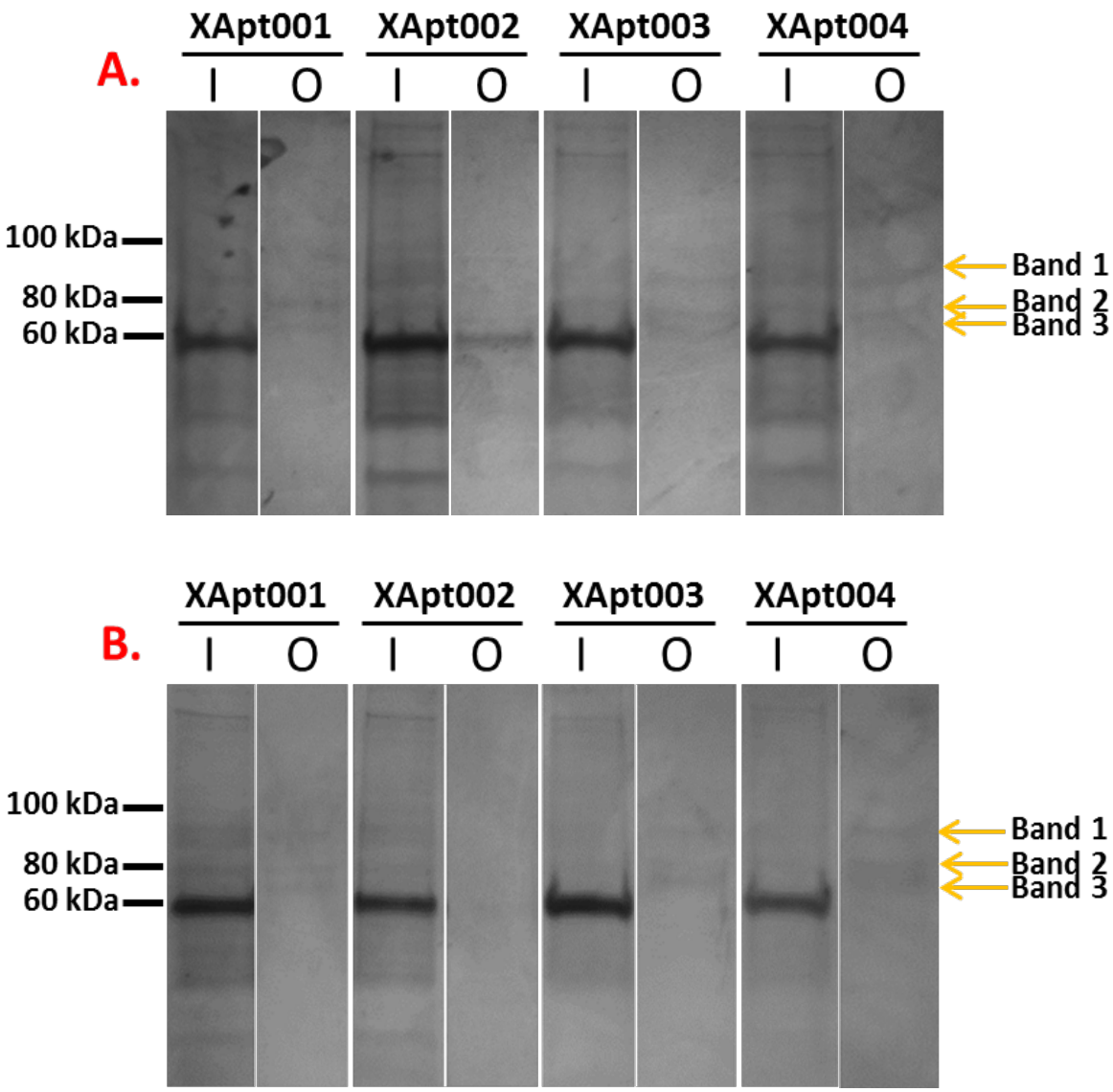

Figure 3.30 – Visualisation of aptoprecipitations, utilising biotinylated aptamers to pull out the aptamer target from SVGp12 (A) and U87MG (B) cell lysate. Biotinylated aptamers were incubated with cell lysate to bind the aptamer target. The subsequent aptamer-protein complex was pulled out of the cell lysate by streptavidin-agarose beads and detected via SDS-PAGE. The cell lysate used to pull down the aptamer target is denoted as the input (I) and the protein target eluted from the aptamer was the output (O). Based on the aptoprecipitations for both cell lysates, the aptamers targeted similar proteins of similar molecular weights. Bands can be seen around 70 kDa and 90 kDa in a similar configuration to those seen previously, a 90 kDa protein indicative of PDE1C isoform 3 (band 1) and two 70 kDa proteins indicative of acetylated PDE1C (band 2) and PDE1C not acetylated (band 3). Controls were produced separately in the absence of any aptamer (not shown).

After visualisation, proteins were seen that were similar to those detected by XApt004 during the denaturing Western blot. Two bands were visible at 70 kDa and one band at 90 kDa for most aptoprecipitations. The 90kDa band was not visible for aptoprecipitations produced using the aptamer XApt002, using either cell lysate. XApt002 was unsuccessful at precipitating any target using the U87MG cell lysate. This could either have been caused by a low concentration of the target within the lysate, or it could be that the aptamers affinity for the target is low. The most successful precipitations were the ones which used the aptamers XApt001, XApt003 and XApt004, with all displaying three bands suggestive of two 70 kDa proteins and a 90kDa protein.

Chapter 4: Discussion

4.1 Discussion

Over the last 10 years, personalised treatment regimens, involving surgery, radiotherapy and chemotherapy have not significantly improved glioma survival rates (Sant *et al.*, 2012, Kohler *et al.*, 2011). Although cancerous cells are more sensitive to DNA damaging agents, they lack specificity and may result in unwanted damage to healthy tissue producing side effects (Dietrich *et al.*, 2008). There is therefore a need for more targeted treatments, with the ability to discriminate between healthy and cancerous cells, without producing adverse effects. As part of glioma treatment, aptamers may be able to provide specificity where current treatments are lacking and deliver therapeutic payloads directly to the tumour in-order to circumvent therapy associated side effects. This study set out to identify novel DNA aptamers that were specific to glioblastoma, through known and unknown targets.

4.2 Producing sensitive and specific cell-SELEX and counter-SELEX procedures

Over the last 24 years, since the first description of aptamer selection by SELEX from Gold and Tuerk in 1990, the method has evolved to increase the overall efficacy of aptamer identification. One of the first improvements was the incorporation of a negative selection, designed to filter out non-specific aptamers that may interact with analogues of the specific target (Jenison *et al.*, 1994). This early improvement provided the basic foundations on which many different SELEX methodologies have been built. Although different, each utilises an amplified aptamer library through iterative negative and positive selections, followed by amplification, purification and quantification to identify specific aptamers to the desired target of choice (Aquino-Jarquin and Toscano-Garibay, 2011). Methods to identify aptamers towards cells and purified proteins, through cell-SELEX and counter-SELEX respectively were adapted from (Sefah *et al.*, 2010a) and (Navani *et al.*, 2009). SELEX involves the iterative application of ssDNA aptamers towards the targets, through negative and positive selections. SELEX selections were followed by

amplification via PCR, purification via ethanol precipitation and quantification via gel electrophoresis.

4.2.1 Amplification of DNA aptamers by TD-PCR

Amplification of DNA aptamers via PCR is an important part of the SELEX procedure. The initial library entered in to SELEX must be amplified to ensure adequate copies are available for aptamer identification. Aptamers eluted from selections must also be amplified ready for re-selection during the next iterative round of SELEX. Non-specific sequences may compete with the aptamers for binding sites and inefficient amplification could lead to low numbers of aptamer copies (Sefah *et al.*, 2010a). Amplification should be as specific as possible, whilst retaining the ability to expand the pool of aptamers. With these considerations a TD-PCR programme was utilised to amplify DNA aptamers.

The TD-PCR programme was produced by the addition of a touch-down phase to the standard PCR programme (Korbie and Mattick, 2008). The touch-down phase consisted of 10 cycles, starting with an annealing temperature 10˚C higher than conventional PCR. By gradually reducing the annealing temperature 1˚C per cycle, a population of aptamers was produced with high specificity. The efficiency of PCR is highly dependent on the annealing temperature used which is dictated by primer melting temperatures (T_m). Primers may partially or non-specifically hybridise to the template strand if a low annealing temperature is used, producing unwanted products (Bell and DeMarini, 1991). Conversely a high annealing temperature will increase the specificity of PCR products, as the primers will only anneal where interactions are the strongest and therefore most specific. Although a higher annealing temperature decreases PCR artefacts, product yield may be reduced as the amount of amplified products is decreased.

The aptamer population was further amplified by 10 cycles of the second standard phase with an optimal annealing temperature of 50˚C. The TD-PCR was more efficient than the standard programme, displaying increased amplification of aptamers and minimal non-specific amplification despite a higher number of cycles

(Fig 3.1).TD-PCR circumvents issues surrounding the annealing temperature by utilising two phases for product amplification. The first phase (TD phase) gradually reduces the annealing temperature, from high to optimal, progressively producing a small population of copies with increased specificity. The second phase amplifies these copies under normal optimal conditions, to ensure an adequate yield is obtained. In this study, the TD-PCR programme was compared to the standard PCR programme through optimising the number of cycles. Too much cycling increased the chances of unwanted artefacts and decreased the yield of specific product. Not enough cycling produced low amounts of amplification, but reduced artefacts and therefore an optimal number of cycles were further investigated. In comparison with the standard PCR programme, TD-PCR was shown to maintain a high level of specificity whilst increasing the amplification of DNA aptamers.

Previously TD-PCR has been used in conjunction with asymmetric PCR within SELEX to select DNA aptamers towards the H3N2 virus (Wongphatcharachai *et al.*, 2013). Asymmetric PCR generates ssDNA aptamers by increasing the ratio of the forward primer to the reverse primer, as opposed to the dsDNA aptamers produced by standard PCR programmes (Marimuthu *et al.*, 2012). Asymmetric PCR ensures the production of ssDNA, were as the dsDNA is denatured and snap-cooled to produce ssDNA aptamers. Although the asymmetric PCR is efficient in producing ssDNA (Svobodova *et al.*, 2012), by decreasing the ratio of the reverse primer to prevent dsDNA from forming, the diversity of the aptamer pool is halved. This is because the aptamer pool is lacking adequate copies of the complementary anti-sense sequence. Whether the production of ssDNA aptamers is more important than the diversity of the aptamer pool is questionable.

4.2.2 Purification of DNA aptamers via ethanol precipitation

The stringency of SELEX selections should be controlled, as SELEX selections with low stringency could decrease the aptamers affinity to the desired target. To control the stringency of SELEX selections, amplified DNA aptamers are purified to concentrate the aptamers (Tuerk and Gold, 1990). The purification of aptamers

needs to be as efficient as possible to maximise yield and reduce the loss of any sequences during the procedure.

An inexpensive and common method of DNA purification is ethanol precipitation. The method works on the principle that DNA is not soluble in high concentrations of ethanol. This is normally facilitated by the addition of a salt, which interferes with the polar interactions between the DNA and water allowing the oligonucleotides to fall out of solution. Ethanol is commonly utilised as it is inexpensive over commercial kits, which are prone to inefficient purification as the length of the DNA becomes smaller. Kits normally require the addition of isopropanol to reduce the loss of small fragments, however this increases the time needed to air dry the resulting pellet of DNA to remove residual isopropanol.

Efforts to improve the purification of DNA aptamers were taken by trialling an alternative ethanol precipitation method (Fregel *et al.*, 2010), which used ammonium acetate salt at low concentrations and the DNA carrier glycogen. The advantages of substituting sodium acetate for ammonium acetate have been well documented previously (Crouse and Amorese, 1987). The use of ammonium acetate prevents the co-precipitation of dNTPs that are required for amplification, as well proteins such as *Taq* polymerase. Glycogen carries DNA by polar interactions with the polar DNA which facilitates purification (Gaillard and Strauss, 1990). The addition of glycogen showed no additional benefit when used at either concentration of 5 mg/ml or 10 mg/ml. The addition of glycogen did not seem to confer any advantage, but could have interfered with DNA-protein interactions as previously documented (Gaillard and Strauss, 1990). These interactions are necessary for successful aptamer identification and so, the modified methods using glycogen was excluded. The standard ethanol precipitation procedure, where the mixture was incubated at -80˚C for 1 hour, precipitated the DNA most efficiently. In retrospect, DNA precipitation using the standard protocol would still have co-precipitated dNTPs and other PCR reagents and so, ammonium acetate could have been used instead of sodium acetate to circumvent this.

4.2.3 Utilisation of minimal biological material for aptamer identification

4.2.3.1 Minimal cell number for aptamer identification

SELEX selections are normally produced using a high number of cells, typically they are carried out using $1x10^6$ cells (Sefah *et al.*, 2010b, Meyer *et al.*, 2013)Two groups have previously utilised the glioblastoma cell line U87MG to identify specific RNA and DNA aptamers (Cerchia *et al.*, 2009, Kang *et al.*, 2012). Cerchia *et al.,* identified RNA aptamers using $1x10^7$ cells, whilst Kang *et al.,* isolated DNA aptamers using a minimum of $1x10^6$ cells. The present study isolated one aptamer following five iterative rounds of cell-SELEX, using 100 cells. Although one aptamer was identified, whether it is specific or not is still yet to be determined. Additionally, only one aptamer was identified, which could imply a limit of detection was reached. Whilst this may be the case, this provides a novel route for the use of primary tissues that are available in premium amounts.

Selections are routinely carried out on cell lines as they are more widely available than primary tissues. Cell lines are produced by the immortalisation of a cell that was once part of a primary tissue; however the patient from whom it was sourced does not necessarily ubiquitously express all biomarkers that are indicative of the disease. This is especially the case where the tumour is highly heterogenous, displaying multiple cell types with varying phenotypes, like glioblastoma. Therefore primary tissues may offer a better variety of biomarkers.

Although primary tissues may be more useful in the identification of novel biomarkers, they are only available in small amounts. A surgeon may reduce the amount of biopsied tissue or reduce the area that is to be resected to preserve higher order functioning brain tissue. Short-term cultures established from primary tissue often grow slowly. The cells may acquire mutations as a consequence of cell culture, leading to aptamers targeting biomarkers that are non-specific (Sampson *et al.*, 2000). The use of primary tissue may also allow for personalised treatments; however quick aptamer identification would be required to prevent mortalities.

To facilitate aptamer identification to 100 cells, TD-PCR programme was optimised during each round, by determining the most efficient number of phase two cycles required for aptamer amplification. Despite using a small number of cells, aptamers were still present following 5 rounds of selection. Aptamers identified using a small number of cells may have better binding affinities than aptamers isolated using large cell numbers. There would be a limited number of targets using small cell numbers and therefore, stringency is increased as a consequence of heightened competition for binding sites.

4.2.3.2 Minimal amount of protein for aptamer identification

Aptamers can be targeted towards proteins indicative of disease by exposing an aptamer library to immobilised purified protein or peptide. Purified proteins or peptides may be purchased commercially, although they can be expensive, therefore, there is a requirement for a counter-SELEX procedure that is able to identify aptamers using minimal amounts of protein. Hicke *et al.,* identified aptamers towards DNA aptamers towards tenascin-C, which is over-expressed in tumorous cells (Hicke *et al.*, 2001). Specific aptamers were isolated following eight rounds of selection, however the group did not document the amount of protein used for each round. The smallest amount of protein utilised for selection was 15ng/µl for aptamers identified towards PDE1C during rounds 5 and 6 of SELEX. Similar to the previous cell-SELEX procedure, TD-PCR was tailored for each round of counter-SELEX selection. Whilst DNA aptamers were identified towards PDE1C, a high amount of non-specific DNA sequences were present within the final pool of aptamers at round 6 (not shown). This was problematic when cloning; many colonies entered into colony PCR showed non-specific insertions within the plasmid. Most of the non-specific sequences were 50-90bps in length and were likely to have been the result of primer-dimer formation (Roux, 1995). The presence of primer-dimers indicated a low concentration of template. Rather than hybridising to the aptamer template, a forward primer non-specifically binds to a reverse primer and *Taq* polymerase initiates amplification of small sequences. In-order to prevent this from happening in future counter-SELEX procedures, the

primer concentration could be lowered to prevent dimerisation. Alternatively, aptamers could be cloned during an earlier round when the aptamer concentration is higher.

The incorporation of capillary electrophoresis (CE-SELEX) during counter-SELEX could also have been used to improve aptamer identification towards purified proteins, by increasing the enrichment efficiency following each round (Mosing *et al.*, 2005). CE-SELEX separates aptamers bound to the target from free aptamers based on different electrophoretic profiles. Aptamers are eluted from the fraction containing aptamer-bound target, which is amplified and incorporated back in to the following round of selection. CE-SELEX also decreases the presence of non-specific aptamers that may be present after elution, this results in selective aptamers being amplified by PCR. The amplified aptamers are then reincorporated back in to following rounds, producing SELEX selections with a high rate of enrichment. Mosing*, et al.,* (2005) used CE-SELEX to identify aptamers towards HIV-1 reverse transcriptase in four rounds of selection. They noted that aptamers were usually selected in 8-12 rounds of standard SELEX, whilst highly specific and selective aptamers were selected in a much smaller number of iterative rounds. Consequently, by reducing the number of SELEX rounds, the amount of biological material needed for aptamer identification was also reduced, therefore, the incorporation of CE-SELEX may help identify aptamers to a protein target whilst reducing the amount of purified protein needed.

4.3 The identification and validation of DNA aptamers towards short-term cultures

Aptamers are routinely identified using cell lines and have been identified to numerous cancer cell lines such as leukaemia (Shangguan *et al.*, 2006), lung cancer (Chen *et al.*, 2008) and prostate cancer (Lupold *et al.*, 2002). Previously, two groups have selected aptamers towards the glioblastoma cell line U87MG. Cerchia *et al.,* isolated RNA aptamers towards the U87MG cell line where as Kang *et al.,* identified DNA aptamers (Cerchia *et al.*, 2009, Kang *et al.*, 2012). Whilst the nucleotide basis

of library was different, the basic foundations to select aptamers to the target cells were very similar, as both utilised a negative selection to filter non-specific sequences in-order to potentiate the identification of specific aptamers to a target (Sefah *et al.*, 2010a).

In the present study, a DNA aptamer library underwent a negative selection of NHA primary cells to identify selective and specific aptamers to primary glioblastoma cells derived from patient biopsies. The main aim of this study was to determine whether biopsy samples could be utilised to generate novel aptamers.

4.3.1 Aptamers identified towards primary cells

A total of 7 unique aptamers were identified towards BTNW390 and BTNW914 primary cells in the present study. Elucidated sequences were analysed though Clustal omega to group the aptamers based on similarity. Clustal omega grouped the aptamers in to four separate families (I-IV), with two aptamers (CLL006 and CLL007) showing no similarity to any other aptamer and therefore, were separated into their own family (Table 4.1).

Table 4.1 – Families of aptamers derived against primary cells, based on sequence similarities as determined by Clustal omega.

Family	Aptamer name	Primary culture used for cell-SELEX selection
I	CLL002(U)	BTNW390, BTNW914
	CLL003	BTNW390
	CLL005	BTNW914
II	CLL001(U)	BTNW390, BTNW914
	CLL004	BTNW914
III	CLL006	BTNW914
IV	CLL007	BTNW914

Each family was further analysed by Clustal Omega to elucidate which positions were similar. Whilst the information gained was used to predict sequences of

interest for five aptamers, the remaining two were not analysed further because they were not similar to any other sequence. MFold was used to predict the secondary structures of all sequences, including the sense strand and the anti-sense strand, to determine whether similar sequences produce similar shapes, but also to determine whether homologous sequences were present within stem loops or not.

A 65-TAAC-68 sequence was synonymous throughout family I members. The homologous sequence was contained within a stem loop for all family members and therefore, could represent a potential binding site for the target. CLL003 and CLL005 were almost identical to one another, with the only difference being a single base change at position (A38G). Due to the high similarity between the two aptamers, it was likely that both aptamers targeted the same protein, which may be found in both short-term cultures, as observed for CLL002(U) which was isolated from both BTNW390 and BTNW914 primary cells. All of these findings also hold true for the anti-sense strands, which are complementary to the sense strand.

Family II exhibited multiple sites of homology, including 53-TGA-55, 65-GAC-67 and 76-AAGGA-80. Based on the predicted secondary structures, the short TGA sequence was contained within stem loops for all family members and may represent a binding site or a site of importance. The GAC sequence was also present within CLL001(U); this was similar for CLL004 with the exception of the adenine nucleotide being part of a stem loop. It is likely that this sequence is not a possible binding site, but rather a site of importance that is either important to the overall aptamer structure or confers some stability when bound to the target. Similarly, the AGGAA sequence is predicted to be part of a stem loop for CLL001(U), however for CLL04 the adenine at position 76 was part of a stem loop and 79-GA-80 was part of a different stem loop, whilst the 78-AG-79 segment was in a similar position. Although different for each sequence, the structures are not exact and may represent a binding site or site of importance.

CLL001(U) from family II and CLL002(U) from family I may offer better affinities than the other aptamer sequences. The number of times an aptamer is sequenced correlates to the number of copies within the aptamer pool from which it was

cloned (Ellington and Szostak, 1990). If there is a higher concentration of one aptamer sequence following multiple rounds of selection, it can be postulated that the aptamer has better binding characteristics for the target. CLL001(U) was sequenced from 50% of plasmids with aptamer insert and may have better binding characteristics than other family II members. Similarly, CLL002(U) was sequenced from 14% of positive clones and may have better binding characteristics than other aptamers within family I.

4.3.2 CLL aptamers in comparison to DNA aptamers derived against the U87MG cell line

During a previous study within the group, DNA aptamers were selected towards the cell line U87MG. The aptamer library was identical to the one used in the present study and a number of aptamers were isolated and sequenced. Overall, out of 10 positive clones, 7 aptamer sequences 106bps in length were identified towards U87MG and were denoted U87TDM. The U87TDM aptamers were compared to the CLL aptamers derived against short-term cell cultures to check for any homology between the sequences. Homologous sequences could imply that the aptamers target similar biomarkers; conversely, any dissimilar CLL sequences could implicate aptamers that target novel biomarkers not present in the glioblastoma cell line. Sequence homology was determined as previously performed; Clustal Omega software grouped the sequences based on similarities (fig 4.1), before individual groups were further analysed to elucidate the similar positions between the sequences (fig 4.2). Any groups that contained only CLL aptamers or only U87TDM aptamers were ignored.

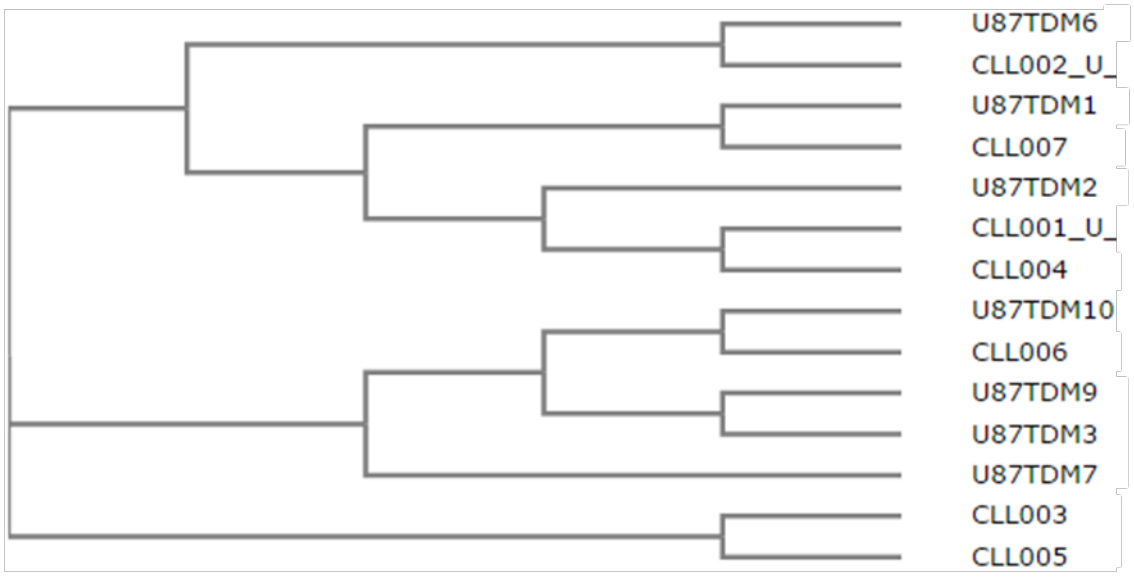

Figure 4.1 – A phylogram grouping CLL aptamers and U87TDM aptamers based on sequence similarities, as determined by Clustal Omega software. The aptamer sequences were grouped in to 3 large families, which contained numerous sub-groups based on the extent of similarities between the aptamers. CLL aptamers and U87TDM aptamers were present in the majority of groups, showing that homologous sequences were present between the aptamers, which were isolated from primary cells and cell lines respectively. CLL003 and CLL005 were not grouped with any U87TDM aptamers, but instead resided within their own family.

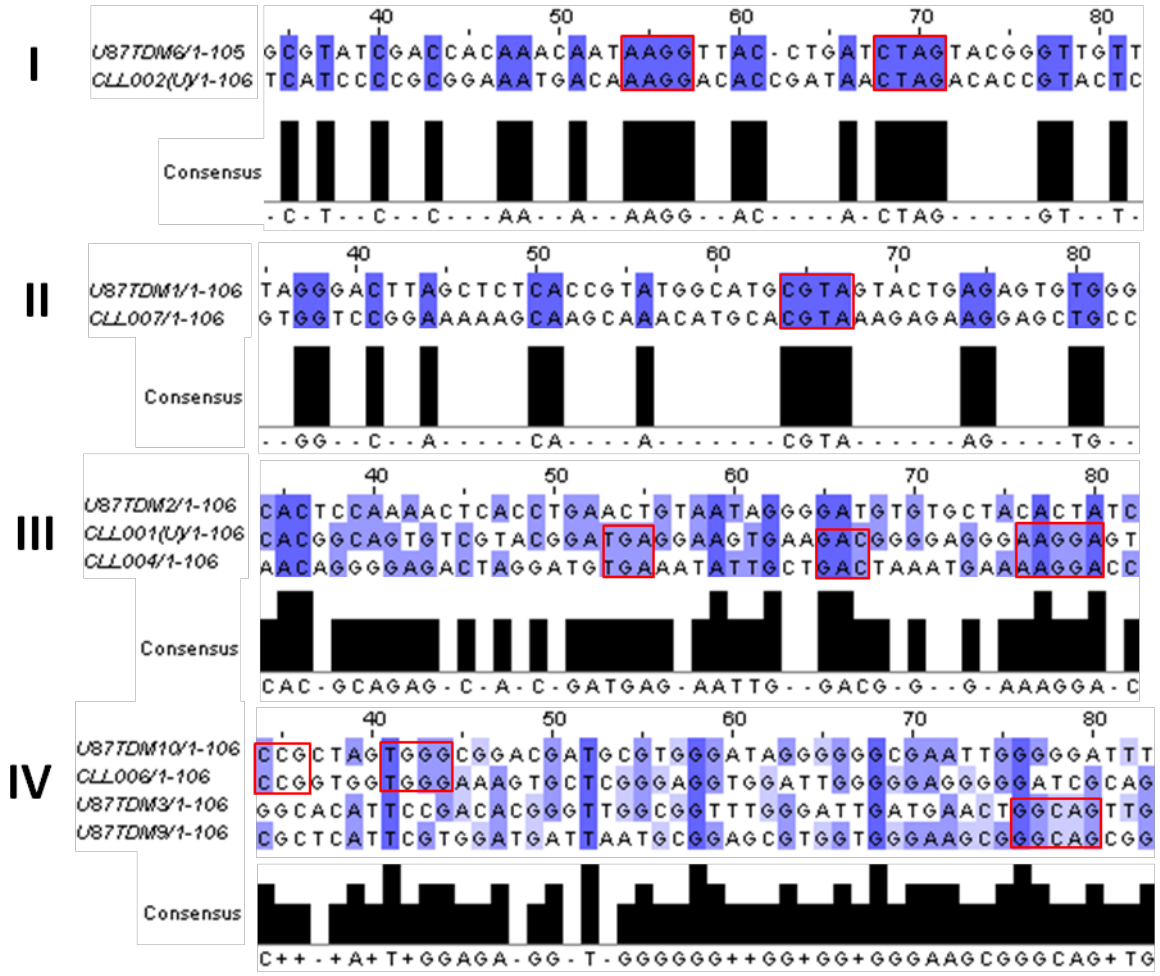

Figure 4.2 – Consensus sequences between familial CLL and U87TDM aptamers, determined by Clustal Omega software. Phylogenetic analysis identified sequences that were similar; these were subsequently entered through Clustal Omega separately to highlight conserved regions. Conserved regions are highlighted in red boxes. U87TDM2 was included in sub-group III as it was deemed to have sufficient homology with the other aptamers within the group, indicated by the length of the line before the sequence branched off. U87TDM7 was not included in sub-group IV because it did not contain sufficient homology with the other aptamers within the sub-group and therefore, could have skewed the results. CLL003 and 005 were ignored because they were not similar to any U87TDM aptamers.

Phylogenetic analysis showed many CLL and U87TDM aptamers to be related. The aptamers CLL006 and CLL007 did not show any similarity to any other aptamer selected towards short-term cultures, however Clustal highlighted similarities between them and some of the U87TDM aptamers. CLL006 had multiple sites of homology with U87TDM1, including a large 64-CGTA-77 conserved region, which could implicate the sequence as a potential binding site or site of importance.

CLL006 was paired with three U87TDM aptamers, although it shared most homology with U87TDM10 with conserved regions of 34-CCG-36 and 41-TGGG-44.

Interestingly, CLL002(U) was no longer grouped with CLL003 or CLL005 and was instead grouped with U87TDM6 as the two sequences shared more homology, than CLL002(U) did with CLL003 and CLL005. The aptamers CLL002(U) and U87TDM10 shared conserved regions of 54-AAGG-57 and 68-CTAG-71. As Clustal Omega could not recognise a significant amount of homology between CLL003/CLL005 and any of the U87TDM aptamers, they may target a biomarker that was present in either primary cultures used, which are not present in the U87MG cell line.

4.3.3 Validating target interaction using aptamers identified towards short term cultures

The aptamers CLL001(U) and CLL002(U) were tested to determine whether they interacted with any target. Native cell lysate was extracted from five tissue samples, which were biopsied from patients with grade IV glioblastoma. The protein extracts were analysed by Western blotting and biotinylated sense aptamer was used to probe the PVDF membrane.

The results of the Western blot were inconclusive. Whilst a brown band was observed for each patient sample, the banding was erratic and could have suggested that there were non-specific interactions. Conversely, banding may have been erratic because of the absence SDS, which binds the proteins to give it a negative charge. A negative charge would allow the protein to be separated based on size without the charge of the protein having an effect. These results require further investigation to determine whether these and other CLL aptamers bound to a target or not. If the bands were a byproduct of non-specific interactions, then the sense aptamer may not be the selective aptamer that targets the protein, instead the selective and specific aptamer may be the anti-sense sequence. Whilst biotinylating the aptamer aids in acknowledging aptamer-protein interaction, it cannot be ruled out that biotinylation perturbed the aptamer from interacting with the target protein.

Oligohistochemistry using glioblastoma tissue sections provided mixed results. CLL001(U) aptamer-protein interaction was evident for BTNW914 which distinctly stained the cell membrane brown. Staining was not as apparent for the remaining tissue slides prepared, nonetheless this implied that the aptamers targeted and bound a protein present on the cell surface. Conversely, background staining caused by naturally occurring biotin cannot be ruled out. Other appropriate validation studies may be helpful in determining aptamer-target interaction, such as localisation studies using fluorescently labelled aptamers instead of biotinylated aptamers.

4.3.4 Utilising primary cells to identify novel aptamers

To the best of the author's knowledge, this is the first time primary cells extracted and cultured from humans have been utilised in-order to identify aptamers. A cell-SELEX protocol using 100 cells per cycle was produced utilising cell lines. This showed that aptamers could be identified on a minimal amount of starting tissue such as cells from a biopsy, and in fact in the future short-term culture of the biopsy material may not be required. Whilst this means that a biopsy is required, which still carries inherent risks, the amount of tissue excised could be minimalised.

Whilst this study is the first example to use primary human cells in short-term culture within cell-SELEX, another SELEX methodology, known as tissue-slide SELEX, utilises primary tissue minimally in-order to identify selective and specific aptamers (Li *et al.*, 2009). Tissue-slide selection uses thinly sliced paraffin embedded tissue sections to identify aptamers to intracellular as well as extracellular biomarkers. Li *et al.,* used tissue-slide SELEX to identify ssDNA aptamers to breast cancer tissue, following 12 rounds of selection one specific aptamer, BC15, was identified. Although aptamer identification is dependent on efficient removal of paraffin and antigens being retrieved effectively (Shi *et al.*, 2006), it may provide a more effective route to personalised aptamers as the tissue can be mapped to determine whether whole tissue sample is cancerous or not. If non-cancerous cells are still present, non-specific aptamers may be produced which could potentiate therapeutic associated side effects. Both methods offer various advantages and

disadvantages towards personalised therapeutic regimens involving aptamers. The best method of aptamer identification may involve a combination of both; however any aptamers selected would still require testing to determine whether they are specific, tolerable and whether they are internalised in to the target cells in order to deliver chemotherapeutic payloads.

4.4 The identification and validation of DNA aptamers towards EGFRvIII peptide

The EGFRvIII mutant receptor is an attractive candidate for ligand targeting because the molecular aberration is cancer specific and has not been observed in healthy tissue (Sok *et al.*, 2006). Monoclonal antibodies have been produced that specifically target EGFRvIII without cross-reacting with EGFRwt, however none have been approved for clinical use thus far (Sampson *et al.*, 2000). Previous attempts to select aptamers towards this truncated protein have thus far shown mixed results, with two groups selecting RNA and DNA aptamers that cross-react with the wild type equivalent (Liu *et al.*, 2009, Li *et al.*, 2011). In the present study, a DNA aptamer library was negatively selected against EGFRwt to mitigate or ameliorate aptamer cross-reactivity. A peptide indicative of the mutated region (amino acids 6-19) was employed as the target epitope during positive selection and 10 novel DNA aptamer sequences were identified.

4.4.1 Aptamers identified towards EGFRvIII peptide

Ten DNA aptamers were isolated towards the EGFRvIII peptide, all with unique nucleotide sequences. Clustal Omega software was used to group the sequences based on sequence similarities which were further elucidated by analysing the families individually. The EGFRvIII aptamers were grouped in to 3 large families (Table 4.2).

Table 4.2 – Families of aptamers derived against EGFRvIII peptide, based on sequence similarities as determined by Clustal omega.

Family	Aptamer name
Family A	EGFRvIII1
	EGFRvIII2
	EGFRvIII6
	EGFRvIII8
Family B	EGFRvIII3
	EGFRvIII4
Family C	EGFRvIII5
	EGFRvIII7
	EGFRvIII9
	EGFRvIII10

EGFRvIII DNA aptamer sequences within family A displayed multiple homologous sequences including 62-CGA-64, 75-GAA-77 and 80-CTC-82. All of which could imply sites of importance, however no single conserved sequence was observed throughout all aptamers within the group. Whilst this could be explained by the aptamers having multiple sites in which the EGFRvIII peptide could bind, it was unlikely because there were no similarities between the conserved regions. Conversely, it could be that none of these conserved regions bind the peptide and instead, serve the aptamer by increasing aptamer-peptide stability when bound. The adenine nucleotide at position 64 was synonymous through all members within family A, and could potentially be the nucleotide which interacts with the EGFRvIII on its own.

Family B consisted of two EGFRvIII aptamers; EGFRvIII3 and 4, which displayed multiple sites of homology that were one or two nucleotides long. As these similarities consist of a small number of nucleotides, it was difficult to predict a potential binding site. Nevertheless, the 61-GNANGG-66 region could be a possible binding site, as these similarities were predicted to be present within a stem loop

and could implicate multiple positions in which the aptamer interacts with the peptide target.

Four EGFRvIII DNA aptamer sequences were grouped in to family C. Similar to family A, Clustal Omega determined multiple sites of homology to be present between the sequences; however no single conserved sequence was present throughout all sequences within the group. An adenine and thymine nucleotide was synonymous at positions 51 and 66 respectively, throughout all EGFRvIII aptamers within the family. These positions could potentially be the binding site in which the aptamer interacts with the EGFRvIII peptide.

No single sequence from any family was observed more than once during sequencing from clones displaying positive insert. An explanation for this could have been that the counter-SELEX selections were not stringent, even though the concentration of the peptide was decreased in an attempt to increase stringency. This was not enough to make the selections competitive and the resulting sequences could potentially have low affinity to the peptide target.

4.4.2 Validating target interaction using aptamer identified towards EGFRvIII

Four aptamers were chosen from differing families based on GT content which has implications on the aptamer stability. A high GT content will give the aptamer an advantage as it is more stable because of the increased number of hydrogen bonds that can occur. Native cell lysate from five glioblastoma tissue samples were analysed via Western blot, which were subsequently probed with each biotinylated sense aptamer.

Western blot analyses did not show any interaction between the biotinylated aptamers sense sequences and the EGFRvIII peptide, in both denaturing and non-denaturing conditions. Similar to the CLL aptamer validation studies, biotinylation could have altered the aptamers conformation or blocked the aptamer binding site, leading to no interaction being observed. Whilst this may be the case, the specific

and selective aptamer may not be the sense sequence, but could potentially be the anti-sense sequence instead. All five patients were *EGFR* amplification positive, whilst it is plausible that the tissues did not contain the EGFRvIII mutation, it was unlikely as 75% of patients that exhibit *EGFR* amplification also co-express the truncated variant. Further studies are therefore warranted to determine if the aptamers target EGFRvIII, such as surface plasmon resonance (SPR) or electrophoretic mobility shift assay.

4.4.3 EGFRvIII specific aptamers in glioblastoma therapy

EGFRvIII is an attractive target as it is unique expressed in glioblastoma and not healthy tissues, drastically reducing the chances of collateral damage and subsequent side effects (Sok *et al.*, 2006). Previously selected aptamers that target both EGFRvIII and EGFRwt have shown the protein to be internalised and degraded more efficiently upon aptamer inhibition (Li *et al.*, 2011). Whilst these effects would undoubtedly increase positive outcomes within a therapy regimen, the protein may not be ubiquitously expressed throughout the tumour cell population. Lopez-Gines *et al.,* studied *EGFR* amplification levels in gliobastoma patients and saw that some patients displayed multiple copies of the gene in as less than 1% of cells tested. As *EGFR* amplification is a pre-requisite for the EGFRvIII version to be present (Luwor *et al.*, 2004), not all of the cells may express the aberration.

4.4 The identification and validation of DNA aptamers towards PDE1C

PDE1C offers another attractive candidate for targeting as the enzyme has been shown to be upregulated in glioblastoma as a consequence of gene amplification (Rowther *et al.*, 2012). Upon inhibition, cells become less mitogenic and growth is slowed. PDE1C is an intracellular second messenger that cleaves cAMP and cGMP to AMP and GMP respectively (Goraya and Cooper, 2005). The reaction is produced in a calmodulin-dependent manner that concludes with metabolic effects. Previous studies have shown PDE1C upregulation to correlate with proliferative behaviour; therefore inhibition of this target may lead to a significant survival advantage (Rowther *et al.*, 2012).

To the best of the author's knowledge, this is the first time aptamers have been targeted to PDE1C. A negative selection of GST was produced to circumvent aptamers non-specifically targeting GST-tags fused with the full length PDE1C protein, which was utilised during positive selections.

4.4.1 Aptamers identified towards PDE1C

From seventeen clones positive for aptamer insert, 4 unique DNA aptamer sequences were isolated through counter-SELEX towards PDE1C. Clustal Omega determined that two of these sequences were related by similar nucleotides at similar positions, whilst the other two were segregated in their own families showing that they were not similar to any of the other sequences (Table 4.3).

Table 4.3 – Families of aptamers derived against EGFRvIII peptide, based on sequence similarities as determined by Clustal omega.

Family	Aptamer name
Family A	XApt001
Family B	XApt002
Family C	XApt003
	XApt004

Families A and B only consisted of one aptamer and as there was no other sequences similar to these two sequences, they were not analysed further. XApt003 and XApt004 were grouped together because they contained regions that were conserved throughout either sequence. The longest sequence conserved throughout both PDE1C aptamers was 72-AGGG-75, however there are multiple regions of homology that are close to one another from position 58 to 79. This could imply that the aptamers binding site was located within this particular segment of the sequence, as it was likely that there are many positions that interact with the target.

Most of the clones that showed positive for aptamer insert were in fact non-specific sequences, likely to have been produced during amplification by TD-PCR. This

suggested the counter-SELEX selections were too stringent and too many iterative rounds were produced, as aptamers were lost and non-specific products dominated the aptamer pool. This was not apparent using gel electrophoresis to qualitatively assess the amount of aptamers still present. Increasing the concentration of protein during selection would have circumvented this, as would a decrease in the number of iterative rounds produced.

4.4.2 Validating target interaction using aptamer identified towards PDE1C

PDE1C is present within astrocytic cell lines, consequently cell lysate from SVGp12 and U87MG were extracted and analysed by Western blot. The sense sequence of all PDE1C aptamers selected was biotinylated and used to probe the PVDF membrane that contained denatured proteins from the cell lines. Upon visualisation, only one aptamer, XApt004, detected proteins were as no signal was shown for the remaining aptamer sequences. XApt004 detected three proteins which are thought to be similar in molecular weight. The XApt004 aptamer interacted with two proteins both of which were 70kDa in size. The lower band at 70kDa was indicative of the inactive PDE1C protein, whereas the higher band was the active PDE1C which is acetylated at amino acid position 1. Furthermore, a 90kDa protein was detected; this protein may be the PDE1C isoform 3 which is also present in astrocytic cells (Yan *et al.*, 1996). The band for PDE1C isoform 3 was faint indicating cellular levels of this protein may be low or the aptamer may not bind efficiently to this spliced variant. These results are similar to those produced by Giachini *et al.,* who studied PDE1C over-expression in hypertensive rats. Using a PDE1C antibody, a similar pattern was observed with two proteins 70 kDa in size being detected and a 87 kDa protein being detected (Giachini *et al.*, 2011). The PDE1C isoform 3 was smaller because of the difference in species.

PDE1C aptamers were derived using purified protein in a native conformation; therefore XApt001-003 should only bind to the native configuration and not the denatured configuration. With this in mind, SVGp12 and U87MG cells were gently lysed in native conditions. Subsequently analysis by non-denaturing Western blots showed that these aptamers did indeed bind a protein indicative of PDE1C.

XApt004 was shown to interact with proteins similar in size to various forms of PDE1C and so, the aptamer was utilised as a positive control. A high and a low band were observed for all aptamers successful in detecting protein from the native cell lysates, including the XApt004 positive control, therefore it can be concluded that all aptamers may bind the second messenger PDE1C. XApt002 was not as successful as the other aptamers in detecting the PDE1C than the other aptamers. Aptamer-protein interaction was minimal using native U87MG cell lysate and no bands were present using native cell lysate from SVGp12. In comparison to the Western blot under denaturing conditions, the detection of one band was lost as only two bands was detected wereas three bands were detected during the denature Western blot. This could either have been caused by the non-denaturing conditions having a detrimental effect, as the charge is an added factor when these conditions are used, or the aptamers may not recognise the natural configuration of the protein.

An aptoprecipitation (AP) method was used to pull out the biotinylated PDE1C aptamer bound target out of the cell lysate extracted under native conditions. Isolated proteins were analysed via SDS-PAGE and visualised using coomassie blue staining. Upon visualisation, three bands were observed for most aptamers, with two 70 kDa bands and one 90 kDa bands, which was a similar configuration to that of the Western blot produced under denaturing conditions. In comparison to the native Western blot, XApt002 failed to precipitate a sufficient amount of specific target to be detected. A large amount of protein may have bound non-specific during the AP using SVGp12 cell lysate.

4.4.3 PDE1C specific aptamers in glioblastoma therapy

Aptamers derived against PDE1C may need a vehicle in-order to deliver the ligand intracellular as this is where the protein target is localised. Previous studies have utilised aptamers to deliver interfering RNA intracellular, including small interfering RNA (siRNA) (Tan *et al.*, 2012) and micro RNA (miRNA) (Esposito *et al.*, 2014). It is therefore reasonable to suggest that aptamers could facilitate the delivery of conjugated aptamers intracellularly. Whilst this would help the aptamer gain access

to the target protein, the four aptamers selected have not been proven to have any inhibitory effects and further studies are required.

4.5 Study limitations

During this study, there was many limitations which were mostly caused by the lack of appropriate controls during experiments. Controls are important inclusions that ensure external factors do not obscure the variable being tested.

4.5.1 Aptamer amplification via PCR

DNA aptamers were amplified following each round of selection, using a pre-determined optimal number of PCR cycles. A control was used whilst optimising the number of PCR cycles which lacked any *Taq* polymerase. The control showed that the eluted aptamers were indeed amplified, this was important as amplification showed that the SELEX selection may have been successful. Moreover, *Taq* polymerase has the ability to add an extra level of diversity to the aptamer pool. The enzyme lacks 3'-5' proof-reading and is therefore liable to error, approximately 1 base in every 100,000 will be erroraneous. By adding more diversity to the aptamer pool, aptamers with better properties may be selected over time.

A control lacking in PCR amplification experiments, previously outlined in **Section** was a PCR reaction lacking any template. This conventional control would have ensured the template being amplified was eluted aptamers, and not contamination. Although it is likely that contamination would have been noticeable, using both controls would have definitively shown that the 106bp aptamers were amplified.

4.5.2 Aptamer-protein interaction via Western blots

Several attempts were made throughout the course of this study to determine whether isolated aptamers bound to their intended target. Although methodologies to detect aptamer-PDE1C interaction and aptamer-EGFRvIII interaction were slightly different, the aim of the experiments were the same and both should have included similar controls which were not produced.

Negative controls should have been included during EGFRvIII aptamer validation (see Section 3.4.5). A negative control, in the absence of any aptamer, would have circumvented any doubts with respect to non-specific binding. Furthermore, if any binding was apparent, it would have served as bonified evidence that the aptamer is interaction with a protein contained in the cell lysate.

Positive controls were lacking for both protein interaction experiments, these inclusions would have provided alot of information if produced. It could be concluded that the EGFRvIII aptamers did not bind any protein (see Section 3.4.5), however as a positive control was not produced, it cannot be ruled out that it was the experimental procedure combined with human error. Additionally, during the denaturing Western blot experiments to detect aptamer-PDE1C binding (see Section 3.5.4), if a positive control was introduced, using a commercially available antibody, more definitive conclusions could have been made. Whilst the size of a protein can not be deduced in non-denaturing conditions (see Section 3.5.4), a positive control using purified PDE1C protein would have shown where the PDE1C bands are on the PVDF membrane. By discovering where the known native protein was on the PVDF membrane, conclusions could have been made as to whether it aligned with the bands detected using the isolated aptamers.

4.5.3 Aptamer-protein interaction via oligohistochemistry

Paraffin embedded tissue, from the same sample used to create the short term cultures used within cell-SELEX, was utilised within oligohistochemistry in-order to determine whether the aptamers bound to a target on the cell surface. Whilst some staining was shown, there were inherent limitations within the experiment.

Negative controls were lacking within this experiment. A negative control using non-cancerous tissue may have shown that the aptamer was specific to glioblastoma. Without this control, it could be argued that the staining shown was non-specific, caused by endogenous biotin within the cells. Nonetheless, this could have been avoided with the addition of a quenching step to block the background biotin, in contrast the same experiment could have been performed which lacked

the incubation of the aptamer with the tissue. This negative control would have highlighted the level of background biotin and qualitative observations could have been made on staining intensity.

4.6 Future studies

Aptamers have been attractive alternatives to antibodies ever since the early years of SELEX selection, as they have the ability to target disease with high specificity and high affinity. Nonetheless, before an aptamer may be utilised to its full potential, further studies are necessary in-order to determine binding characteristics, aptamer localisation and pharmacokinetic properties, amongst others.

4.6.1 Establishing aptamer binding sites

Aptamers are generally selected from large libraries of RNA or DNA 20-100 bases in length. A large number of sequence permutations will increase the chances of selecting an aptamer which efficiently binds to the target of choice. Although these targeting ligands have shown promise in the clinical setting, an issue is the cost of synthesising large sequences of DNA or RNA. For these reasons discovering which nucleotides are involved in binding is important, as not all nucleotides may be needed for the aptamer to bind to the target and in-turn, cut the cost of producing the targeting ligand in the clinical setting.

Mutations can be introduced into aptamer sequences by site directed mutagenesis or by synthesising truncated aptamers (Huizenga and Szostak, 1995, Ruckman *et al.*, 1998), however where to introduce mutations may be difficult to determine as the length of the aptamer sequences become larger. Consensus sequence alignment between the aptamers, comparative to the alignments presented throughout this study, may help to determine where important motifs are although this may be inaccurate with small numbers of selected aptamers.

4.6.2 Establishing aptamer affinity towards protein epitope

In the present study, 8 novel DNA aptamers have been identified towards glioblastoma cells and 14 aptamers have been targeted towards biomarkers important to gliomagenesis. The affinity these aptamers have towards the target however, is unknown. By establishing a disassociation constant (K_d), information to the aptamers affinity can be gained. In addition, aptamers that have multiple nucleotide positions that interact with the target have better K_d constants. This may be useful as it could provide information to further implicate a binding site.

The K_d *of a*ptamers derived towards whole cells may be investigated using flow cytometry. Cerchia *et al.,* and Kang *et al.,* were both successful in determining the disassociation constants of their aptamers by tagging the sequences with fluorescent compounds. By incubating the cells with various concentrations of fluorescently labelled aptamer, they were able to determine the aptamers K_d efficiently.

Aptamers identified towards purified proteins already established to be of importance during gliomagenesis, may have their K_d constants checked using surface plasmon resonance (SPR), which detects refracted light emitted upon aptamer-protein interaction. Kaar and Yung used SPR to determine the K_d of $VEGF_{165}$ specific aptamers (Kaur and Yung, 2012). Whilst this methodology may be effective in determine affinities to protein that are not membrane bound, affinities may be different when the protein is in its natural environment. Analysis by flow cytometry may provide more accurate information whether proteins are membrane bound and not free within the cytoplasm.

4.6.3 Establishing aptamer target epitope

Aptamers derived through cell-SELEX have the potential to identify novel biomarkers characteristic of disease, whilst simultaneously identifying a targeting ligand. The process uses a negative selection in the form of a whole cell with no or little pathological evidence of the disease, however no indications are given as to what the specific protein is (Sefah *et al.*, 2010a). It is important to know the protein

which is targeted, mutated proteins may be exclusive to the disease, but over-expressed proteins may be present in non-cancerous tissue. Further studies may be utilised, such as the aptoprecipitation protocol described in the present study, to isolate the target from native cell lysate which could be identified through mass spectrometry.

4.6.4 Establishing aptamer localisation and enzymatic inhibition

Novel DNA aptamers identified towards primary cells could be utilised for glioblastoma specific intracellular delivery of chemotherapeutics, with the aim of reducing therapy associated side effects that are not well tolerated in older patients (Brandes *et al.*, 2008). The aptamer must be internalised within the cell for this potential to become reality and therefore, cellular localisation studies must be produced to show the aptamers are internalised efficiently. Aptamer localisation may be deduced by incubating the aptamer, tagged with a fluorophore, with live cells characteristic of the glioblastoma (Graham and Zarbl, 2012). Confocal microscopy of the cells, following aptamer incubation, will elucidate whether the aptamers are internalised or not.

In this study, aptamers were selected towards PDE1C with the aim of producing a targeting ligand that would inhibit the enzymatic activity of the protein, which may reduce proliferative activity within glioblastoma tumours. Even though aptamers are well known to target active sites and therefore, induce inhibition (Section 1.2.2), the PDE1C aptamers identified may interact with the protein without affecting function. An ELISA study could be produced to determine the rate at which the substrates, cAMP and cGMP, are catalytically changed to AMP and GMP (Gilbert *et al.*, 2007). Decreased levels of the catalysed product will indicate an aptamer with inhibitory effects and may be used to decrease the activity of downstream mediators.

4.6.5 Enhancing the pharmacokinetic profile of aptamers

The first therapeutic aptamer approved by the FDA, Pegaptanib, showed that the aptamer must be modified to increase the aptamer half-life within serum (Ruckman *et al.*, 1998). Nucleases present within serum will degrade the oliognucleotides reducing the half-life of the aptamer, which could result in the aptamer failing to exert any therapeutic effects or deliver conjugated chemotherapies. To reduce nuclease degredation, individual nucleotides within the aptamer sequence may be modified at various positions (Fig 4.3).

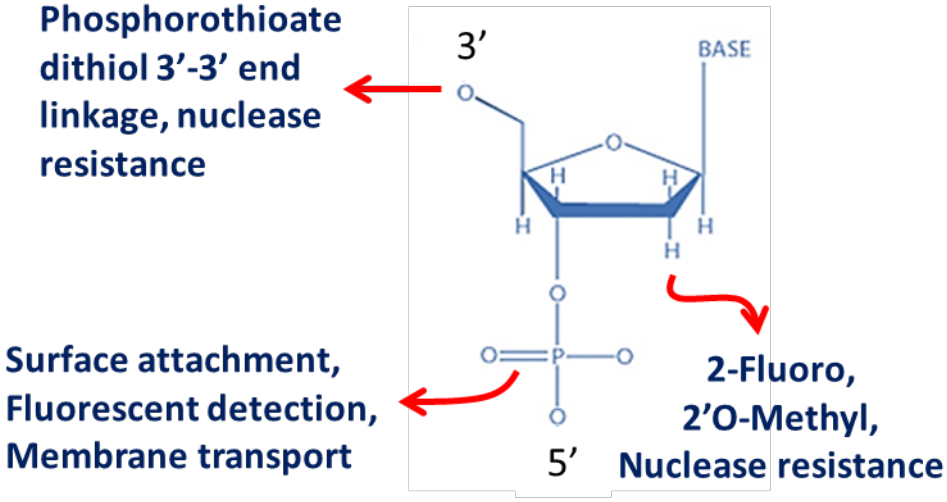

Figure 4.3 – Examples of nucleotide modifications to reduce degredation, increase half-life and facilitate functionality. Without intervention, aptamers will be degraded by nucleases within the serum. The half-life of administered aptamers may be increased following modifications, such as 2'fluoro or 2'O-methyl modifications. Aptamers may also be modified at the 3` end of the sequence using phosphorothioate dithiol linkages, in contrast the 5` end is normally reserved for conjugations to increase aptamer functionality.

Although these modifications may reduce oligonucleotide degradation, aptamers be quickly filtered from the blood by renal filtration. Unmodified aptamers are generally 5-15 kDa, which is far below the threshold that would see the aptamer be retained within the circulating blood. Glomerular filtration will result in molecules being removed from the blood that are less than 30-40kDa (Ruggiero *et al.*, 2010), however previous studies have utilised large moieties of polyethylene glycol or

cholesterol to limit aptamer excretion through the renal system (Rusconi *et al.*, 2004, Da Pieve *et al.*, 2012).

4.7 Conclusion

A total of 22 novel DNA aptamers have been identified towards glioblastoma cells and purified proteins known to be important for gliomagenesis. Whilst validation studies have shown two aptamers derived using short-term cultures to interact with glioblastoma cells, more studies into the specificity and selectivity of the ligands are necessary to ensure the binding is specific. Aptamers targeted to EGFRvIII failed to show any interaction during validation studies when using the biotinylated sense sequence, further studies using the anti-sense aptamer sequence are required to determine whether this is the specific aptamer sequence. Validation studies using aptamers isolated towards PDE1C, by western blot and AP analyses, have shown the derived ligands to target a protein similar in molecular weight to PDE1C and its various isoforms. These aptamer sequences have the potential to target the protein; however whether they have inhibitory effects is still to be established. A cell-SELEX methodology was described, utilising TD-PCR and 100 cells, one aptamer was sequenced following five rounds of cell-SELEX. Though this showed aptamers may be identified using a small number of cells, caution is advised as aptamers may be lost if too many iterative cycles are performed. The described procedure could potentially be used to select a panel of personalised aptamers to each patient following tumour biopsy. Excised tissue would need to be mapped to ensure the sample contains little non-cancerous tissue; however the time taken to test the aptamers could result in disease progression. Nevertheless, heterogenous cell populations will express varied biomarkers which can be utilised to provide personalised therapies and ultimately improve the outlook for glioblastoma patients.

Appendix : Miscallaenous aptamer sequences

Appendix 1: Non-specifc PDE1C aptamer sequences

4Forward:

CCCTCGAGTTTACCGCAGAATTCATACCACTTGACCATGTTAATAAGCTATGCCCACCATAAG TGACCTGACTGAATTCTCTCCCTATAGTGAGTCGTATTAGGAT

4Reverse failed

7Forward:

ATCCTAATACGACTCACTATAGGGAGAATTCTGCGGTAAACTCGAGGG

7Reverse failed

8Forward failed

8Reverse:

ATCCTAATACGACTCACTATGGCCGGGCGGTGGAATTCTGCGGTAAACTCGAGGG

9Forward:

ATCCTAATACGACTCACTATGGCCACACGGAATTCTGCGGNNAACTCGAGGG

9Reverse failed

10Forward:

CCCTCGAGTTTACCGCAGAATTCACCCCACAAGCCACACGCATCGATTGCCCGCCTATAGTGA GTCGTATTAGGAT

10Reverse:

ATCCTAATACGACTCACTATAGGCGGGCAATCGATGCGTGTGGCTTGTGGGGTGAATTCTGC GGTAAACTCGAGGG

11Forward:

ATCCTAATACGACTCACTATGCACAACCAGCCATGGGGAATTCTGCGGTAAACTCGAGGG

11Reverse failed

12Forward:

CCCTCGAGTTTACCGCAGAATTCATGAGCTGACCGCGTACTGTGCCCGGTATAGTGAGTCGT ATTAGGAT

12Reverse:

CCCTCGAGTTTACCGCAGAATTCGGCATGTCCCTCTGGCGGCATAGTGAGTCGTATTAGGAT

13Forward:

CCCTCGAGTTTACCGCAGAATTCGGCATGTCCCTCTGGCGGCATAGTGAGTCGTATTAGGAT

13Reverse failed

14Forward:

CCCTCGAGTTTACCGCAGAATTCGGCATGTCCCTCTGGCGGCATAGTGAGTCGTATTAGGAT

14Reverse failed

15Forward:

ATCCTAATACGACTCACTATGCACCCGGACCGTACAGCGCTAGAATTCTGCGGTAAACTCGAGGG

15Reverse failed

16Forward:

CCCTCGAGTTTACCGCAGAATTCCCCCGCCCCCCGCCATAGTGAGTCGTATTAGGAT

16Reverse:

ATCCTAATACGACTCACTATGGCGGGGGGCGGGGGAATTCTGCGGTAAACTCGAGGG

References

AHLSTROM, M., PEKKINEN, M., HUTTUNEN, M. & LAMBERG-ALLARDT, C. 2005. Dexamethasone down-regulates cAMP-phosphodiesterase in human osteosarcoma cells. *Biochem Pharmacol,* 69**,** 267-75.

AQUINO-JARQUIN, G. & TOSCANO-GARIBAY, J. D. 2011. RNA aptamer evolution: two decades of SELEction. *Int J Mol Sci,* 12**,** 9155-71.

ATHANASSIOU, H., SYNODINOU, M., MARAGOUDAKIS, E., PARASKEVAIDIS, M., VERIGOS, C., MISAILIDOU, D., ANTONADOU, D., SARIS, G., BEROUKAS, K. & KARAGEORGIS, P. 2005. Randomized phase II study of temozolomide and radiotherapy compared with radiotherapy alone in newly diagnosed glioblastoma multiforme. *J Clin Oncol,* 23**,** 2372-7.

BAGALKOT, V., FAROKHZAD, O. C., LANGER, R. & JON, S. 2006. An aptamer-doxorubicin physical conjugate as a novel targeted drug-delivery platform. *Angew Chem Int Ed Engl,* 45**,** 8149-52.

BANKS, W. A. 2009. Characteristics of compounds that cross the blood-brain barrier. *BMC Neurol,* 9 Suppl 1**,** S3.

BAO, S., WU, Q., MCLENDON, R. E., HAO, Y., SHI, Q., HJELMELAND, A. B., DEWHIRST, M. W., BIGNER, D. D. & RICH, J. N. 2006. Glioma stem cells promote radioresistance by preferential activation of the DNA damage response. *Nature,* 444**,** 756-60.

BATES, P. J., LABER, D. A., MILLER, D. M., THOMAS, S. D. & TRENT, J. O. 2009. Discovery and development of the G-rich oligonucleotide AS1411 as a novel treatment for cancer. *Experimental and molecular pathology,* 86**,** 151-164.

BELL, D. A. & DEMARINI, D. M. 1991. Excessive cycling converts PCR products to random-length higher molecular weight fragments. *Nucleic Acids Res,* 19**,** 5079.

BONDY, M. L., SCHEURER, M. E., MALMER, B., BARNHOLTZ-SLOAN, J. S., DAVIS, F. G., IL'YASOVA, D., KRUCHKO, C., MCCARTHY, B. J., RAJARAMAN, P., SCHWARTZBAUM, J. A., SADETZKI, S., SCHLEHOFER, B., TIHAN, T., WIEMELS, J. L., WRENSCH, M., BUFFLER, P. A. & BRAIN TUMOR EPIDEMIOLOGY, C. 2008. Brain tumor epidemiology: consensus from the Brain Tumor Epidemiology Consortium. *Cancer,* 113**,** 1953-68.

BRANDES, A. A., FRANCESCHI, E., TOSONI, A., BENEVENTO, F., SCOPECE, L., MAZZOCCHI, V., BACCI, A., AGATI, R., CALBUCCI, F. & ERMANI, M. 2009. Temozolomide concomitant and adjuvant to radiotherapy in elderly patients with glioblastoma. *Cancer,* 115**,** 3512-3518.

BRANDES, A. A., TOSONI, A., CAVALLO, G., RENI, M., FRANCESCHI, E., BONALDI, L., BERTORELLE, R., GARDIMAN, M., GHIMENTON, C., IUZZOLINO, P., PESSION, A., BLATT, V. & ERMANI, M. 2006. Correlations between O6-methylguanine DNA methyltransferase promoter methylation status, 1p and 19q deletions, and response to temozolomide in anaplastic and recurrent oligodendroglioma: a prospective GICNO study. *J Clin Oncol,* 24**,** 4746-53.

BRANDES, A. A., TOSONI, A., FRANCESCHI, E., RENI, M., GATTA, G. & VECHT, C. 2008. Glioblastoma in adults. *Crit Rev Oncol Hematol,* 67**,** 139-52.

CAVALIERE, R., LOPES, M. B. S. & SCHIFF, D. 2005. Low-grade gliomas: an update on pathology and therapy. *The Lancet Neurology,* 4**,** 760-770.

CERCHIA, L., ESPOSITO, C. L., JACOBS, A. H., TAVITIAN, B. & DE FRANCISCIS, V. 2009. Differential SELEX in human glioma cell lines. *PLoS One,* 4**,** e7971.

CHALMERS, A. 2011. *Understanding radiotherapy and its potential for use in novel combination trials* [Online]. National Cancer Research Institute. Available: http://www2.ncri.org.uk/ctrad/documents/tsr/ncri_ctrad_tsr_-_glioma_-_april_2011.pdf [Accessed 14/12/13.

CHAMBERLAIN, M. C. 2010. Temozolomide: therapeutic limitations in the treatment of adult high-grade gliomas. *Expert Rev Neurother,* 10**,** 1537-44.

CHEN, H. W., MEDLEY, C. D., SEFAH, K., SHANGGUAN, D., TANG, Z., MENG, L., SMITH, J. E. & TAN, W. 2008. Molecular recognition of small-cell lung cancer cells using aptamers. *ChemMedChem,* 3**,** 991-1001.

CHENG, C., CHEN, Y. H., LENNOX, K. A., BEHLKE, M. A. & DAVIDSON, B. L. 2013. In vivo SELEX for Identification of Brain-penetrating Aptamers. *Mol Ther Nucleic Acids,* 2**,** e67.

CHU, C. T., EVERISS, K. D., WIKSTRAND, C. J., BATRA, S. K., KUNG, H. J. & BIGNER, D. D. 1997. Receptor dimerization is not a factor in the signalling activity of a transforming variant epidermal growth factor receptor (EGFRvIII). *Biochem J,* 324 (Pt 3)**,** 855-61.

CHU, T. C., III, J. W. M., LAVERY, L. A., FAULKNER, S., ROSENBLUM, M. G., ELLINGTON, A. D. & LEVY, M. 2006. Aptamer:Toxin Conjugates that Specifically Target Prostate Tumor Cells. *Cancer Res.,* 66.

CROUSE, J. & AMORESE, D. 1987. Ethanol precipitation: ammonium acetate as an alternative to sodium acetate. *Focus,* 9**,** 3-5.

CRUK. 2014. *Brain, other CNS and intracranial tumours incidence statistics* [Online]. Available: http://www.cancerresearchuk.org/cancer-info/cancerstats/types/brain/incidence/.

DA PIEVE, C., BLACKSHAW, E., MISSAILIDIS, S. & PERKINS, A. C. 2012. PEGylation and biodistribution of an anti-MUC1 aptamer in MCF-7 tumor-bearing mice. *Bioconjug Chem,* 23**,** 1377-81.

DAHIA, P. L. 2000. PTEN, a unique tumor suppressor gene. *Endocr Relat Cancer,* 7**,** 115-29.

DASSIE, J. P., LIU, X.-Y., THOMAS, G. S., WHITAKER, R. M., THIEL, K. W., STOCKDALE, K. R., MEYERHOLZ, D. K., MCCAFFREY, A. P., MCNAMARA II, J. O. & GIANGRANDE, P. H. 2009. Systemic administration of optimized aptamer-siRNA chimeras promotes regression of PSMA-expressing tumors. *Nat Biotech,* 27**,** 839-846.

DAVIES, G. C., RYAN, P. E., RAHMAN, L., ZAJAC-KAYE, M. & LIPKOWITZ, S. 2006. EGFRvIII undergoes activation-dependent downregulation mediated by the Cbl proteins. *Oncogene,* 25**,** 6497-509.

DEMUTH, T. & BERENS, M. E. 2004. Molecular mechanisms of glioma cell migration and invasion. *Journal of neuro-oncology,* 70**,** 217-28.

DHAR, S., GU, F. X., LANGER, R., FAROKHZAD, O. C. & LIPPARD, S. J. 2008. Targeted delivery of cisplatin to prostate cancer cells by aptamer functionalized Pt(IV) prodrug-PLGA–PEG nanoparticles. *Proceedings of the National Academy of Sciences,* 105**,** 17356-17361.

DIETRICH, J., MONJE, M., WEFEL, J. & MEYERS, C. 2008. Clinical patterns and biological correlates of cognitive dysfunction associated with cancer therapy. *Oncologist,* 13**,** 1285-95.

DOLLINS, C. M., NAIR, S. & SULLENGER, B. A. 2008. Aptamers in immunotherapy. *Human gene therapy,* 19**,** 443-450.

DUCONGE, F. & TOULME, J. J. 1999. In vitro selection identifies key determinants for loop-loop interactions: RNA aptamers selective for the TAR RNA element of HIV-1. *RNA,* 5**,** 1605-14.

DUFFAU, H. 2013. A new philosophy in surgery for diffuse low-grade glioma (DLGG): oncological and functional outcomes. *Neurochirurgie,* 59**,** 2-8.

ELLENBOGEN, J. R., DAVIES, P., ELDRIDGE, P. R. & JENKINSON, M. D. 2013. Unusual patterns of recurrence in low grade gliomas. *J Clin Neurosci*.

ELLER, J. L., LONGO, S. L., KYLE, M. M., BASSANO, D., HICKLIN, D. J. & CANUTE, G. W. 2005. Anti-epidermal growth factor receptor monoclonal antibody cetuximab augments radiation effects in glioblastoma multiforme in vitro and in vivo. *Neurosurgery,* 56**,** 155-62; discussion 162.

ELLINGTON, A. D. & SZOSTAK, J. W. 1990. In vitro selection of RNA molecules that bind specific ligands. *Nature,* 346**,** 818-22.

ENGELHARD, H. H., STELEA, A. & COCHRAN, E. J. 2002. Oligodendroglioma: pathology and molecular biology. *Surg Neurol,* 58**,** 111-7; discussion 117.

ENGSTROM, P. G., TOMMEI, D., STRICKER, S. H., ENDER, C., POLLARD, S. M. & BERTONE, P. 2012. Digital transcriptome profiling of normal and glioblastoma-derived neural stem cells identifies genes associated with patient survival. *Genome Med,* 4**,** 76.

ESPOSITO, C. L., CERCHIA, L., CATUOGNO, S., DE VITA, G., DASSIE, J. P., SANTAMARIA, G., SWIDERSKI, P., CONDORELLI, G., GIANGRANDE, P. H. & DE FRANCISCIS, V. 2014. Multifunctional aptamer-miRNA conjugates for targeted cancer therapy. *Mol Ther,* 22**,** 1151-63.

FAN, K. J. & PEZESHKPOUR, G. H. 1992. Ethnic distribution of primary central nervous system tumors in Washington, DC, 1971 to 1985. *J Natl Med Assoc,* 84**,** 858-63.

FAN, Q. W., CHENG, C. K., GUSTAFSON, W. C., CHARRON, E., ZIPPER, P., WONG, R. A., CHEN, J., LAU, J., KNOBBE-THOMSEN, C., WELLER, M., JURA, N., REIFENBERGER, G., SHOKAT, K. M. & WEISS, W. A. 2013. EGFR phosphorylates tumor-derived EGFRvIII driving STAT3/5 and progression in glioblastoma. *Cancer Cell,* 24**,** 438-49.

FITZWATER, T. & POLISKY, B. 1996. A SELEX primer. *Methods Enzymol,* 267**,** 275-301.

FOY, J. W., RITTENHOUSE, K., MODI, M. & PATEL, M. 2007. Local tolerance and systemic safety of pegaptanib sodium in the dog and rabbit. *J Ocul Pharmacol Ther,* 23**,** 452-66.

FREGEL, R., GONZALEZ, A. & CABRERA, V. M. 2010. Improved ethanol precipitation of DNA. *Electrophoresis,* 31**,** 1350-2.

GAILLARD, C. & STRAUSS, F. 1990. Ethanol precipitation of DNA with linear polyacrylamide as carrier. *Nucleic acids research,* 18**,** 378.

GAJADHAR, A. S., BOGDANOVIC, E., MUNOZ, D. M. & GUHA, A. 2012. In situ analysis of mutant EGFRs prevalent in glioblastoma multiforme reveals aberrant dimerization, activation, and differential response to anti-EGFR targeted therapy. *Mol Cancer Res,* 10**,** 428-40.

GE, H., GONG, X. & TANG, C. K. 2002. Evidence of high incidence of EGFRvIII expression and coexpression with EGFR in human invasive breast cancer by laser capture microdissection and immunohistochemical analysis. *Int J Cancer,* 98**,** 357-61.

GIACHINI, F. R., LIMA, V. V., CARNEIRO, F. S., TOSTES, R. C. & WEBB, R. C. 2011. Decreased cGMP level contributes to increased contraction in arteries from hypertensive rats: role of phosphodiesterase 1. *Hypertension,* 57**,** 655-63.

GILBERT, J. C., DEFEO-FRAULINI, T., HUTABARAT, R. M., HORVATH, C. J., MERLINO, P. G., MARSH, H. N., HEALY, J. M., BOUFAKHREDDINE, S., HOLOHAN, T. V. & SCHAUB, R. G. 2007. First-in-human evaluation of anti von Willebrand factor therapeutic aptamer ARC1779 in healthy volunteers. *Circulation,* 116**,** 2678-86.

GOODENBERGER, M. L. & JENKINS, R. B. 2012. Genetics of adult glioma. *Cancer Genetics,* 205**,** 613-621.

GORAYA, T. A. & COOPER, D. M. 2005. Ca2+-calmodulin-dependent phosphodiesterase (PDE1): current perspectives. *Cell Signal,* 17**,** 789-97.

GRAHAM, J. C. & ZARBL, H. 2012. Use of Cell-SELEX to Generate DNA Aptamers as Molecular Probes of HPV-Associated Cervical Cancer Cells. *PLoS One,* 7**,** e36103.

GRANDAL, M. V., ZANDI, R., PEDERSEN, M. W., WILLUMSEN, B. M., VAN DEURS, B. & POULSEN, H. S. 2007. EGFRvIII escapes down-regulation due to impaired internalization and sorting to lysosomes. *Carcinogenesis,* 28**,** 1408-17.

GUO, J., GAO, X., SU, L., XIA, H., GU, G., PANG, Z., JIANG, X., YAO, L., CHEN, J. & CHEN, H. 2011. Aptamer-functionalized PEG-PLGA nanoparticles for enhanced anti-glioma drug delivery. *Biomaterials,* 32**,** 8010-20.

GUPTA, P., HAN, S.-Y., HOLGADO-MADRUGA, M., MITRA, S. S., LI, G., NITTA, R. T. & WONG, A. J. 2010. Development of an EGFRvIII specific recombinant antibody. *BMC biotechnology,* 10**,** 72.

HARDING, S. L., ANDREW. MCLAUGHLAN, BARBARA. WILLIE, LYDIA 2008. Ranibizumab and pegaptanib for the treatment of age-related macular degeneration. *In:* NHS (ed.) 2 ed. London: NICE publications.

HARTMANN, C., HENTSCHEL, B., WICK, W., CAPPER, D., FELSBERG, J., SIMON, M., WESTPHAL, M., SCHACKERT, G., MEYERMANN, R., PIETSCH, T., REIFENBERGER, G., WELLER, M., LOEFFLER, M. & VON DEIMLING, A. 2010. Patients with IDH1 wild type anaplastic astrocytomas exhibit worse prognosis than IDH1-mutated glioblastomas, and IDH1 mutation status accounts for the unfavorable prognostic effect of higher age: implications for classification of gliomas. *Acta Neuropathol,* 120**,** 707-18.

HARTMANN, C., MEYER, J., BALSS, J., CAPPER, D., MUELLER, W., CHRISTIANS, A., FELSBERG, J., WOLTER, M., MAWRIN, C., WICK, W., WELLER, M., HEROLD-MENDE, C., UNTERBERG, A., JEUKEN, J. W., WESSELING, P., REIFENBERGER, G. & VON DEIMLING, A. 2009. Type and frequency of IDH1 and IDH2 mutations are related to astrocytic and oligodendroglial differentiation and age: a study of 1,010 diffuse gliomas. *Acta Neuropathol,* 118**,** 469-74.

HASSELBALCH, B., LASSEN, U., HANSEN, S., HOLMBERG, M., SORENSEN, M., KOSTELJANETZ, M., BROHOLM, H., STOCKHAUSEN, M. T. & POULSEN, H. S. 2010. Cetuximab, bevacizumab, and irinotecan for patients with primary glioblastoma and progression after radiation therapy and temozolomide: a phase II trial. *Neuro Oncol,* 12**,** 508-16.

HICKE, B. J., MARION, C., CHANG, Y. F., GOULD, T., LYNOTT, C. K., PARMA, D., SCHMIDT, P. G. & WARREN, S. 2001. Tenascin-C aptamers are generated using tumor cells and purified protein. *J Biol Chem,* 276**,** 48644-54.

HUANG, Y. F., SHANGGUAN, D., LIU, H., PHILLIPS, J. A., ZHANG, X., CHEN, Y. & TAN, W. 2009. Molecular assembly of an aptamer–drug conjugate for targeted drug delivery to tumor cells. *ChemBioChem,* 10**,** 862-868.

HUIZENGA, D. E. & SZOSTAK, J. W. 1995. A DNA aptamer that binds adenosine and ATP. *Biochemistry,* 34**,** 656-665.

IKEBUKURO, K., TAKASE, M. & SODE, K. 2007. Selection of DNA aptamers that inhibit enzymatic activity of PQQGDH and its application. *Nucleic Acids Symp Ser (Oxf)***,** 403-4.

IRESON, C. R. & KELLAND, L. R. 2006. Discovery and development of anticancer aptamers. *Mol Cancer Ther,* 5**,** 2957-62.

ISHIDA, S., USUI, T., YAMASHIRO, K., KAJI, Y., AMANO, S., OGURA, Y., HIDA, T., OGUCHI, Y., AMBATI, J., MILLER, J. W., GRAGOUDAS, E. S., NG, Y. S., D'AMORE, P. A., SHIMA, D. T. & ADAMIS, A. P. 2003. VEGF164-mediated inflammation is required for pathological, but not physiological, ischemia-induced retinal neovascularization. *J Exp Med,* 198**,** 483-9.

JENISON, R. D., GILL, S. C., PARDI, A. & POLISKY, B. 1994. High-resolution molecular discrimination by RNA. *Science,* 263**,** 1425-9.

KANCHA, R. K., VON BUBNOFF, N. & DUYSTER, J. 2013. Asymmetric kinase dimer formation is crucial for the activation of oncogenic EGFRvIII but not for ERBB3 phosphorylation. *Cell Commun Signal,* 11**,** 39.

KANG, D., WANG, J., ZHANG, W., SONG, Y., LI, X., ZOU, Y., ZHU, M., ZHU, Z., CHEN, F. & YANG, C. J. 2012. Selection of DNA Aptamers against Glioblastoma Cells with High Affinity and Specificity. *PLoS One,* 7**,** e42731.

KAPPELLE, A. C., POSTMA, T. J., TAPHOORN, M. J., GROENEVELD, G. J., VAN DEN BENT, M. J., VAN GROENINGEN, C. J., ZONNENBERG, B. A., SNEEUW, K. C. & HEIMANS, J. J. 2001. PCV chemotherapy for recurrent glioblastoma multiforme. *Neurology,* 56**,** 118-20.

KARCHER, S., STEINER, H.-H., AHMADI, R., ZOUBAA, S., VASVARI, G., BAUER, H., UNTERBERG, A. & HEROLD-MENDE, C. 2006. Different angiogenic phenotypes in primary and secondary glioblastomas. *International Journal of Cancer,* 118**,** 2182-2189.

KAUR, H. & YUNG, L.-Y. L. 2012. Probing High Affinity Sequences of DNA Aptamer against VEGF₁₆₅. *PLoS One,* 7**,** e31196.

KLUSSMANN, S., NOLTE, A., BALD, R., ERDMANN, V. A. & FURSTE, J. P. 1996. Mirror-image RNA that binds D-adenosine. *Nat Biotechnol,* 14**,** 1112-5.

KOHLER, B. A., WARD, E., MCCARTHY, B. J., SCHYMURA, M. J., RIES, L. A. G., EHEMAN, C., JEMAL, A., ANDERSON, R. N., AJANI, U. A. & EDWARDS, B. K. 2011. Annual Report to the Nation on the Status of Cancer, 1975–2007, Featuring Tumors of the Brain and Other Nervous System. *Journal of the National Cancer Institute*.

KORBIE, D. J. & MATTICK, J. S. 2008. Touchdown PCR for increased specificity and sensitivity in PCR amplification. *Nat Protoc,* 3**,** 1452-6.

KOUWENHOVEN, M. C., KROS, J. M., FRENCH, P. J., BIEMOND-TER STEGE, E. M., GRAVELAND, W. J., TAPHOORN, M. J., BRANDES, A. A. & VAN DEN BENT, M. J. 2006. 1p/19q loss within oligodendroglioma is predictive for response to first line temozolomide but not to salvage treatment. *Eur J Cancer,* 42**,** 2499-503.

LACROIX, M., ABI-SAID, D., FOURNEY, D. R., GOKASLAN, Z. L., SHI, W., DEMONTE, F., LANG, F. F., MCCUTCHEON, I. E., HASSENBUSCH, S. J., HOLLAND, E., HESS, K., MICHAEL, C., MILLER, D. & SAWAYA, R. 2001. A multivariate analysis of 416 patients with glioblastoma multiforme: prognosis, extent of resection, and survival. *Journal of neurosurgery,* 95**,** 190-8.

LEWANDOWSKA, M. A., FURTAK, J., SZYLBERG, T., ROSZKOWSKI, K., WINDORBSKA, W., RYTLEWSKA, J. & JOZWICKI, W. 2014. An analysis of the prognostic value of IDH1 (isocitrate dehydrogenase 1) mutation in Polish glioma patients. *Mol Diagn Ther,* 18**,** 45-53.

LI, N., NGUYEN, H. H., BYROM, M. & ELLINGTON, A. D. 2011. Inhibition of cell proliferation by an anti-EGFR aptamer. *PLoS One,* 6**,** e20299.

LI, S., XU, H., DING, H., HUANG, Y., CAO, X., YANG, G., LI, J., XIE, Z., MENG, Y., LI, X., ZHAO, Q., SHEN, B. & SHAO, N. 2009. Identification of an aptamer targeting hnRNP A1 by tissue slide-based SELEX. *Journal of Pathology,* 218**,** 327-336.

LIN, Y. & JAYASENA, S. D. 1997. Inhibition of multiple thermostable DNA polymerases by a heterodimeric aptamer. *J Mol Biol,* 271**,** 100-11.

LIU, Y., KUAN, C. T., MI, J., ZHANG, X., CLARY, B. M., BIGNER, D. D. & SULLENGER, B. A. 2009. Aptamers selected against the unglycosylated EGFRvIII ectodomain and delivered intracellularly reduce membrane-bound EGFRvIII and induce apoptosis. *Biol Chem,* 390**,** 137-44.

LIU, Z., DUAN, J. H., SONG, Y. M., MA, J., WANG, F. D., LU, X. & YANG, X. D. 2012. Novel HER2 aptamer selectively delivers cytotoxic drug to HER2-positive breast cancer cells in vitro. *J Transl Med,* 10**,** 148.

LOKKER, N. A., SULLIVAN, C. M., HOLLENBACH, S. J., ISRAEL, M. A. & GIESE, N. A. 2002. Platelet-derived growth factor (PDGF) autocrine signaling regulates survival and mitogenic pathways in glioblastoma cells: evidence that the novel PDGF-C and PDGF-D ligands may play a role in the development of brain tumors. *Cancer Res,* 62**,** 3729-35.

LOPEZ-GINES, C., GIL-BENSO, R., FERRER-LUNA, R., BENITO, R., SERNA, E., GONZALEZ-DARDER, J., QUILIS, V., MONLEON, D., CELDA, B. & CERDA-NICOLAS, M. 2010. New pattern of EGFR amplification in glioblastoma and the relationship of gene copy number with gene expression profile. *Mod Pathol,* 23**,** 856-65.

LOUIS, D. N., OHGAKI, H., WIESTLER, O. D., CAVENEE, W. K., BURGER, P. C., JOUVET, A., SCHEITHAUER, B. W. & KLEIHUES, P. 2007. The 2007 WHO classification of tumours of the central nervous system. *Acta Neuropathol,* 114**,** 97-109.

LUPOLD, S. E., HICKE, B. J., LIN, Y. & COFFEY, D. S. 2002. Identification and characterization of nuclease-stabilized RNA molecules that bind human prostate cancer cells via the prostate-specific membrane antigen. *Cancer Res,* 62**,** 4029-33.

LUWOR, R. B., ZHU, H. J., WALKER, F., VITALI, A. A., PERERA, R. M., BURGESS, A. W., SCOTT, A. M. & JOHNS, T. G. 2004. The tumor-specific de2-7 epidermal growth factor receptor (EGFR) promotes cells survival and heterodimerizes with the wild-type EGFR. *Oncogene,* 23**,** 6095-104.

MARIMUTHU, C., TANG, T. H., TOMINAGA, J., TAN, S. C. & GOPINATH, S. C. 2012. Single-stranded DNA (ssDNA) production in DNA aptamer generation. *Analyst,* 137**,** 1307-15.

MARTENS, T., MATSCHKE, J., MÜLLER, C., RIETHDORF, S., BALABANOV, S., WESTPHAL, M. & HEESE, O. 2013. Skeletal spread of an anaplastic astrocytoma (WHO grade III) and preservation of histopathological properties within metastases. *Clinical Neurology and Neurosurgery,* 115**,** 323-328.

MASUI, K., CLOUGHESY, T. F. & MISCHEL, P. S. 2012. Review: molecular pathology in adult high-grade gliomas: from molecular diagnostics to target therapies. *Neuropathol Appl Neurobiol,* 38**,** 271-91.

MAYER, G. 2009. The chemical biology of aptamers. *Angew Chem Int Ed Engl,* 48**,** 2672-89.

MENDONSA, S. D. & BOWSER, M. T. 2004. In vitro selection of high-affinity DNA ligands for human IgE using capillary electrophoresis. *Anal Chem,* 76**,** 5387-92.

MEYER, S., MAUFORT, J. P., NIE, J., STEWART, R., MCINTOSH, B. E., CONTI, L. R., AHMAD, K. M., SOH, H. T. & THOMSON, J. A. 2013. Development of an Efficient Targeted Cell-SELEX Procedure for DNA Aptamer Reagents. *PLoS One,* 8**,** e71798.

MOK, W. & LI, Y. 2008. Recent Progress in Nucleic Acid Aptamer-Based Biosensors and Bioassays. *Sensors,* 8**,** 7050-7084.

MOSING, R. K., MENDONSA, S. D. & BOWSER, M. T. 2005. Capillary electrophoresis-SELEX selection of aptamers with affinity for HIV-1 reverse transcriptase. *Analytical chemistry,* 77**,** 6107-6112.

NAVANI, N. K., MOK, W. K. & YINGFU, L. 2009. In vitro selection of protein-binding DNA aptamers as ligands for biosensing applications. *Methods Mol Biol,* 504**,** 399-415.

NEWHAUSER, W. D. & DURANTE, M. 2011. Assessing the risk of second malignancies after modern radiotherapy. *Nature reviews. Cancer,* 11**,** 438-48.

NICE 2001. Guidance on the use of temozolomide for the treatment of recurrent malignant glioma. London.

NICE 2007. Carmustine implants and temozolomide for the treatment of newly diagnosed high-grade glioma.

OHGAKI, H. 2009. Epidemiology of brain tumors. *Methods Mol Biol,* 472**,** 323-42.

OHGAKI, H., DESSEN, P., JOURDE, B., HORSTMANN, S., NISHIKAWA, T., DI PATRE, P. L., BURKHARD, C., SCHULER, D., PROBST-HENSCH, N. M., MAIORKA, P. C., BAEZA, N., PISANI, P., YONEKAWA, Y., YASARGIL, M. G., LUTOLF, U. M. & KLEIHUES, P. 2004. Genetic pathways to glioblastoma: a population-based study. *Cancer research,* 64**,** 6892-9.

OHGAKI, H. & KLEIHUES, P. 2005. Population-based studies on incidence, survival rates, and genetic alterations in astrocytic and oligodendroglial gliomas. *Journal of neuropathology and experimental neurology,* 64**,** 479-89.

OHGAKI, H. & KLEIHUES, P. 2007. Genetic pathways to primary and secondary glioblastoma. *Am J Pathol,* 170**,** 1445-53.

OKITA, Y., NARITA, Y., MIYAKITA, Y., OHNO, M., MATSUSHITA, Y., FUKUSHIMA, S., SUMI, M., ICHIMURA, K., KAYAMA, T. & SHIBUI, S. 2012. IDH1/2 mutation is a prognostic marker for survival and predicts response to chemotherapy for grade II gliomas concomitantly treated with radiation therapy. *Int J Oncol,* 41**,** 1325-36.

OSTROM, Q. T., GITTLEMAN, H., FARAH, P., ONDRACEK, A., CHEN, Y., WOLINSKY, Y., STROUP, N. E., KRUCHKO, C. & BARNHOLTZ-SLOAN, J. S. 2013. CBTRUS Statistical Report: Primary Brain and Central Nervous System Tumors Diagnosed in the United States in 2006-2010. *Neuro Oncol,* 15 Suppl 2**,** ii1-ii56.

PEIFFER, J. & KLEIHUES, P. 1999. Hans-Joachim Scherer (1906-1945), pioneer in glioma research. *Brain Pathol,* 9**,** 241-5.

PREUSSER, M., CHARLES JANZER, R., FELSBERG, J., REIFENBERGER, G., HAMOU, M. F., DISERENS, A. C., STUPP, R., GORLIA, T., MAROSI, C., HEINZL, H., HAINFELLNER, J. A. & HEGI, M. 2008. Anti-O6-methylguanine-methyltransferase (MGMT) immunohistochemistry in glioblastoma multiforme: observer variability and lack of association with patient survival impede its use as clinical biomarker. *Brain Pathol,* 18**,** 520-32.

PRIGENT, S. A., NAGANE, M., LIN, H., HUVAR, I., BOSS, G. R., FERAMISCO, J. R., CAVENEE, W. K. & HUANG, H. S. 1996. Enhanced tumorigenic behavior of

glioblastoma cells expressing a truncated epidermal growth factor receptor is mediated through the Ras-Shc-Grb2 pathway. *J Biol Chem,* 271**,** 25639-45.

REIFENBERGER, G. & COLLINS, V. P. 2004. Pathology and molecular genetics of astrocytic gliomas. *J Mol Med (Berl),* 82**,** 656-70.

RICARD, D., IDBAIH, A., DUCRAY, F., LAHUTTE, M., HOANG-XUAN, K. & DELATTRE, J.-Y. 2012. Primary brain tumours in adults. *The Lancet,* 379**,** 1984-1996.

ROSENBERG, J. E., BAMBURY, R. M., VAN ALLEN, E. M., DRABKIN, H. A., LARA, P. N., JR., HARZSTARK, A. L., WAGLE, N., FIGLIN, R. A., SMITH, G. W., GARRAWAY, L. A., CHOUEIRI, T., ERLANDSSON, F. & LABER, D. A. 2014. A phase II trial of AS1411 (a novel nucleolin-targeted DNA aptamer) in metastatic renal cell carcinoma. *Invest New Drugs,* 32**,** 178-87.

ROUX, K. H. 1995. Optimization and troubleshooting in PCR. *PCR Methods Appl,* 4**,** S185-94.

ROWTHER, F., B., DAWSON, T., ASHTON, K., DARLING, J. & WARR, T. 2012. Depletion of Ca2+/CAM-stimulated Phosphodiesterase 1C (PDE1C) attenuates proliferation, migration, and invasion of adult high-grade astrocytoma cells. *Neuro Oncol,* 14**,** 7-20.

RUCKMAN, J., GREEN, L. S., BEESON, J., WAUGH, S., GILLETTE, W. L., HENNINGER, D. D., CLAESSON-WELSH, L. & JANJIC, N. 1998. 2'-Fluoropyrimidine RNA-based aptamers to the 165-amino acid form of vascular endothelial growth factor (VEGF165). Inhibition of receptor binding and VEGF-induced vascular permeability through interactions requiring the exon 7-encoded domain. *J Biol Chem,* 273**,** 20556-67.

RUGGIERO, A., VILLA, C. H., BANDER, E., REY, D. A., BERGKVIST, M., BATT, C. A., MANOVA-TODOROVA, K., DEEN, W. M., SCHEINBERG, D. A. & MCDEVITT, M. R. 2010. Paradoxical glomerular filtration of carbon nanotubes. *Proc Natl Acad Sci U S A,* 107**,** 12369-74.

RUSCONI, C. P., ROBERTS, J. D., PITOC, G. A., NIMJEE, S. M., WHITE, R. R., QUICK JR, G., SCARDINO, E., FAY, W. P. & SULLENGER, B. A. 2004. Antidote-mediated control of an anticoagulant aptamer in vivo. *Nat Biotech,* 22**,** 1423-1428.

RUSYN, I., ASAKURA, S., PACHKOWSKI, B., BRADFORD, B. U., DENISSENKO, M. F., PETERS, J. M., HOLLAND, S. M., REDDY, J. K., CUNNINGHAM, M. L. & SWENBERG, J. A. 2004. Expression of Base Excision DNA Repair Genes Is a Sensitive Biomarker for in Vivo Detection of Chemical-induced Chronic Oxidative Stress Identification of the Molecular Source of Radicals Responsible for DNA Damage by Peroxisome Proliferators. *Cancer research,* 64**,** 1050-1057.

RYBALKIN, S. D., RYBALKINA, I., BEAVO, J. A. & BORNFELDT, K. E. 2002. Cyclic nucleotide phosphodiesterase 1C promotes human arterial smooth muscle cell proliferation. *Circ Res,* 90**,** 151-7.

SALMAGGI, A., BOIARDI, A., GELATI, M., RUSSO, A., CALATOZZOLO, C., CIUSANI, E., SCIACCA, F. L., OTTOLINA, A., PARATI, E. A., LA PORTA, C., ALESSANDRI, G., MARRAS, C., CROCI, D. & DE ROSSI, M. 2006. Glioblastoma-derived tumorospheres identify a population of tumor stem-like cells with angiogenic potential and enhanced multidrug resistance phenotype. *Glia,* 54**,** 850-60.

SALVATI, M., FORMICHELLA, A. I., D'ELIA, A., BROGNA, C., FRATI, A., GIANGASPERO, F., DELFINI, R. & SANTORO, A. 2009. Cerebral glioblastoma with oligodendrogliomal component: analysis of 36 cases. *Journal of neuro-oncology,* 94**,** 129-34.

SAMPSON, J. H., CROTTY, L. E., LEE, S., ARCHER, G. E., ASHLEY, D. M., WIKSTRAND, C. J., HALE, L. P., SMALL, C., DRANOFF, G., FRIEDMAN, A. H., FRIEDMAN, H. S. & BIGNER, D. D. 2000. Unarmed, tumor-specific monoclonal antibody effectively treats brain tumors. *Proceedings of the National Academy of Sciences,* 97**,** 7503-7508.

SANAI, N., MARTINO, J. & BERGER, M. S. 2012. Morbidity profile following aggressive resection of parietal lobe gliomas. *Journal of neurosurgery,* 116**,** 1182-6.

SANT, M., MINICOZZI, P., LAGORIO, S., BØRGE JOHANNESEN, T., MARCOS-GRAGERA, R., FRANCISCI, S. & THE, E. W. G. 2012. Survival of European patients with central nervous system tumors. *International Journal of Cancer,* 131**,** 173-185.

SARKARIA, J. N., KITANGE, G. J., JAMES, C. D., PLUMMER, R., CALVERT, H., WELLER, M. & WICK, W. 2008. Mechanisms of chemoresistance to alkylating agents in malignant glioma. *Clin Cancer Res,* 14**,** 2900-8.

SCHLEHUBER, S. & SKERRA, A. 2005. Anticalins as an alternative to antibody technology. *Expert Opin Biol Ther,* 5**,** 1453-62.

SCHMIDT, F., FISCHER, J., HERRLINGER, U., DIETZ, K., DICHGANS, J. & WELLER, M. 2006. PCV chemotherapy for recurrent glioblastoma. *Neurology,* 66**,** 587-9.

SCHWARTZBAUM, J. A., FISHER, J. L., ALDAPE, K. D. & WRENSCH, M. 2006. Epidemiology and molecular pathology of glioma. *Nat Clin Pract Neurol,* 2**,** 494-503; quiz 1 p following 516.

SEFAH, K., SHANGGUAN, D., XIONG, X., O'DONOGHUE, M. B. & TAN, W. 2010a. Development of DNA aptamers using Cell-SELEX. *Nat Protoc,* 5**,** 1169-85.

SEFAH, K., SHANGGUAN, D., XIONG, X., O'DONOGHUE, M. B. & TAN, W. 2010b. Development of DNA aptamers using Cell-SELEX. *Nature Protocols,* 5**,** 1169-1185.

SHANGGUAN, D., LI, Y., TANG, Z., CAO, Z. C., CHEN, H. W., MALLIKARATCHY, P., SEFAH, K., YANG, C. J. & TAN, W. 2006. Aptamers evolved from live cells as effective molecular probes for cancer study. *Proc Natl Acad Sci U S A,* 103**,** 11838-43.

SHANGGUAN, D., MENG, L., CAO, Z. C., XIAO, Z., FANG, X., LI, Y., CARDONA, D., WITEK, R. P., LIU, C. & TAN, W. 2008. Identification of liver cancer-specific aptamers using whole live cells. *Anal Chem,* 80**,** 721-8.

SHI, S.-R., LIU, C., BALGLEY, B. M., LEE, C. & TAYLOR, C. R. 2006. Protein extraction from formalin-fixed, paraffin-embedded tissue sections: quality evaluation by mass spectrometry. *Journal of Histochemistry & Cytochemistry,* 54**,** 739-743.

SHIMIZU, K., MURATA, T., WATANABE, Y., SATO, C., MORITA, H. & TAGAWA, T. 2009. Characterization of phosphodiesterase 1 in human malignant melanoma cell lines. *Anticancer Res,* 29**,** 1119-22.

SIMMONS, S. C., JAMSA, H., SILVA, D., CORTEZ, C. M., MCKENZIE, E. A., BITU, C. C., SALO, S., NURMENNIEMI, S., NYBERG, P., RISTELI, J., DEALMEIDA, C. E., BRENCHLEY, P. E., SALO, T. & MISSAILIDIS, S. 2014. Anti-heparanase aptamers as potential diagnostic and therapeutic agents for oral cancer. *PLoS One,* 9**,** e96846.

SOK, J. C., COPPELLI, F. M., THOMAS, S. M., LANGO, M. N., XI, S., HUNT, J. L., FREILINO, M. L., GRANER, M. W., WIKSTRAND, C. J. & BIGNER, D. D. 2006. Mutant epidermal growth factor receptor (EGFRvIII) contributes to head and neck cancer growth and resistance to EGFR targeting. *Clinical Cancer Research,* 12**,** 5064-5073.

SONG, S., WANG, L., LI, J., FAN, C. & ZHAO, J. 2008. Aptamer-based biosensors. *TrAC Trends in Analytical Chemistry,* 27**,** 108-117.

SOUNDARARAJAN, S., CHEN, W., SPICER, E. K., COURTENAY-LUCK, N. & FERNANDES, D. J. 2008. The nucleolin targeting aptamer AS1411 destabilizes Bcl-2 messenger RNA in human breast cancer cells. *Cancer Res,* 68**,** 2358-65.

SOUNDARARAJAN, S., WANG, L., SRIDHARAN, V., CHEN, W., COURTENAY-LUCK, N., JONES, D., SPICER, E. K. & FERNANDES, D. J. 2009. Plasma membrane nucleolin is a receptor for the anticancer aptamer AS1411 in MV4-11 leukemia cells. *Mol Pharmacol,* 76**,** 984-91.

STOLTENBURG, R., REINEMANN, C. & STREHLITZ, B. 2005. FluMag-SELEX as an advantageous method for DNA aptamer selection. *Anal Bioanal Chem,* 383**,** 83-91.

STUPP, R., MASON, W. P., VAN DEN BENT, M. J., WELLER, M., FISHER, B., TAPHOORN, M. J. B., BELANGER, K., BRANDES, A. A., MAROSI, C., BOGDAHN, U., CURSCHMANN, J., JANZER, R. C., LUDWIN, S. K., GORLIA, T., ALLGEIER, A., LACOMBE, D., CAIRNCROSS, J. G., EISENHAUER, E. & MIRIMANOFF, R. O. 2005. Radiotherapy plus Concomitant and Adjuvant Temozolomide for Glioblastoma. *New England Journal of Medicine,* 352**,** 987-996.

SUGAWA, N., EKSTRAND, A. J., JAMES, C. D. & COLLINS, V. P. 1990. Identical splicing of aberrant epidermal growth factor receptor transcripts from amplified rearranged genes in human glioblastomas. *Proc Natl Acad Sci U S A,* 87**,** 8602-6.

SURMA-AHO, O., NIEMELA, M., VILKKI, J., KOURI, M., BRANDER, A., SALONEN, O., PAETAU, A., KALLIO, M., PYYKKONEN, J. & JAASKELAINEN, J. 2001. Adverse long-term effects of brain radiotherapy in adult low-grade glioma patients. *Neurology,* 56**,** 1285-90.

SVOBODOVA, M., PINTO, A., NADAL, P. & CK, O. S. 2012. Comparison of different methods for generation of single-stranded DNA for SELEX processes. *Anal Bioanal Chem,* 404**,** 835-42.

TAN, M., VERNES, J. M., CHAN, J., CUELLAR, T. L., ASUNDI, A., NELSON, C., YIP, V., SHEN, B., VANDLEN, R., SIEBEL, C. & MENG, Y. G. 2012. Real-time quantification of antibody-short interfering RNA conjugate in serum by antigen capture reverse transcription-polymerase chain reaction. *Anal Biochem,* 430**,** 171-8.

TIEDE, C., TANG, A. A., DEACON, S. E., MANDAL, U., NETTLESHIP, J. E., OWEN, R. L., GEORGE, S. E., HARRISON, D. J., OWENS, R. J., TOMLINSON, D. C. & MCPHERSON, M. J. 2014. Adhiron: a stable and versatile peptide display scaffold for molecular recognition applications. *Protein Eng Des Sel,* 27**,** 145-55.

TOWNSHEND, B., AUBRY, I., MARCELLUS, R. C., GEHRING, K. & TREMBLAY, M. L. 2010. An RNA aptamer that selectively inhibits the enzymatic activity of protein tyrosine phosphatase 1B in vitro. *ChemBioChem,* 11**,** 1583-93.

TUERK, C. & GOLD, L. 1990. Systematic evolution of ligands by exponential enrichment: RNA ligands to bacteriophage T4 DNA polymerase. *Science,* 249**,** 505-10.

VAN DEN BENT, M. J. 2010. Interobserver variation of the histopathological diagnosis in clinical trials on glioma: a clinician's perspective. *Acta Neuropathol,* 120**,** 297-304.

VATTER, S., PAHLKE, G., DEITMER, J. W. & EISENBRAND, G. 2005. Differential phosphodiesterase expression and cytosolic Ca2+ in human CNS tumour cells and in non-malignant and malignant cells of rat origin. *J Neurochem,* 93**,** 321-9.

VOGT, N., LEFEVRE, S. H., APIOU, F., DUTRILLAUX, A. M., COR, A., LEURAUD, P., POUPON, M. F., DUTRILLAUX, B., DEBATISSE, M. & MALFOY, B. 2004. Molecular structure of double-minute chromosomes bearing amplified copies of the

epidermal growth factor receptor gene in gliomas. *Proc Natl Acad Sci U S A,* 101**,** 11368-73.

VON BOSSANYI, P., SALLABA, J., DIETZMANN, K., WARICH-KIRCHES, M. & KIRCHES, E. 1998. Correlation of TGF-alpha and EGF-receptor expression with proliferative activity in human astrocytic gliomas. *Pathol Res Pract,* 194**,** 141-7.

WATERMAN, H., KATZ, M., RUBIN, C., SHTIEGMAN, K., LAVI, S., ELSON, A., JOVIN, T. & YARDEN, Y. 2002. A mutant EGF-receptor defective in ubiquitylation and endocytosis unveils a role for Grb2 in negative signaling. *EMBO J,* 21**,** 303-13.

WELLER, M. 2011. Novel diagnostic and therapeutic approaches to malignant glioma. *Swiss Med Wkly,* 24**,** 13210.

WEN, P. Y. & KESARI, S. 2008. Malignant gliomas in adults. *The New England journal of medicine,* 359**,** 492-507.

WONGPHATCHARACHAI, M., WANG, P., ENOMOTO, S., WEBBY, R. J., GRAMER, M. R., AMONSIN, A. & SREEVATSAN, S. 2013. Neutralizing DNA aptamers against swine influenza H3N2 viruses. *J Clin Microbiol,* 51**,** 46-54.

YAN, C., ZHAO, A. Z., BENTLEY, J. K. & BEAVO, J. A. 1996. The calmodulin-dependent phosphodiesterase gene PDE1C encodes several functionally different splice variants in a tissue-specific manner. *Journal of Biological Chemistry,* 271**,** 25699-25706.

YOUNT, G. L., HAAS-KOGAN, D. A., VIDAIR, C. A., HAAS, M., DEWEY, W. C. & ISRAEL, M. A. 1996. Cell cycle synchrony unmasks the influence of p53 function on radiosensitivity of human glioblastoma cells. *Cancer Res,* 56**,** 500-6.

ZHANG, X., GUREASKO, J., SHEN, K., COLE, P. A. & KURIYAN, J. 2006. An allosteric mechanism for activation of the kinase domain of epidermal growth factor receptor. *Cell,* 125**,** 1137-49.